1997

Seismic velocities and depositional environments, upper Morrow Formation, Texas

Jens R. Halverson
San Jose State University

SEISMIC VELOCITIES AND DEPOSITIONAL ENVIRONMENTS, UPPER MORROW FORMATION, TEXAS

A Thesis Presented to

The Faculty of the Department of Geology

San Jose State University

In Partial Fulfillment of the

Requirements for the Degree

Master of Science

by

Jens R. Halverson

December 1997

UMI Number: 1388195

UMI
300 North Zeeb Road
Ann Arbor, MI 48103

APPROVED FOR THE DEPARTMENT OF GEOLOGY BY:

Dr. Calvin H. Stevens, Professor of Geology

Dr. David W. Andersen, Professor of Geology

Dr. John P. Brooke, Professor of Geology

APPROVED FOR THE UNIVERSITY BY:

ABSTRACT

SEISMIC VELOCITIES AND DEPOSITIONAL ENVIRONMENTS, UPPER MORROW FORMATION, TEXAS

by Jens R. Halverson

The upper Morrow Formation in the western Anadarko Basin, northeastern Texas Panhandle, was studied using 360 km of seismic inversion data integrated with data from 80 wells. The goals were to use seismic data to interpret the lithologies, depositional environments, evolving paleogeography, and changing sea level represented by this stratigraphic interval.

Seismic interval velocity contouring, based upon wavelet character, and correlation with borehole data provided the basis for the interpretations. Characteristic seismic signatures of three lithologies, sandstone, shale, and clayey siltstone, were recognized.

Sandstone anomalies, concentrated at three seismic horizons, were mapped. The highest and lowest horizons are interpreted to represent deltaic distributary channel systems, whereas the middle horizon is interpreted to represent a meandering fluvial system. These seismic horizons are also interpreted to represent three minor progradational pulses of 4^{th}- to 5^{th}-order global stratigraphic cycles produced by repeated glaciation in the southern hemisphere, with possible tectonically generated pulses superimposed.

ACKNOWLEDGMENTS

Appreciation is herein expressed to the thesis committee, which consists of Dr. Calvin H. Stevens, Dr. David W. Andersen, and Dr. John P. Brooke. Dr. Stevens played the role of thesis advisor and senior editor. His extensive experience in geology was made manifest by his many insightful comments and suggestions. Dr. Andersen made many contributions to the editing of the manuscript. His comments on the illustrations and his perspective as a sedimentologist were especially helpful. Dr. Brooke was the geophysicist on the thesis committee; he reviewed the geophysical aspects of the thesis for technical competency. I am grateful to the thesis committee for all of its efforts made on my behalf.

Acknowledgment is made to Seisdata Services, Inc.; Teknica, Inc. (USA); Seismos Energy Company, and Seismic Interpretations, Inc. for access to and release of the seismic data.

I am grateful for the financial and moral support of Dr. D. E. Halverson, Dorothy Halverson, Karen Rencher, and Dr. Mark Rencher.

DEDICATION

This work is dedicated to the 500,000 workers of the petroleum industry who lost their jobs in the mid-1980's because they did their work too well. Through their collective creativity and expertise they discovered too much oil and gas, thereby prompting the Saudi Arabians to flood the world oil market, overproducing by 800 percent; this action caused the collapse of the price of crude oil on the world markets and caused the demise of the petroleum industry in the United States.

TABLE OF CONTENTS

LIST OF ILLUSTRATIONS

LIST OF PLATES

INTRODUCTION

This research was conceived as a detailed investigation of the environments of deposition and the evolving paleogeography of the upper Morrow Formation as interpreted through the use of wavelet character analysis of seismic data. The zone of interest is the completely buried upper Morrow Formation located approximately 3,050 m (10,000 ft) below the surface on the northern flank of the western Anadarko Basin of North America. The specific study area is in the northeastern part of Lipscomb County in the Texas Panhandle (Fig. 1). This 50 km by 50 km (30 by 30 mile) county is located upon the high plains of the Midcontinent, approximately 160 km (100 miles) northeast of Amarillo, Texas. This geographic area was selected due to the availability of high-quality reflection seismic data, color seismic inversion processed data, and sufficient subsurface well control for integrated geologic and geophysical research. In addition, the seismic stratigraphic study of Darden Field (Halverson, 1988), which is in the research area, suggested that seismic inversion processing and seismic interval velocity mapping might be suitable techniques for completing the stratigraphic picture within this area of sparse well control.

Previously, the structural interpretation techniques used in this area involved mapping reflection seismic data to complete the structural picture between sparse well control. This sparse well control is attested to by the fact that, within the 900 sections that comprise Lipscomb County, fewer than twenty-five wells penetrate the lower Paleozoic to the

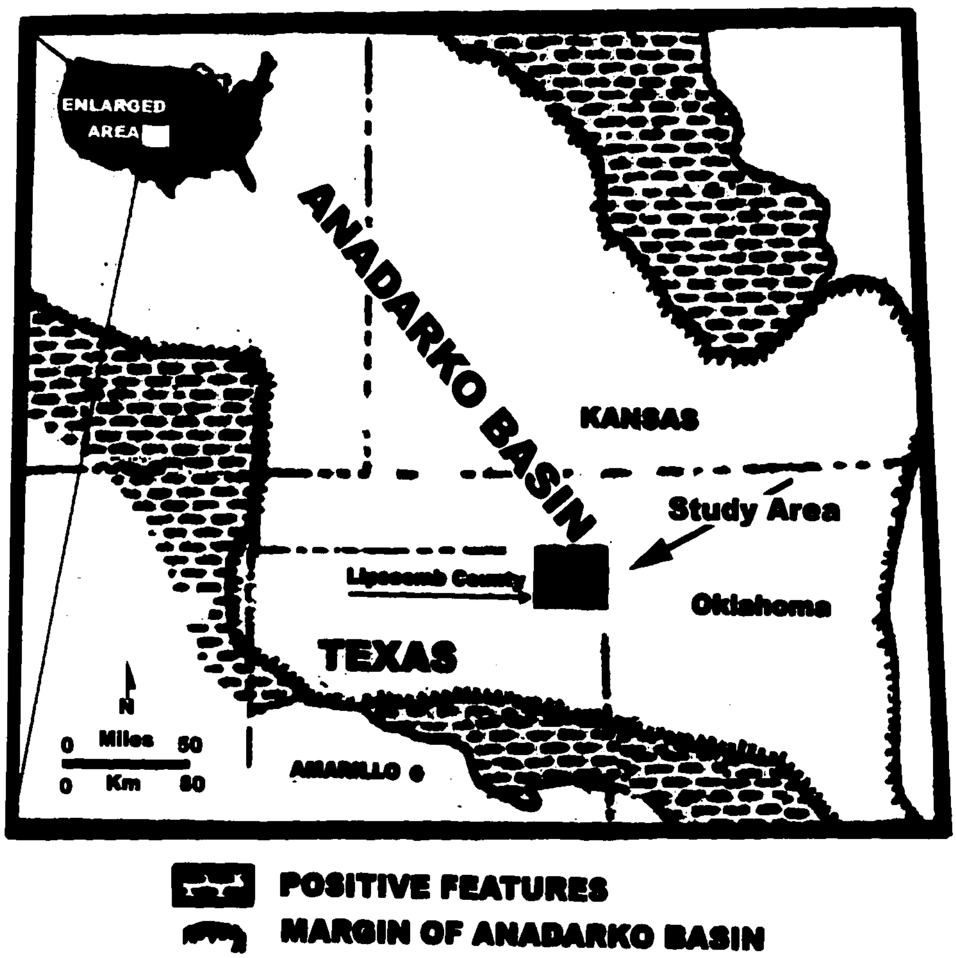

Figure 1. The study area in the western Anadarko Basin of North America (adapted from Swanson, 1979).

Ordovician Simpson Formation at a depth of ~5,000 m (16,500 ft) below the surface. Additionally, within the 300 sections comprising the study area, only several hundred wells penetrate the upper Morrow Formation, which is at an average depth of ~3,050 m (10,000 ft) below the surface.

For this study, 360 km (225 miles) of color seismic inversion data were integrated with geologic data from 80 wells to map several seismic horizons, lithologic units reflecting seismic energy that can be correlated over a large geographic area, within the upper Morrow Formation. The mapped seismic horizons for this study are most analogous to geologic isopachous maps, which represent both the areal extent of a lithologic unit and its varying thickness. The interpretations and mapping utilized for this research include methods described by Lindseth (1976) and methods from the Darden Field case study described by Halverson (1988), as well as methods to be described herein.

The final maps generated for this study are a series of interval velocity maps of seismic horizons within the upper Morrow Formation. The most probable lithologies of the maps of each seismic horizon were determined by the integration of the seismic inversion data with the geologic well control.

The ultimate goal of this geologic and geophysical investigation, realized through the interpretation of these interval velocity maps, is to provide the data needed for a determination of the depositional environments, a history of changing relative sea level, and a description of the evolving paleogeography within the study area during the deposition of the upper Morrow Formation.

GEOLOGIC SETTING

Tectonic History

The tectonic history of the Anadarko Basin area has been summarized by Perry (1989). Crustal consolidation and regional high-grade metamorphism occurred during the middle Proterozoic (1.3 to 1.4 Ga), at which time the structural grain (N 60 W) of the basin was developed. During the late Proterozoic, the proto-Anadarko Basin (southern Oklahoma aulacogen) originated as the failed arm of a triple junction along a rifted continental margin (Fig. 2). Thick lower Paleozoic deposits accumulated within this rifted structural low. During the Late Mississippian to Early Permian, as the North American plate collided with Gondwanaland to form the supercontinent Pangaea, this area was subjected to compressional stresses of continental proportions. This collision formed a fold and thrust belt along the southern flank of the southern Oklahoma aulacogen. Thrust loading depressed the lithosphere resulting in the development of a foreland basin, the Anadarko Basin, on the northern flank of the aulacogen (Figs. 3, 4).

Mississippian and Pennsylvanian Stratigraphy

A generalized stratigraphic column of the Morrow Formation and encompassing units is shown in Figure 5. An unnamed Mississippian limestone of Chesterian age, informally called the "Chester" or the "Mississippian limestone," is separated from the overlying lower Morrow

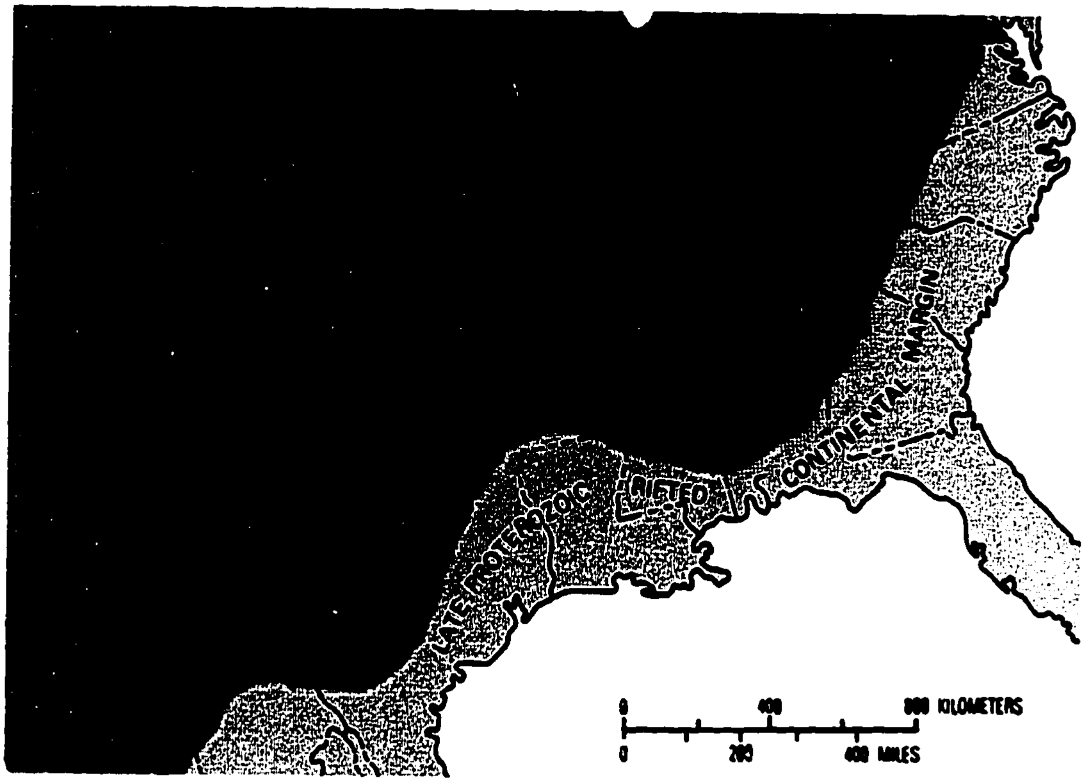

Figure 2. The late Proterozoic rifted continental margin and associated rifts (red). The proto-Anadarko Basin or southern Oklahoma aulacogen originated as the failed arm of a triple junction (adapted from Perry, 1989).

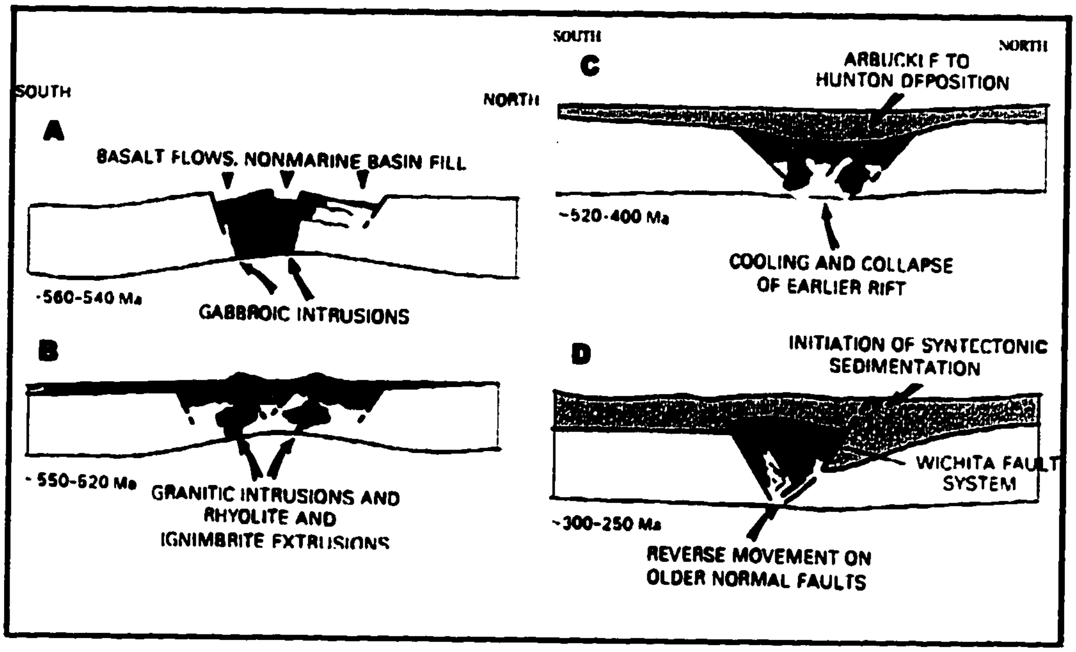

Figure 3. The geologic evolution of the southern Oklahoma aulacogen. A and B show a rift valley forming with associated igneous intrusive and extrusive rocks. Cooling and collapse at C creates a rift basin, the southern Oklahoma aulacogen, in which thick lower Paleozoic sediments are deposited. D shows the results of the collision between the North American plate and Gondwanaland (adapted from Perry, 1989).

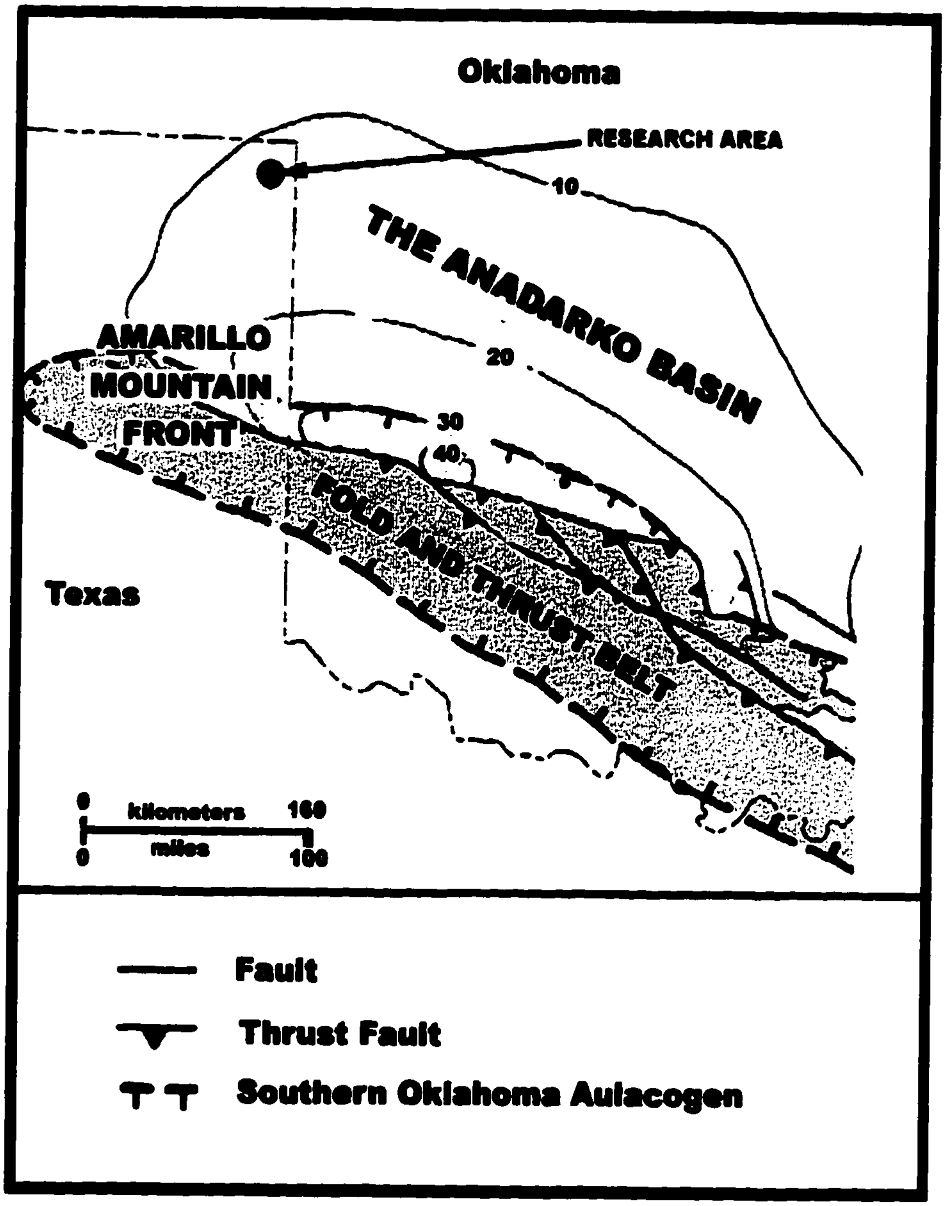

Figure 4. Map of the Anadarko Basin. The Amarillo Mountain front (gray) is part of the fold and thrust belt, which developed along the southern flank of the southern Oklahoma aulacogen. The Anadarko Basin (yellow) is the associated foreland basin (adapted from Perry, 1989). Contoured on depth to basement with a 3,050 m (10,000 ft) contour interval.

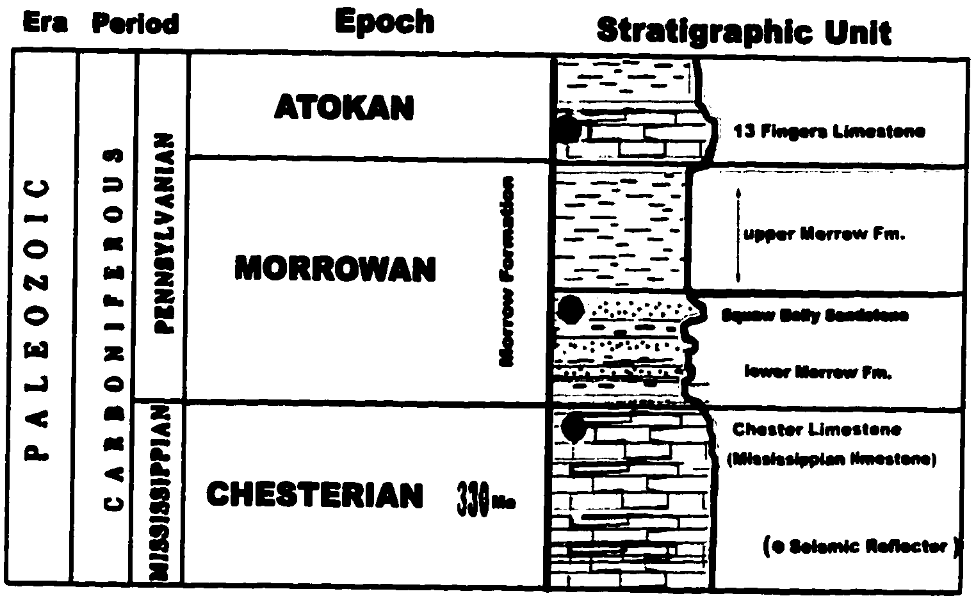

Figure 5. A generalized stratigraphic column of the Morrow Formation and encompassing units (Swanson, 1979). The dash pattern indicates shale, dotted pattern indicates sandstone, and the rectangular pattern indicates limestone. The large black dots represent major seismic reflectors.

Formation by a major unconformity. The lower Morrow Formation, composed of sandstone and shale, lies unconformably upon the Mississippian limestone. The top of the lower Morrow Formation is placed at the top of a prominent sandstone called the Squaw Belly Sandstone (Fig. 5). The upper Morrow Formation is predominantly shale with local sandstone deposits. The overlying Atokan Thirteen Fingers Limestone sequence consists of a series of thin limestone beds interbedded with shale. The top of the Morrow Formation is placed at the base of this limestone sequence.

The Thirteen Fingers Limestone, the Squaw Belly Sandstone, and the Mississippian limestone are major seismic reflectors within this area and provide excellent seismic horizons for correlation. The stratigraphic positions of these reflections are indicated by the black dots on the generalized stratigraphic column (Fig. 5).

Previous Work

Earlier studies of the upper Morrow Formation have been either very general, considering the basin as a whole, or very detailed, investigating specific oil fields. These studies are summarized briefly in chronological order. In the Texas Panhandle, the upper Morrow sandstones have been interpreted to be a part of a complex fluvial and deltaic system based upon paleontologic data, well cores, and well log analysis (Swanson, 1979). In a regional study, Moore (1979) also interpreted the upper Morrow sandstones to be fluvial and deltaic in origin. In the Oklahoma Panhandle, the sandstones were described as fluvial, estuary-mouth bar, marine-barrier bar, and shoreline deposits (Kasino and Davies, 1979). Swanson (1979) interpreted the upper Morrow Formation to be fluvial and deltaic within the western Anadarko Basin, and he has referred to this entire area as the Upper Morrow Deltaic Plain. In southeastern Colorado and southwestern Kansas the upper Morrow sandstones have been interpreted to represent fluvial, deltaic, and estuarine environments (Patterson, 1985; Miller and others, 1991). A generalized map of the paleogeography and paleoenvironments of the late Morrowan, as interpreted by Moore (1979), is shown in Figure 6. Figure 7 illustrates the proposed source areas of the Upper Morrow Deltaic Plain towards the northwest (Swanson, 1979).

Swanson (1979) presented several schematic diagrams (e.g., Fig. 8) representing the different depositional environments along the Upper Morrow Deltaic Plain from its source area to the sea. In his model, sediment was transported through meandering fluvial systems into a deltaic system, ending in distributary channels and associated facies. Figure 8 represents one moment in geologic time.

During the Carboniferous and Permian periods, the sea invaded onto and retreated from the cratonic shelf of North America more than fifty times (Ross and Ross, 1985). These eustatic sea level changes ranged from 100 to 200 m with a recurrence interval of 1.2 to 4.0 Ma (Ross and Ross, 1985), thereby being third-order, global, stratigraphic cycles as described by Miall (1990). Tectonic sea level changes associated with the development of a fold and thrust belt (the Amarillo Mountain front) with its resultant foreland basin (the Anadarko Basin), were superimposed upon the eustatic sea level changes, thus complicating interpretation of the mechanism of sea level change and the distribution of sedimentary facies throughout this period

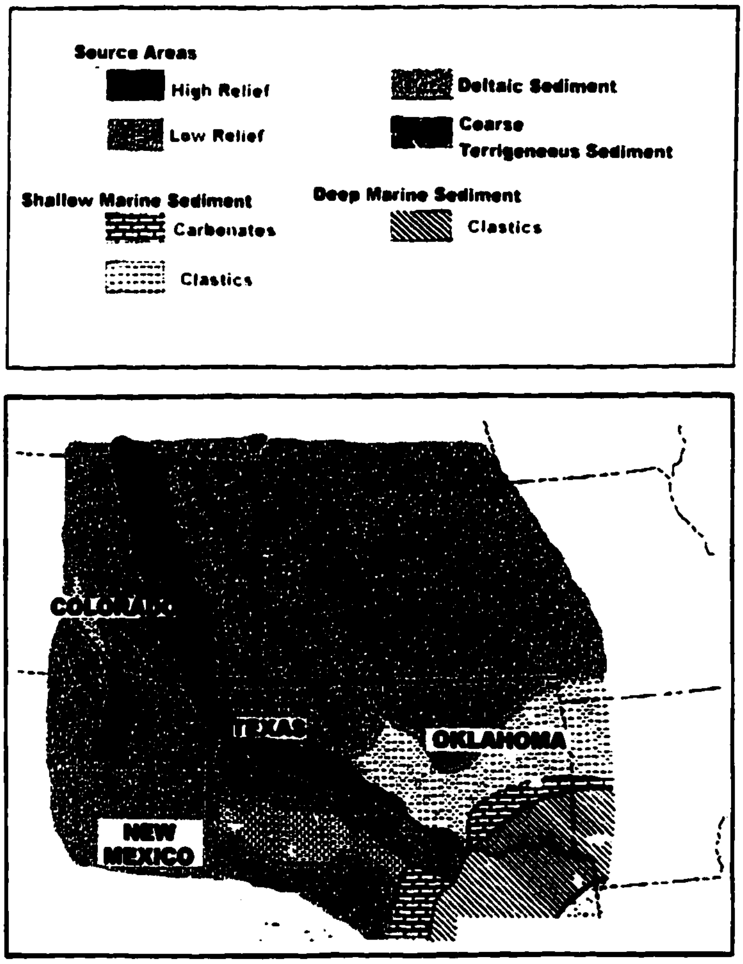

Figure 6. The generalized Morrowan paleogeography of the greater Anadarko Basin. The green represents the Upper Morrow Deltaic Plain. The pink and red represent the source areas of low and high relief, respectively (adapted from Moore, 1979).

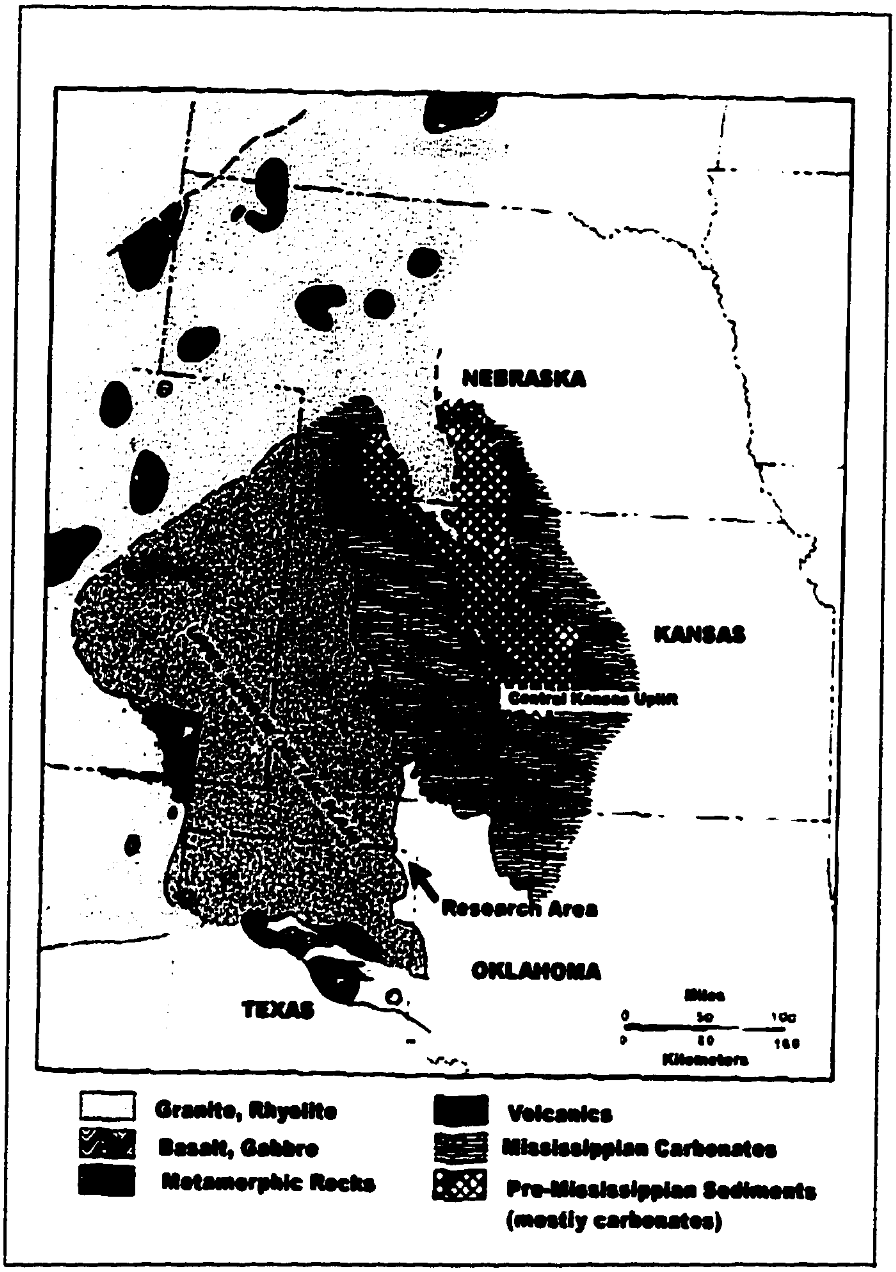

Figure 7. Late Morrowan source areas for sediment deposited in the greater Anadarko Basin. The source areas for the Upper Morrow Deltaic Plain (green) are highlighted above in red and pink (adapted from Swanson, 1979).

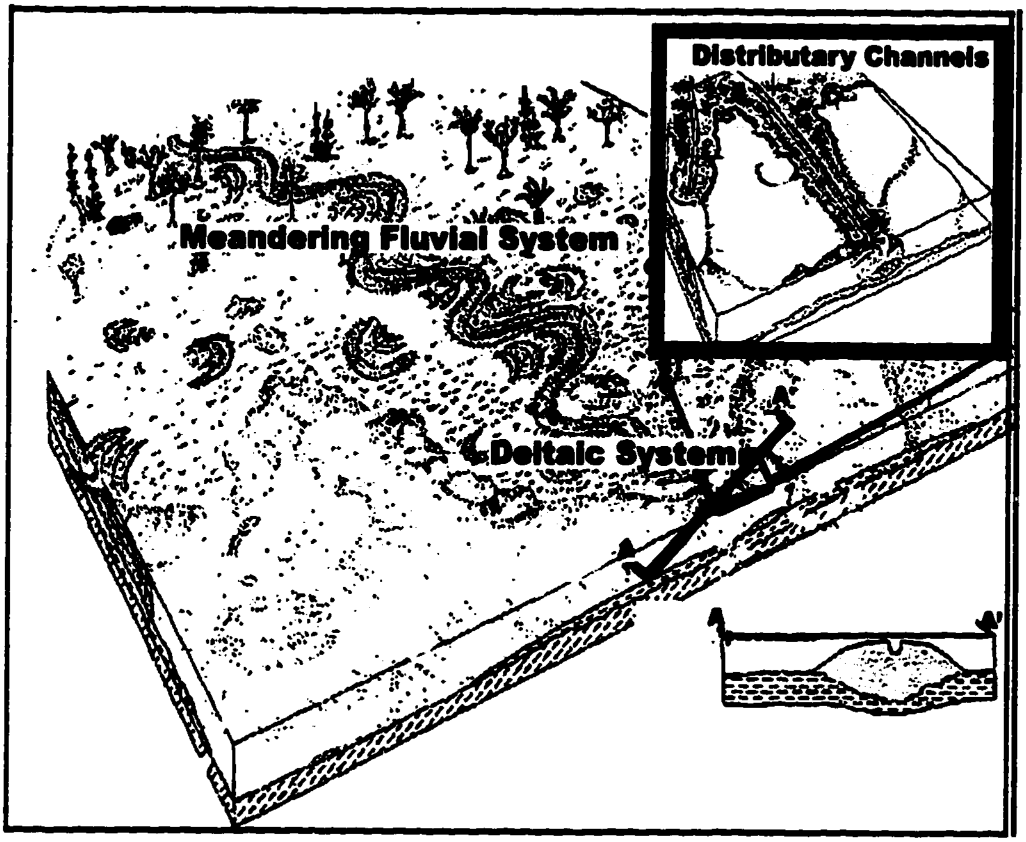

Figure 8. A block diagram of fluvial and deltaic systems. The diagram shows the distribution of sandstone in yellow. Cross-section A - A' bisects a distributary channel. An enlarged plan view of a distributary channel is shown within the red insert (adapted from several diagrams of Swanson, 1979).

of geologic time. The interdependent relationship between tectonic and eustatic sea level changes with the subsequent development of facies patterns within the upper Morrow Formation in the northeastern portion of the Texas Panhandle has not been discussed in detail previously.

METHODS

A key to the accurate interpretation of any seismic stratigraphic study is the procurement of higher quality seismic data than generally is needed for a structural seismic interpretation. The objective of seismic data acquisition and its processing is to obtain the highest dominant frequency and the widest bandwidth (range of frequencies) possible from the reflected seismic signal. Personal experience in the Texas Panhandle portion of the Anadarko Basin has shown that there are two major seismic problems: static corrections ("statics") and the attenuation of seismic energy.

Generally, static corrections are made to compensate for the effects of variations in surface elevation, the thickness and velocity of the weathered layer, and corrections to datum. Energy attenuation is the reduction of the amplitude and/or the complete loss of certain frequencies generated by the energy source. The higher frequencies are the first to be attenuated within the Earth, thereby reducing the bandwidth and often lowering the dominant frequency.

Acquisition and Processing of Reflection Seismic Data

Energy attenuation was a problem in the acquisition of the seismic data along the southern margin of the study area where surficial eolian sand was crossed by the seismic crew. In order to compensate for this problem, the fold, or the number of times the subsurface was sampled at each seismic trace within that specific area, was increased to 48 fold. As the fold was increased, the signal-to-noise ratio of the data also was increased, thereby reducing the effects of attenuation.

The seismic data used in this study were acquired ("shot") using the following acquisition parameters:

- Vibroseis energy source
- Sweep parameters:
  - 12-second sweep
  - 14 to 112 Hertz linear upsweep
- Recording parameters:
  - MDS-10 instrumentation
  - 96 channel
  - 12 to 125 Hertz recording filter
  - 15-second recording length
  - 2-millisecond sample rate
- Geophone group interval:
  - 110 ft (33 m)
  - 24 geophones per group
  - 5 ft (1.5 m) geophone spacing
- Shotpoint interval:
  - 220 ft (67 m)
  - near trace: 330 ft (100 m)
  - far trace: 5,550 ft (1,692 m)
- Fold: 24 (48 fold in eolian areas)

Accurate corrections for statics is a problem due to variations in thickness and lithology within the Ogalala Formation; the "Seeker" and "Vector Stat" programs (trademarks of Seisdata Services, Inc.) were used to make these corrections.

Spectral analysis of a processed seismic trace from the study area indicated a dominant frequency of 45 to 50 Hz with a two and one-half octave bandwidth (14 to 85 Hz). Personal experience has shown the above frequency content, which has a higher dominant frequency and wider bandwidth than the data previously shot in the Texas Panhandle, to be superior.

An Overview of Color Seismic Inversion Processing

In color seismic inversion processing the structural seismic data, the acquisition and processing parameters of which were discussed in the previous section, are the input for the inversion process, and the color-coded display of the seismic inversion section is the output. Seismic inversion processing is a type of inverse modeling, which involves the determination of a geologic model that could have given rise to the observed seismic effects (Sheriff, 1984). In general terms, seismic inversion is a process whereby seismic data are computed backwards in an effort to interpret the geology (lithology, geometry, thickness, etc.) that could have created them.

The seismic data used for this study were processed using the "Seislog" (trademark of Teknica, Inc., USA) seismic inversion algorithm. The algorithm quantifies the amplitudes of the seismic reflections and displays those amplitudes in terms of interval velocities. Analyzing interval velocities and correlating them with geologic data from wells can yield an indication of the relative thickness of a unit reflector in addition to its most probable lithology. Color seismic inversion sections are displayed in depth (as opposed to time as in a traditional structural seismic section) and interval velocity (as opposed to amplitude and polarity). This display facilitates the integration of the well log data with the seismic data and enhances the extraction of stratigraphic information from the seismic wavelet character.

A graphic representation of the seismic inversion process is shown in Figure 9. The seismic wavelet is first extracted from the seismic data, reflection coefficients are generated for each seismic trace, and a low-frequency model designed for a specific geologic area is then added. Finally, a pseudosonic log is generated by the inversion algorithm for each trace, and the velocities are color coded. These color-coded pseudosonic logs, derived from all of the input seismic traces, are displayed beside one another to form the color-coded seismic inversion section. Figure 10 is an example of an interpreted seismic inversion section.

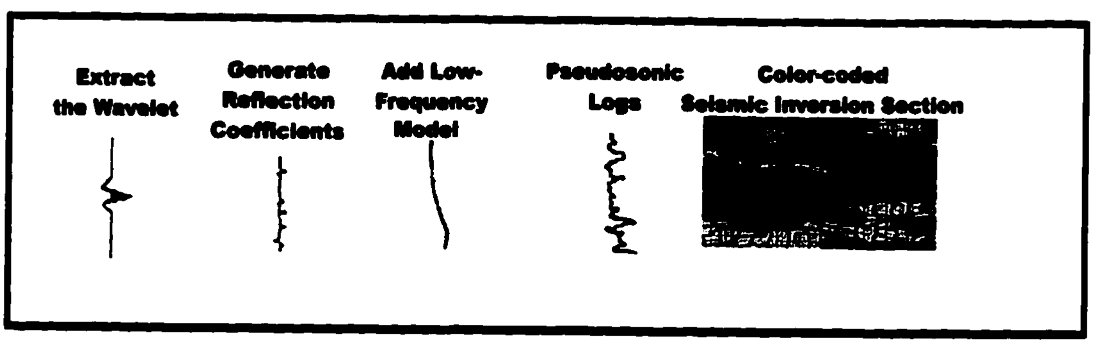

Figure 9. An overview of the seismic inversion process. First, the seismic wavelet is extracted from a representative seismic trace, reflection coefficients are calculated for each trace, and a two-dimensional low frequency model is added. Then, a pseudosonic log is generated by the inversion algorithm for each seismic trace, the interval velocities are color-coded and the pseudosonic logs are all displayed horizontally, resulting in a color seismic inversion section. The examples above are representative of each individual step, but are not individually correlative.

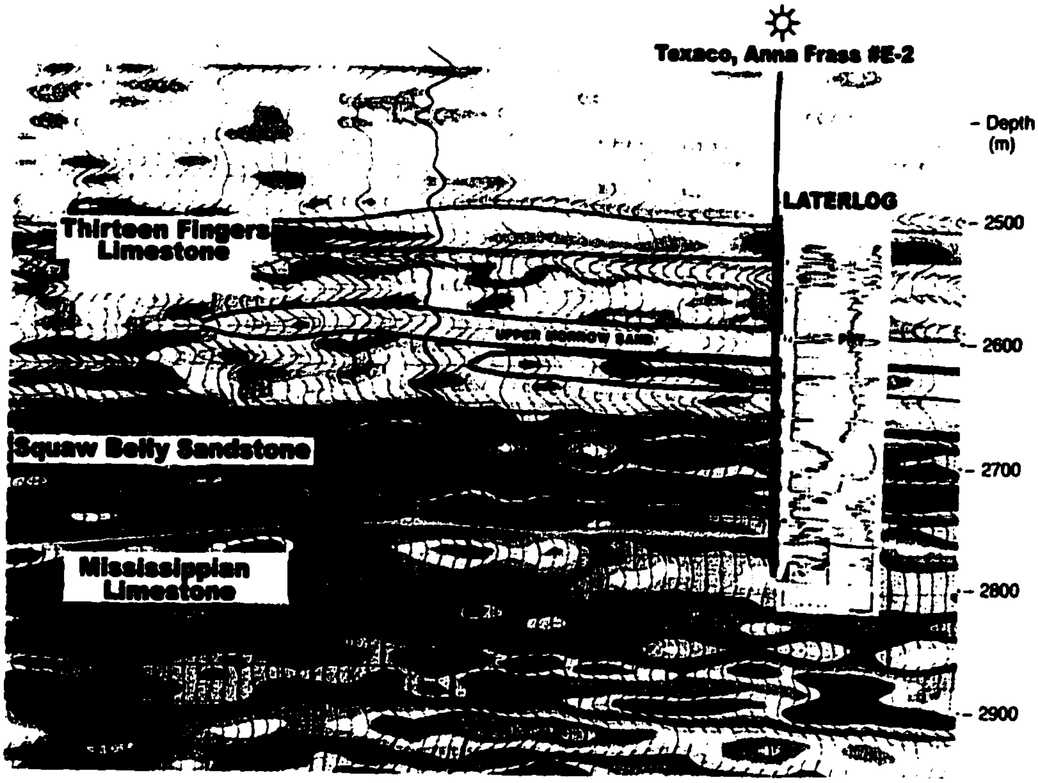

Figure 10. An example of a color-coded seismic inversion section. Interval velocities of the displayed section increase from 10,000 ft/sec (3.05 km/s) to 18,000 ft/sec (5.5 km/s) corresponding to colors grading from light greens, white, and yellows, through browns, reds, blues, and purples.

Seismic Anomalies

The ultimate goal of seismic inversion processing is the identification, interpretation, and mapping of seismic anomalies. For this study a seismic anomaly is considered any reflection within the upper Morrow Formation that has an interval velocity different from that of shale.

Sonic logs indicate that the interval velocity of shale within the study area is between ~10,500 ft/sec and ~11,750 ft/sec (3.21 - 3.59 km/s). This corresponds to 4^{th}- and 5^{th}-order green colors and white on the seismic inversion sections. The seismic inversion sections indicate that the interval velocity of the seismic anomalies within the study area is between ~11, 765 ft/sec and ~14, 266 ft/sec (3.59 km/s - 4.36 km/s). This corresponds to 1^{st}- and 2^{nd}-order yellow, and 1^{st}- through 4^{th}-order brown colors. Additionally, for these anomalies to be considered significant for this study, they must exceed more than approximately ten shotpoints in length, be coherent (acceptable signal to noise ratio), and be correlative across several seismic lines through "line ties", where two seismic lines cross, or "jump correlation," where adjacent seismic lines are correlated at points other than "line ties".

Correlation and Integration of Data Sets

An accurate identification of the stratigraphic position of the seismic anomalies within the upper Morrow Formation was crucial for accurate mapping and subsequent interpretations. Geologic data from wells and geophysical data from seismic inversion sections were interpreted, correlated, and integrated. A total of 360 km (225 miles) of seismic inversion data and logs from eighty wells were used for the interpretation of the geology of the study area.

From a geophysical viewpoint, it is important to note that the correlation of seismic inversion data differs from the correlation of structural reflection seismic data. A seismic inversion section simulates a sonic well log for each seismic trace. Therefore, as in interpretation of well logs, the inflection point above or below a lithologic unit is chosen ("picked") for correlative purposes. This is in contrast to the interpretation of structural reflection seismic sections where the peak or trough of an individual reflection is picked. However, the objective of both methods is the same, i.e., the identification of the boundary between units of differing lithology.

Four major regional reflections were identified on the seismic inversion sections and correlated with the well logs. These reflections originated from the base of the Desmoinesian, the top of the Atokan Thirteen Fingers Limestone, the top of the Morrowan Squaw Belly Sandstone, and the top of the Mississippian limestone. The top of the Atokan Thirteen Fingers Limestone and the top of the Squaw Belly Sandstone, the highest member of the lower Morrow Formation, were picked to bracket the zone of interest within the upper Morrow Formation. The base of the Desmoinesian and the top of the Mississippian limestone were also picked to help correlate in more difficult areas.

In addition to the correlation of reflections around the seismic grid via line ties, each individual seismic anomaly was jump correlated to the nearest parallel seismic line to insure the uniformity of the stratigraphic position for each anomaly.

Eighty well logs within a radius of one-half mile (800 m) from the seismic lines were interpreted, reduced to match the seismic inversion display scale, correlated with the inversion data, and physically spliced next to the nearest correlative shotpoint.

Seismic Interval Velocity Mapping

Once the seismic anomalies had been identified and their stratigraphic position determined by integration of the seismic inversion data with the well data, it became apparent that these seismic anomalies were concentrated at three stratigraphic positions within the upper Morrow Formation. Herein, these seismic horizons are informally referred to as the seismic horizon of the lower upper Morrow Formation, the seismic horizon of the middle upper Morrow Formation, and the seismic horizon of the upper upper Morrow Formation. The anomalies at each stratigraphic level were then mapped separately by contouring the interval velocities of the anomalies from each seismic horizon. Although the contouring is somewhat interpretive, the final mapped seismic horizon generally is similar to a geologic map based solely upon subsurface well control (Halverson, 1988). Figure 11 is an example of such a comparison from the Darden Field study.

Limitations on Seismic Data Interpretation

Envisioning seismic data as the exclusive response of rock interfaces reflecting seismic energy and nothing else can lead to serious pitfalls in interpretation. All imaging tools have limitations of resolution, problems of calibration, and interference from unwanted sources:

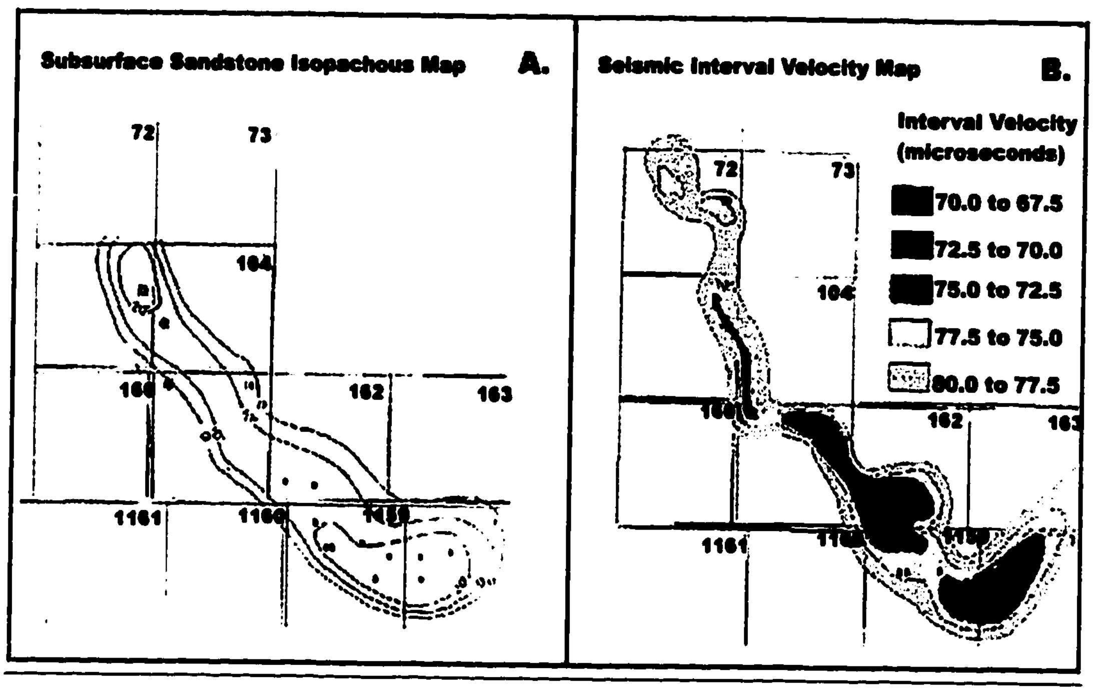

Figure 11. Comparison of maps utilizing different techniques. A subsurface isopach map of an upper Morrow sandstone in Darden field and the seismic interval velocity map of the same interval are shown in A and B, respectively; these maps demonstrate an approximate one-to-one correlation (adapted from Halverson, 1988). The contour interval on the isopach map is 10 ft (~3 m), 2.5 microseconds on the seismic interval velocity map.

noise. The most important factors limiting interpretation of the seismic data within the study area are tuning thickness, the effective Fresnel zone, seismic noise, thin-bed geometry, and wavelet interference.

The Tuning Thickness Concept

The tuning thickness of a lithologic unit is that thickness at which the reflection from the top of the reflector and that from the bottom of the reflector have maximum constructive interference. Consequently, the reflector yields its maximum reflection amplitude at the tuning thickness or tuning point (Neidel and Poggiagliolmi, 1977). As the lithologic unit becomes thicker than the tuning thickness, the wavelet shape changes and becomes two separate reflections because the wavelets from the top and bottom of the unit reflector interfere destructively. Once completely separated, these two reflections correlate with the top and the bottom of the reflector. Below the tuning point, or for thicknesses less than the tuning thickness, the wavelet amplitude decreases as a linear function of unit thickness (Fig. 12).

Geophysical modeling of thin sandstone units within the study area indicates that the maximum tuning thickness is approximately 30 m (Halverson, 1988). Thus, in theory two sandstone units separated by less than 30 m (100 ft) of shale should appear as one seismic reflection or seismic anomaly, with the amplitude of the reflection being a function of cumulative sandstone thickness.

Theoretically, the actual thickness of a thin lithologic unit can be determined by analyzing the reflection amplitude generated from below the tuning point. In practice, changes in the frequency and noise content of the seismic data, lateral variations of interval velocities within the reflector, and the averaging effects of the surface area causing the reflection, make amplitude analysis an indication of relative, rather than absolute, thickness.

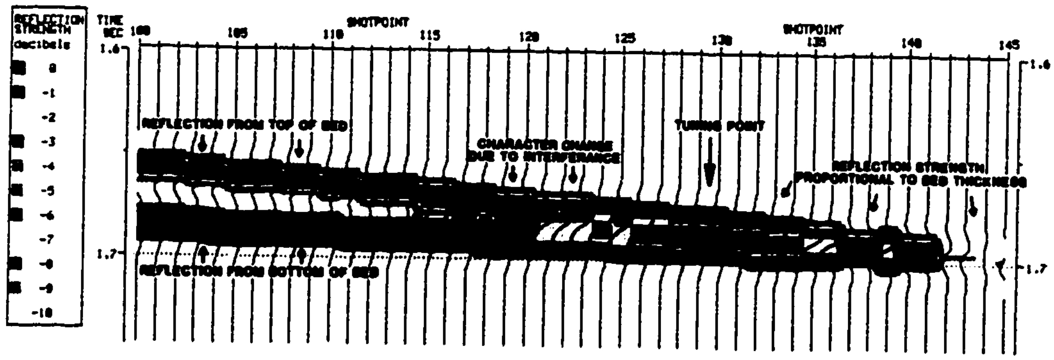

Figure 12. Tuning thickness model. The tuning point of a reflector is the point of maximum constructive interference, which creates the maximum reflection amplitude. The thinner the reflector, below the tuning point, the smaller the reflection amplitude (adapted from Halverson, 1988).

The Effective Fresnel Zone

A seismic reflection received at any given shotpoint from any given reflector actually comes from a circular area upon the reflector's surface instead of the commonly illustrated raypath from a point source upon the reflector. This circular area, called the Fresnel zone, is where reflected energy interferes constructively with itself and is the area primarily responsible for the generation of the reflection (Fig. 13A). A nomogram (Fig. 13B) was used to determine the Fresnel-zone radius for seismic horizons within the upper Morrow Formation in the study area. When calculated using the following parameters, a 2-way travel time of 1.55 seconds, a dominant frequency of 50 Hz., and an average velocity to the reflector of 11,300 ft/s (3.445 km/s), the Fresnel-zone radius is approximately 300 m (1000 ft). There is debate among exploration geophysicists as to what fraction of the Fresnel-zone radius is the dominant reflecting surface, or the effective Fresnel-zone. Generally, the effective Fresnel zone is calculated using ¼ to ½ of the seismic wavelet (Fig. 13A). Therefore, within the research area, the effective Fresnel zone has a radius up to 300 m.

The importance of the effective Fresnel zone is that it affects the seismic tool's resolution; it represents the smallest feature that can be areally imaged in the sub-surface.

Seismic Noise

Noise within the seismic signal can complicate the interpretation of the seismic data by masking true reflections and seismic anomalies. An example of minor seismic noise is shown on Figure 14. On this figure, 2nd-order yellow and 1st -order brown interval velocities that extend for less than approximately 10 shotpoints are most likely caused by noise within the seismic data. Figure 15 is an example of major noise content within a seismic section.

Thin-bed Geometry and Limitations of Resolution

An accurate interpretation of the geology of an area using reflection seismic data relies upon the understanding of the limitations of imaging with the seismic tool, with resolution being a key limitation of this tool. The term "resolution" is defined as "the minimum separation of two bodies before their individual identities are lost " (Sheriff, 1984). The horizontal

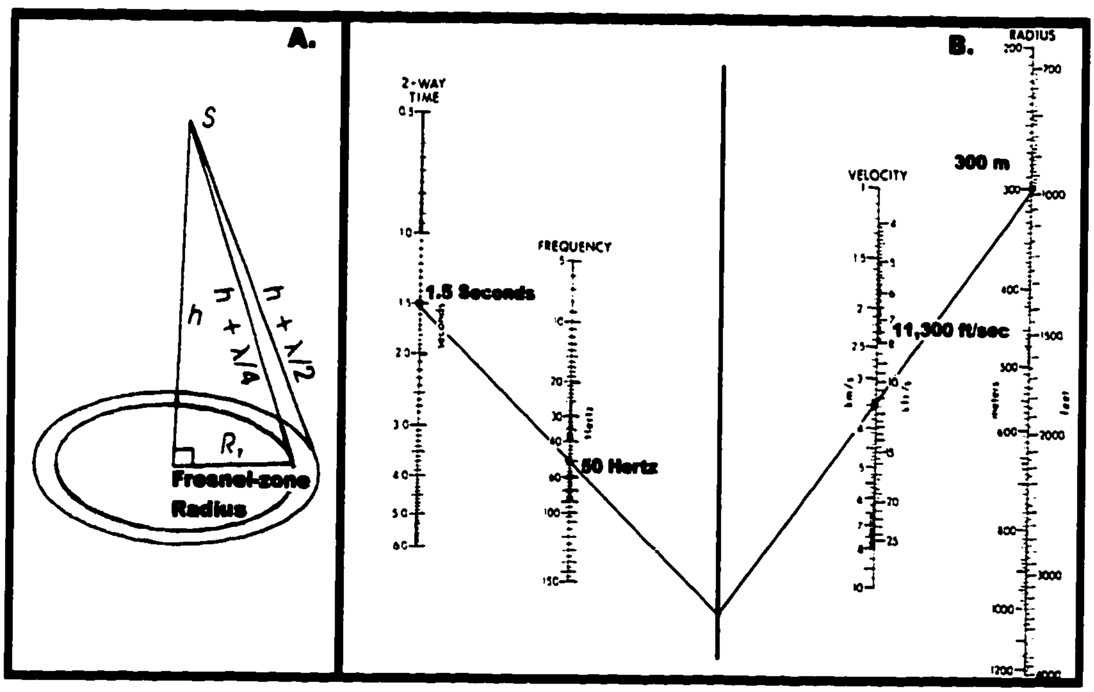

Figure 13. The Fresnel-zone radius (A) and a nomogram (B) used for its calculation. The effective Fresnel zone calculated for seismic horizons within the upper Morrow Formation in the study area is a circle with a radius of 300 m (modified from Sheriff, 1984).

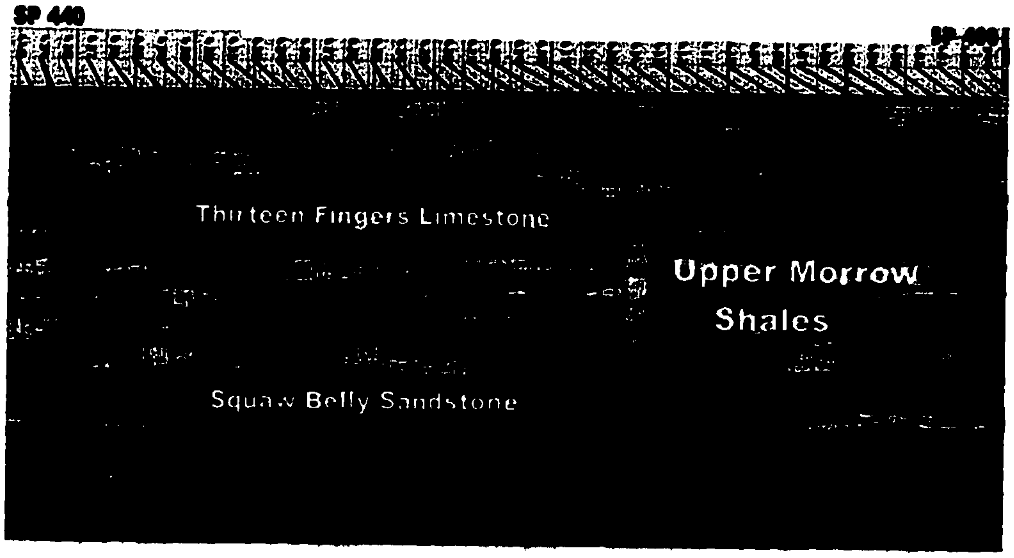

Figure 14. Minor seismic noise in a seismic inversion section superimposed upon the seismic response of a part of the upper Morrow Formation known to be shale based on well log data; a portion of Seismic Line 2 between SP 400 - 440. The yellow and brown colors that extend for less than approximately 10 shotpoints on this section are interpreted to be caused by minor noise within the seismic data because of their lack of continuity.

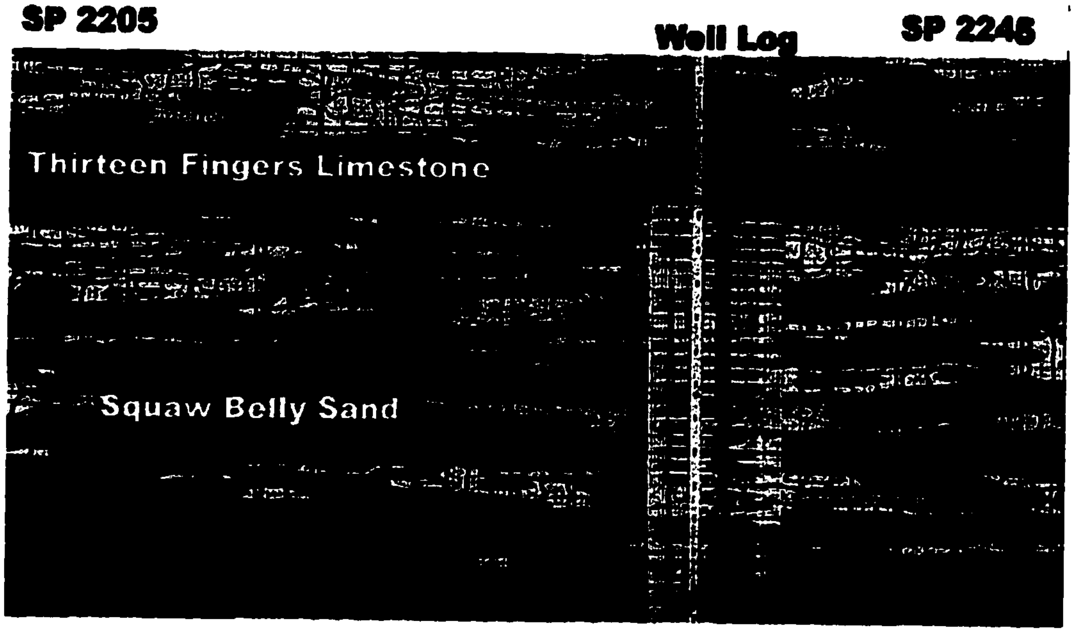

Figure 15. Major seismic noise content superimposed upon the seismic response of shale; a portion of Seismic Line 4 between SP 2205 - 2245. The well log indicates that the interval between the Thirteen Fingers Limestone and the Squaw Belly Sandstone is entirely shale. Geophysical modeling indicates that the spatially limited and randomly scattered reflections, the interval velocities of which are greater than those for shale (yellow and brown interval velocity colors), probably are relics from the computer processing of noise.

resolution of a seismic inversion section is limited by the line spacing of the seismic grid and the effective Fresnel zone for that specific area. The vertical resolution is limited by the dominant frequency and total bandwidth (range of frequencies) of the seismic data. These are real, physical contraints upon the ability of the seismic tool to detect and quantify the areal extent and relative thickness of a lithologic unit.

An additional complication of vertical resolution, particularly in this study area, is the response of the seismic wavelet to different geometries of thin sandstone units. Geophysical modeling of different sandstone and shale thicknesses and their geometries below the tuning point has been published by Anstey (1980). His work has shown that, irrespective of the geometry, the amplitude of the seismic reflection is directly proportional to the cumulative thickness of all the sandstone units (Fig. 16).

Because the tuning thickness within the study area is approximately 30 m (100 ft) for the Morrow Formation, two sandstone units separated by less than 30 m will appear as one seismic reflection. The sandstone units within upper Morrow Formation are spaced vertically closer than 30 m, thus limiting the vertical resolution of the seismic data. A well (NE ¼ of Section 1147, Block 43, H. & T. C. Survey), which ties Seismic Line 1 at SP 305, illustrates the limitation of vertical resolution. The well logs show two sandstone units separated vertically by 20 ft (6 m) of shale with a cumulative sandstone thickness of ~20 ft (Fig. 17). The resultant wavelet from this vertical distribution of sandstone is a single reflection (seismic anomaly) instead of two reflections. Consequently, the two closely spaced but vertically isolated sandstone units appear as if they were one sandstone unit.

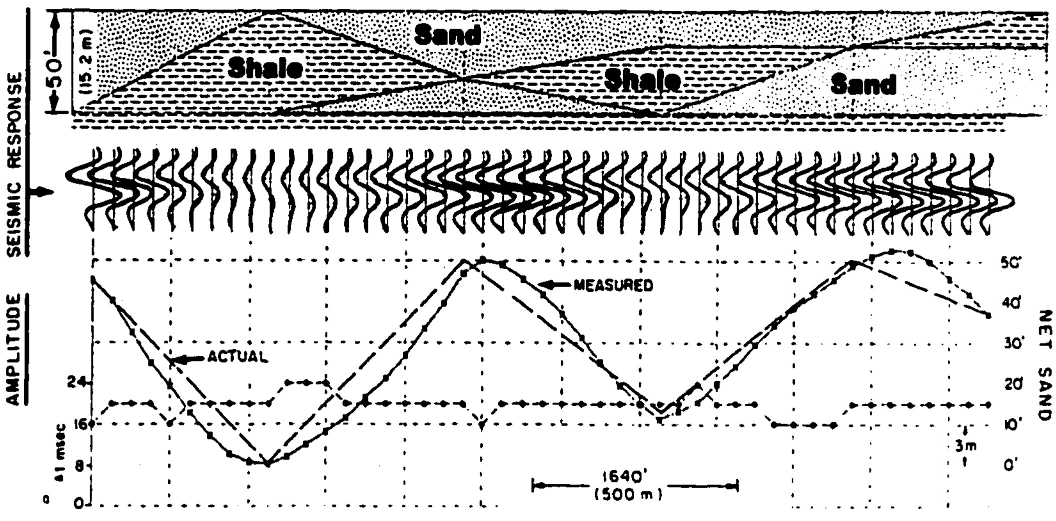

Figure 16. Geophysical modeling of different sandstone and shale geometries. The single seismic reflection shown in the figure above is the seismic response from the cumulative thickness of the sandstone units, the thicknesses of which are below the tuning point. As the model demonstrates, sandstone geometry has no effect upon the amplitude of the reflection nor upon the wavelet character. It is the cumulative sand thickness that affects the wavelet amplitude (modified from Anstey, 1980).

SP 305 SP 275

Figure 17. An example of the problem caused by thin-bed geometry; a portion of Seismic Line 1 between SP 305 - 275. A single seismic reflection, which is the resultant wavelet generated by the two sandstone units shown in the well log, is due to the tuning thickness effect.

Discrepancy between Well Logs and Mapped Interval Velocities

Apparent discrepancies between the cumulative sandstone thicknesses from wells and their seismically interpreted thicknesses can be a problem within the study area. An example is shown by two wells that tie Seismic Line 1 (Fig. 18). The first well, which ties Seismic Line 1 at SP 305 (NW ¼ of Section 1146), has two sandstone units with a cumulative thickness of ~20 ft (6 m) separated vertically by 20 ft (6 m) of clay based upon information from well logs. The second well ties Seismic Line 1 at SP 410 (SW ¼, NE ¼ of Section 1059). This well has two sandstone units with a cumulative sandstone thickness of 25 ft (8 m) separated vertically by 50 ft (15 m) of rock suggested to be clay by the gamma ray log, but with sand or silt contamination as suggested by the resistivity log (Hilchie, 1978). The well logs and their seismic responses from the first and second wells are shown in Figures 19 and 20, respectively.

The sandstone units in both wells generate a single reflection; however, the sandstone in the second well has produced a greater interval velocity than the first well. The interval velocity should appear faster in the second well, which has a greater cumulative sandstone thickness than the first well, but the interval velocity difference between the two sandstone sequences in the two wells is too great for a thickness differential of only 5 feet.

An explanation for this interval velocity discrepancy apparently is the presence of clayey siltstone under both sandstone units in the second well that adds to the cumulative thickness of the non-shale units (see well log in Fig. 20). This increased thickness evidently increases the amplitude of the seismic reflection and consequently increases the observed

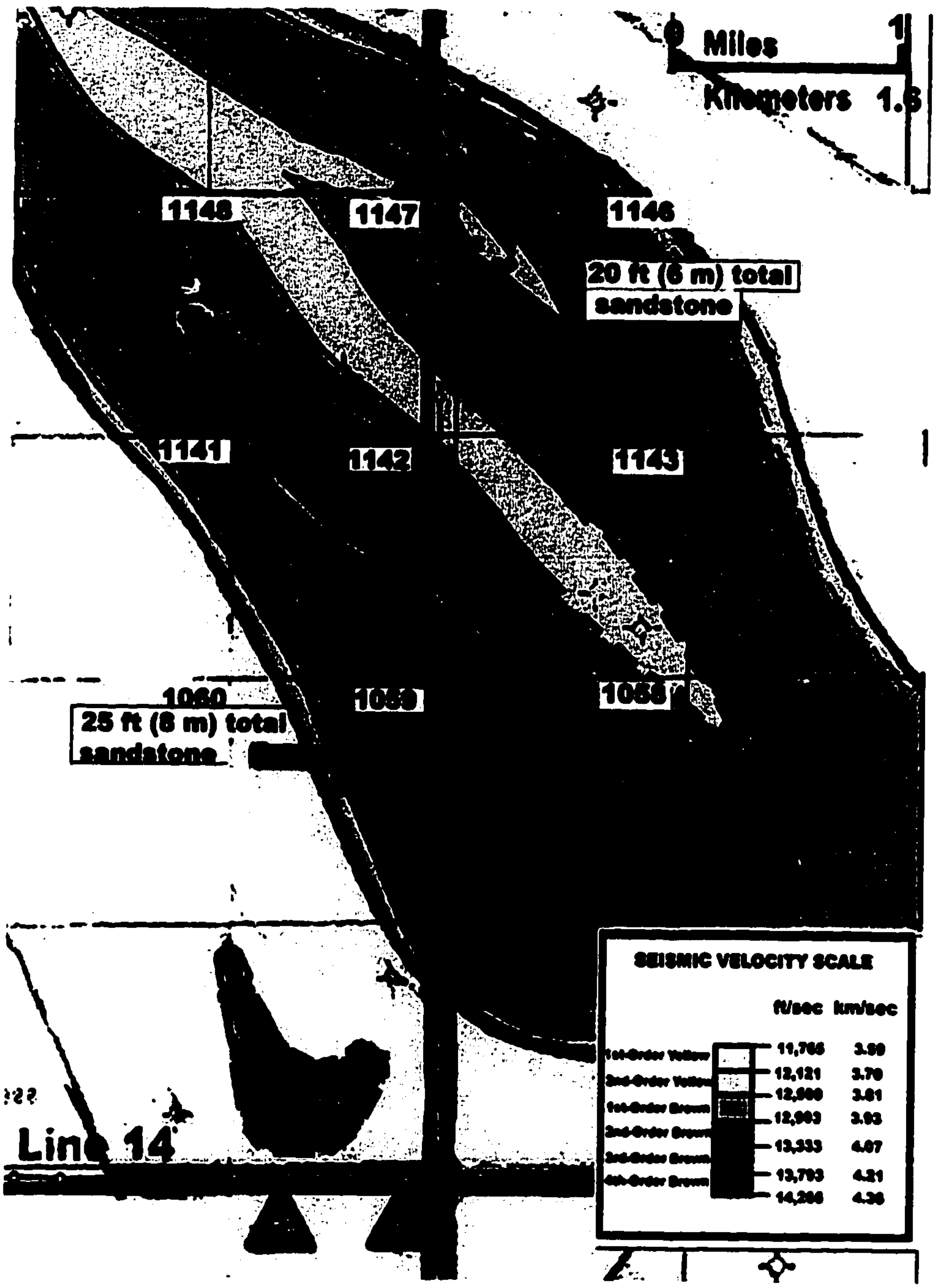

Figure 18. A discrepancy between interval velocities and well-log thickness. The sandstone thickness in the two wells indicated by arrows is similar but seismic-interval velocities suggest greatly differing thicknesses.

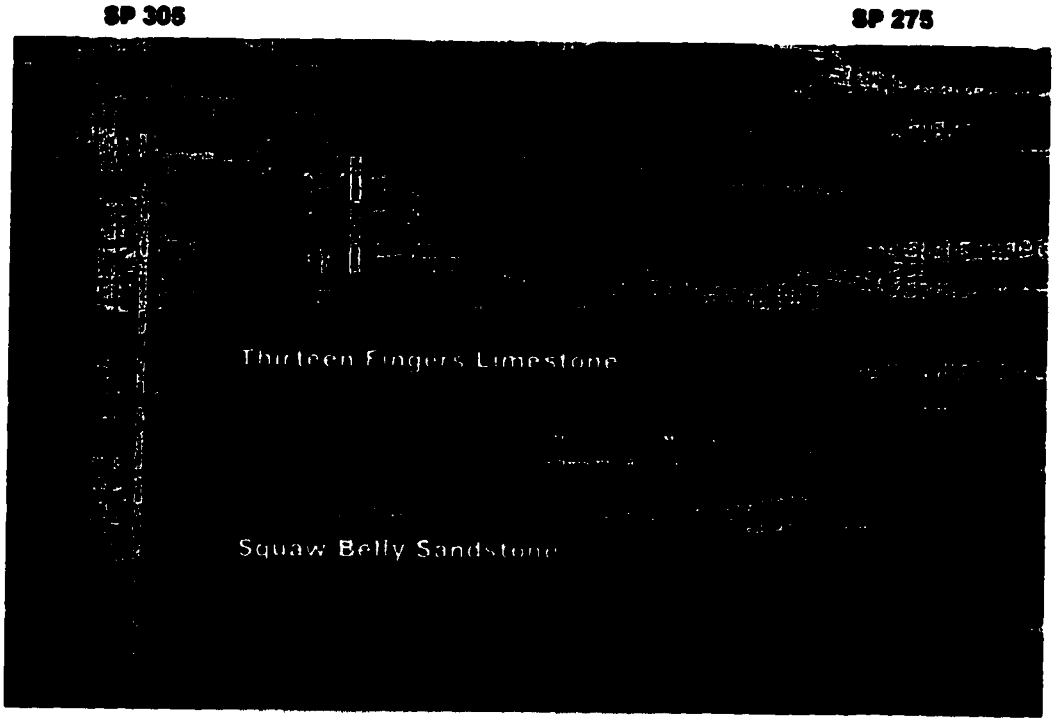

Figure 19. The seismic response to a cumulative sandstone thickness of 20 ft, Seismic Line 1, SP 270 - 310. The well log ties the seismic line at SP 305 and is located in the NW ¼ of Section 1146 (see Fig. 18).

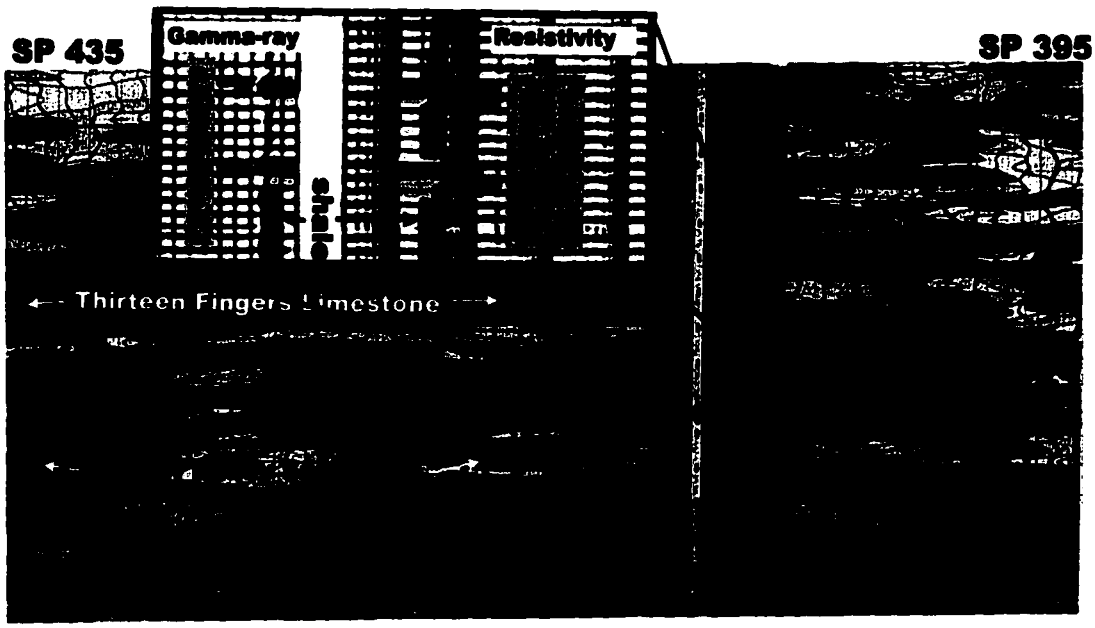

Figure 20. The seismic response to a cumulative sandstone thickness of 25 ft; Seismic Line 1, SP 395 - 435. The well log ties the seismic line at SP 410 (SW ¼, NE ¼ of Section 1059). The log interpretation of additional clayey siltstone (shaley siltstone) increases the cumulative thickness of the reflector to ~40 ft.

interval velocity as calculated by the inversion algorithm. The above scenario yields a more reasonable cumulative thickness differential between the two wells and better accounts for the magnitude of their interval velocity differential. Thus, the seismic tool may detect, as sandstone, an entire depositional unit consisting of sandstone, siltstone, and clayey siltstone rather than just the clean sandstone.

Non-uniqueness: The Thirteen Fingers Limestone Sequence

Non-uniqueness in seismic stratigraphic interpretations means that two or more different geologic scenarios can generate identical seismic responses. Such a situation exists within the study area. An anomalous thickening of the Thirteen Fingers Limestone sequence in the southern part of the study area generates seismic anomalies similar to, and easily mistaken for, upper upper Morrow Formation sandstone anomalies. This happens when the Thirteen Fingers Limestone sequence becomes thicker than its tuning thickness. The thickness of the Thirteen Fingers Limestone sequence near SP 850 on Seismic Line 1 is ~120 ft (36 m), and it generates one reflection (Fig. 21); it then thickens to ~200 ft (55 m) near SP 1250, approximately 10 miles to the south, where it generates two separate and distinct reflections (Fig. 22). Thus, as the limestone sequence thickens and exceeds its tuning point, it generates two reflections. The lower reflection, or the reflection from the base of the limestone sequence, is close to the position where a seismic anomaly from the upper upper Morrow Formation might be expected and could easily be mistaken for such an anomaly. The correct assignment of this seismic anomaly can be made by tracing anomalies from areas where the assignment is certain into areas of uncertainty.

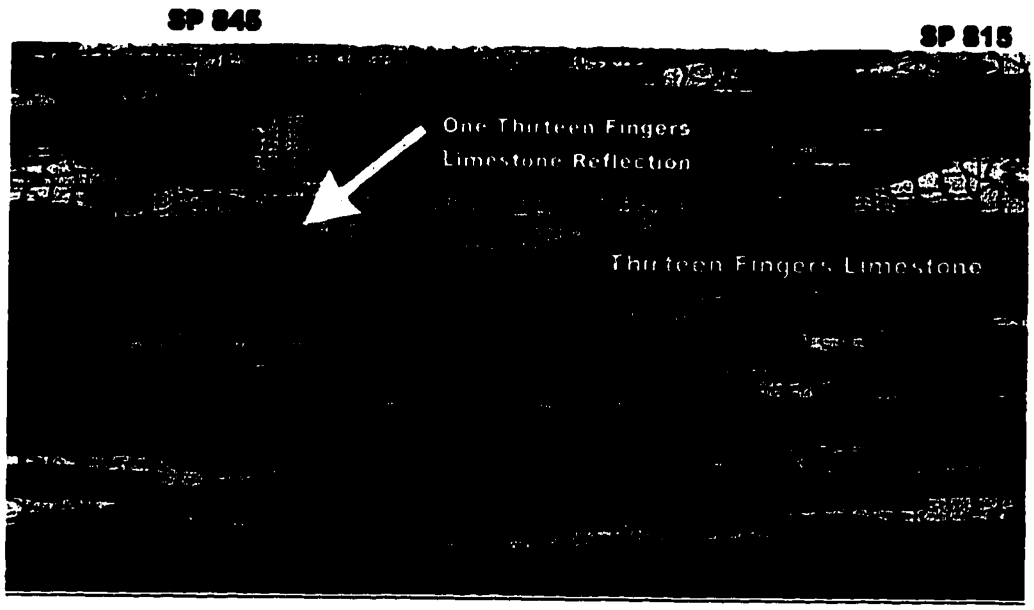

Figure 21. The seismic expression of the Thirteen Fingers Limestone sequence; Seismic Line 1 between SP 815 and SP 845. The Thirteen Fingers Limestone sequence, which is above the red line, is approximately 120 ft (36 m) thick in this area and generates one seismic reflection.

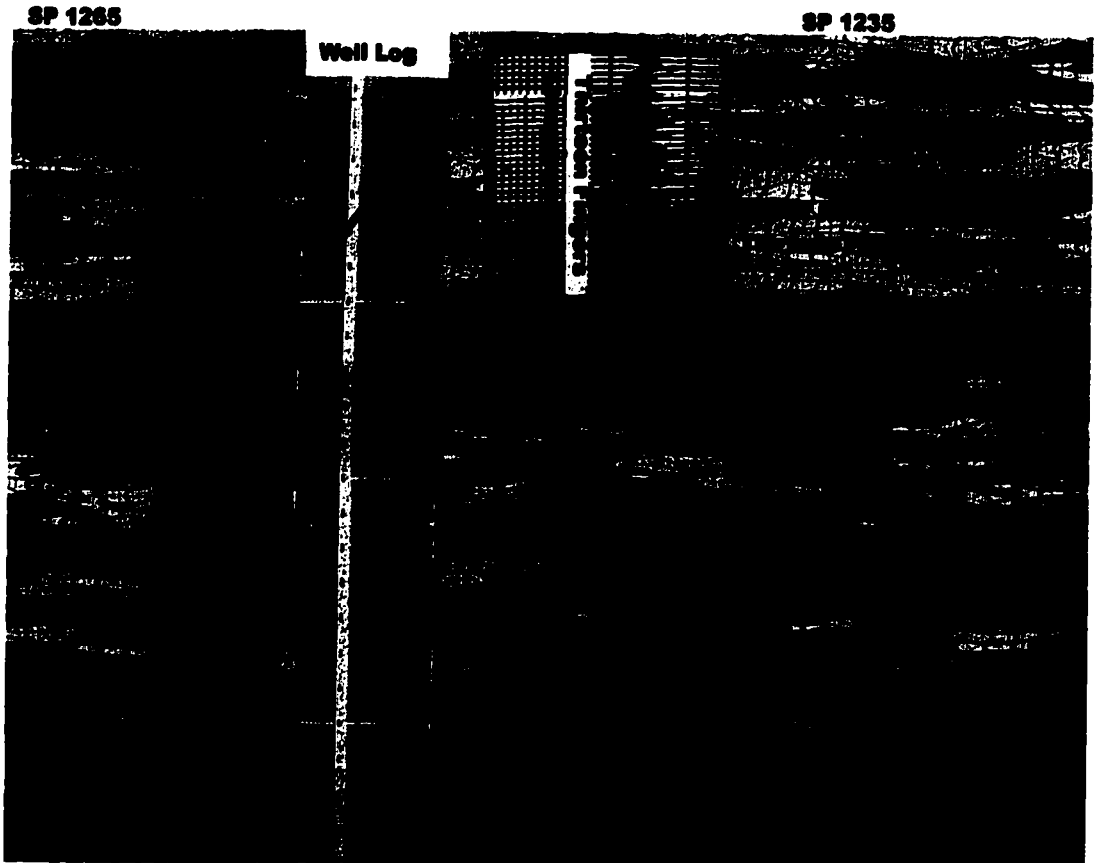

Figure 22. Two Thirteen Fingers Limestone reflections; A portion of Seismic Line 1 between shotpoints 1225 and 1265. In this area, the Thirteen Fingers limestone sequence thickens from 120 ft to over 200 ft (35 m to 70 m). Where the thickness of the sequence exceeds its tuning thickness the reflection separates into two separate reflectors.

LITHOLOGIC DETERMINATION OF SEISMIC ANOMALIES

The ultimate goal of acquiring and processing seismic data is to obtain data of the highest possible quality from which one can make the most accurate geologic interpretations. This is especially true for seismic stratigraphic interpretations. From the seismic data, the nature of seismic anomalies is interpreted after taking into account the effects of noise, geometry of the lithologic units, seismic resolution, tuning thickness, wavelet interference, non-uniqueness of the interpretations, and the size of the Fresnel zone. The probable lithology of each anomaly is then determined by comparison of its range of interval velocities with that of lithologies interpreted from well logs that penetrated these or similar anomalies. The seismic response to units within this study area are interpreted to correspond to three different lithologies: shale, sandstone, and clayey siltstone.

Shale is the predominant lithology within the 100-m- to 200-m-thick upper Morrow Formation, which separates the Atokan Thirteen Fingers Limestone sequence from the Squaw Belly Sandstone. Sonic logs indicate that the interval velocities of the shale range from ~10,500 ft/sec to ~11,750 ft/sec (3.21 - 3.59 km/s). This velocity range corresponds to white and 4^{th}- and 5^{th}-order green interval velocity colors on the seismic inversion sections. The seismic expression of shale is shown in Figure 23.

The seismic expression of an interpreted sandstone anomaly in the lower upper Morrow Formation is shown in Figure 24. The interval velocities of sandstone anomalies from the seismic inversion sections range from 2nd-order yellow through 4th-order brown interval velocity colors, with an average maximum interval velocity in the 2nd- and 3rd-order brown colors (12,900 to 13,500 ft/sec or 3.93 to 4.12 km/s).

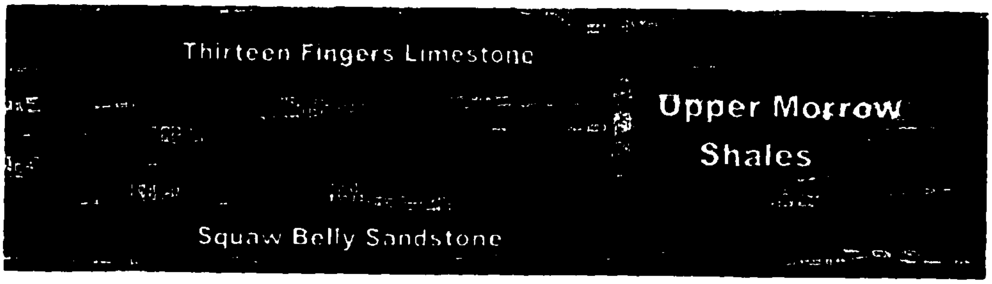

Figure 23. Seismic expression of shale in the upper Morrow Formation; Seismic Line 2, SP 400 - SP 440. The shale is characterized by the greens and white interval velocity colors; the incoherent and randomly scattered reflections of yellow and brown interval velocity colors are caused by seismic noise.

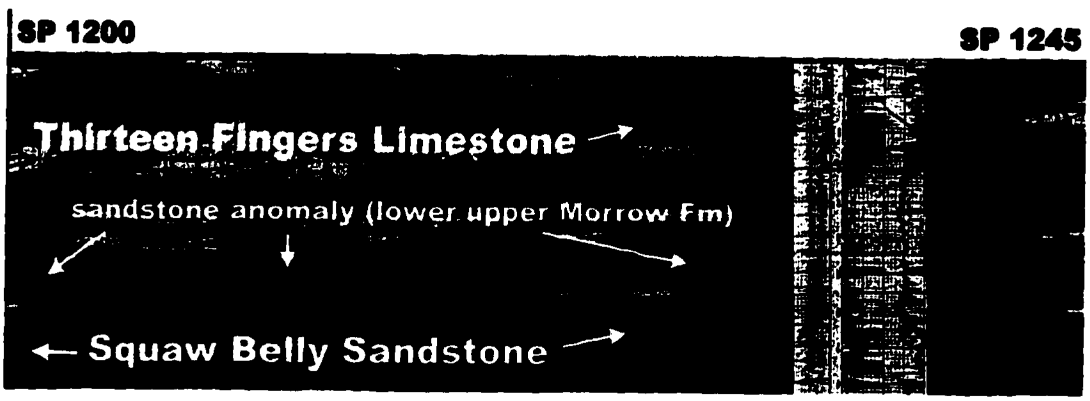

Figure 24. Seismic expression of an upper Morrow sandstone; Seismic Line 5, SP 1200 - SP 1245. The sandstone anomaly is characterized by the yellow and brown interval velocity colors.

Anomalies interpreted as clayey siltstone are characterized by poorly coherent reflections of 1st - and 2nd -order yellow interval velocity colors that extend laterally from sandstone anomalies of the middle upper Morrow Formation seismic horizon (Fig. 25). The apparent thickness determined from the seismic inversion sections indicates that the clayey siltstone anomalies appear to be vertically thicker (~ 50 m to ~75 m on Seismic Line 5) than the laterally adjacent sandstone anomalies (~ 25 m on Seismic Line 5). This is due to differences in the frequency content of the reflected seismic signal from the two different anomalies; the higher frequencies are preferentially attenuated in the reflected signal from the clayey siltstones, so the algorithm produces a greater apparent thickness for that lithology.

Hilchie (1978) described the log characteristics of shaly sandstone (herein referred to as clayey siltstone) as having a gamma ray curve that reads "hot," as it would in shale, but also having a residual response on resistivity measurements that indicates the presence of sand. Informally, these log characteristics commonly are inferred to indicate a "trace sand" in the Texas Panhandle. The seismic expression of a clayey siltstone anomaly is shown on Seismic Line 5 between shotpoints 1025 and 1065 (Fig. 25).

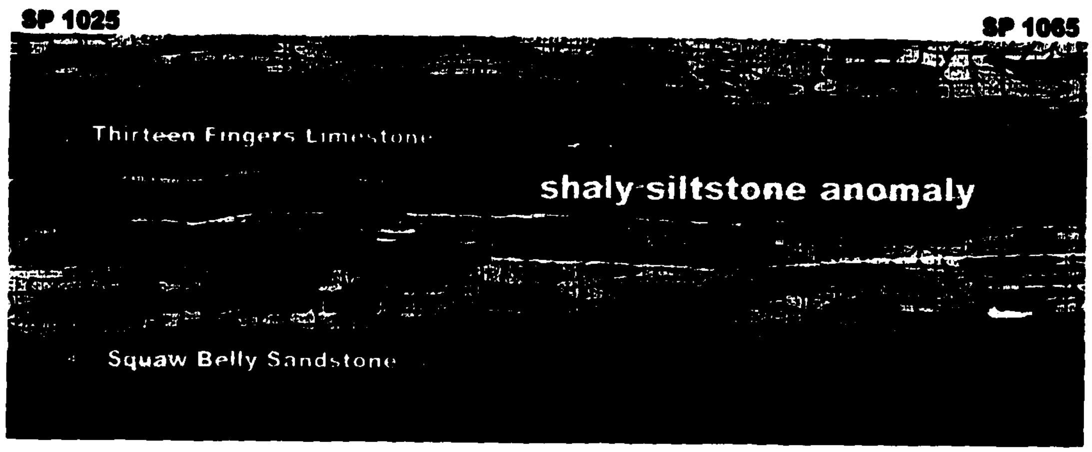

Figure 25. The seismic expression of an interpreted clayey siltstone anomaly ("shaly" siltstone); Seismic Line 5 between SP 1025 and SP 1065.

INTERPRETATION OF DEPOSITIONAL ENVIRONMENTS

The three seismic horizons of the upper Morrow Formation were studied separately and their depositional environments interpreted independently. The interpretations of the environment of deposition are based upon two primary lines of evidence. One is the shape of the well log curves that are characteristic of, but not limited to, specific sandstone environments (Hilchie, 1978). The second is the geomorphic shape of the mapped seismic anomalies.

The maps were generated by contouring interval velocities for each of the seismic horizons. As the contouring proceeded, the seismic line density itself constrained the contoured picture in areas of higher seismic line density, but left areas of lower seismic line density open to a variety of contouring possibilities. Comparing the contoured pattern in the areas of higher density, where the contouring was more constrained, with models that are geologically reasonable, a geologic picture began to form. The contouring within areas of lower seismic line density was open to a variety of contouring possibilities, but the possible geologic models derived from areas of higher density placed constraints upon the contouring within those areas. In this way, the mapped seismic horizon began to take on geologic significance and shape. This was an iterative process whereby the raw seismic data, geologic models, and the contoured map evolved concurrently into a congruent picture.

The Seismic Horizon of the Lower Upper Morrow Formation

The map of the seismic horizon of the lower upper Morrow Formation is presented on Plate I, and is shown in reduced form on Figure 26. While plotting the seismic anomalies on the seismic base map prior to contouring, it became apparent that there was one major trend in the northwest, which is seen on Seismic Lines 7, 27, and the western third of Line14. This trend is divided into five smaller branches towards the southeast, which is farther towards the depocenter of the basin, as seen on Lines 23, 3, 25, 5, and the eastern two thirds of Line 14. The anomalies show a splaying pattern towards the southeast, which abruptly terminates north of Line 2 and east of Line 1. The interval velocity data were first contoured in an area of greater seismic line density where Seismic Lines 27, 5, and 25 tie Seismic Line 14. The contouring within this area of greater seismic line density formed the core pattern of the basinward splaying. This splaying pattern was used as the contouring model for areas of lesser seismic line density, and the "bird's foot" geometry seen on Figure 26 was subsequently formed. A "bird's foot" geometry of sandstone is characteristic of deltaic distributary channel systems (Coleman and Prior, 1982).

Well log analysis from wells that penetrate the anomaly tend to confirm this interpretation. The well log shown in Figure 27, correlated to Seismic Line 27, demonstrates the characteristic inverted bell-shaped curves of a distributary channel (Swanson, 1979), and the well log correlated to Seismic Line 5 (Fig. 28) shows the bell-shaped curves characteristic of a point bar sequence. A point bar sequence is more common in a meandering fluvial system than in a deltaic distributary channel system (Swanson, 1979), and the seismic wavelet character alone can not differentiate between them. However, the inverted bell-shaped curves of the well tied to Seismic Line 27 and especially the overall geomorphic expression ("bird's foot") favor a deltaic distributary channel system interpretation for the entire depositional environment.

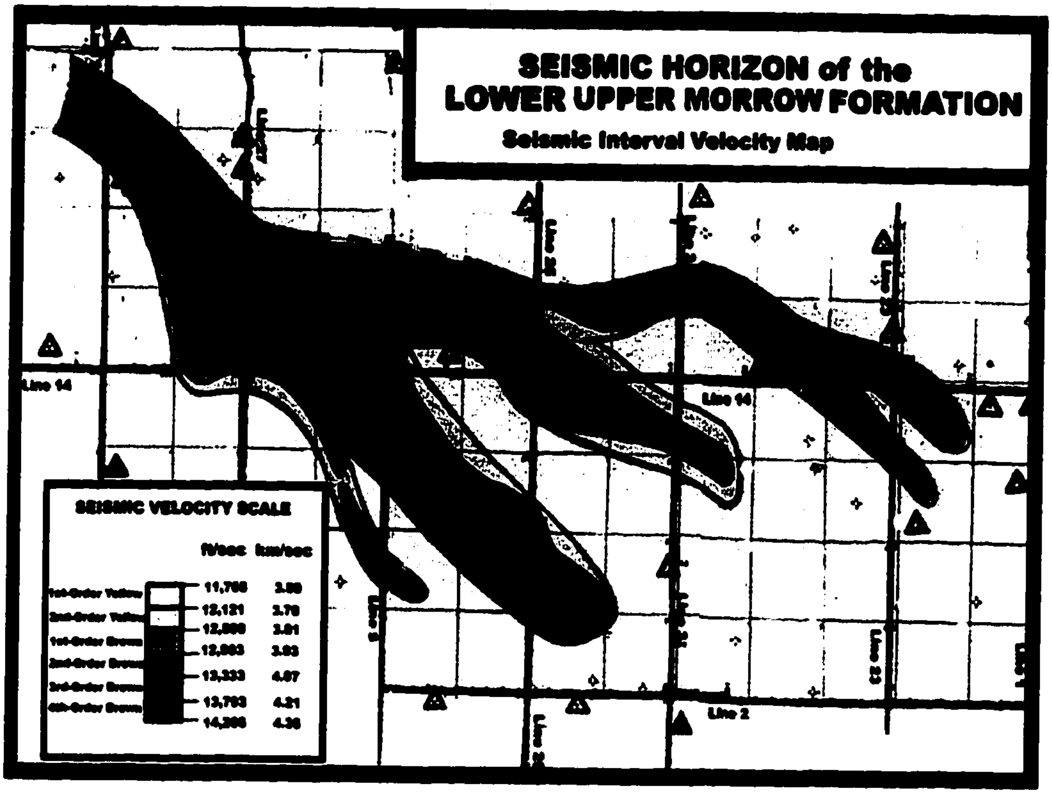

Figure 26. The mapped interval velocities of the seismic horizon of the lower upper Morrow Formation. The "bird's foot" geometry is suggestive of a deltaic distributary channel system. Seismic lines are highlighted in blue; wells tied to the seismic data are indicated by the red triangles.

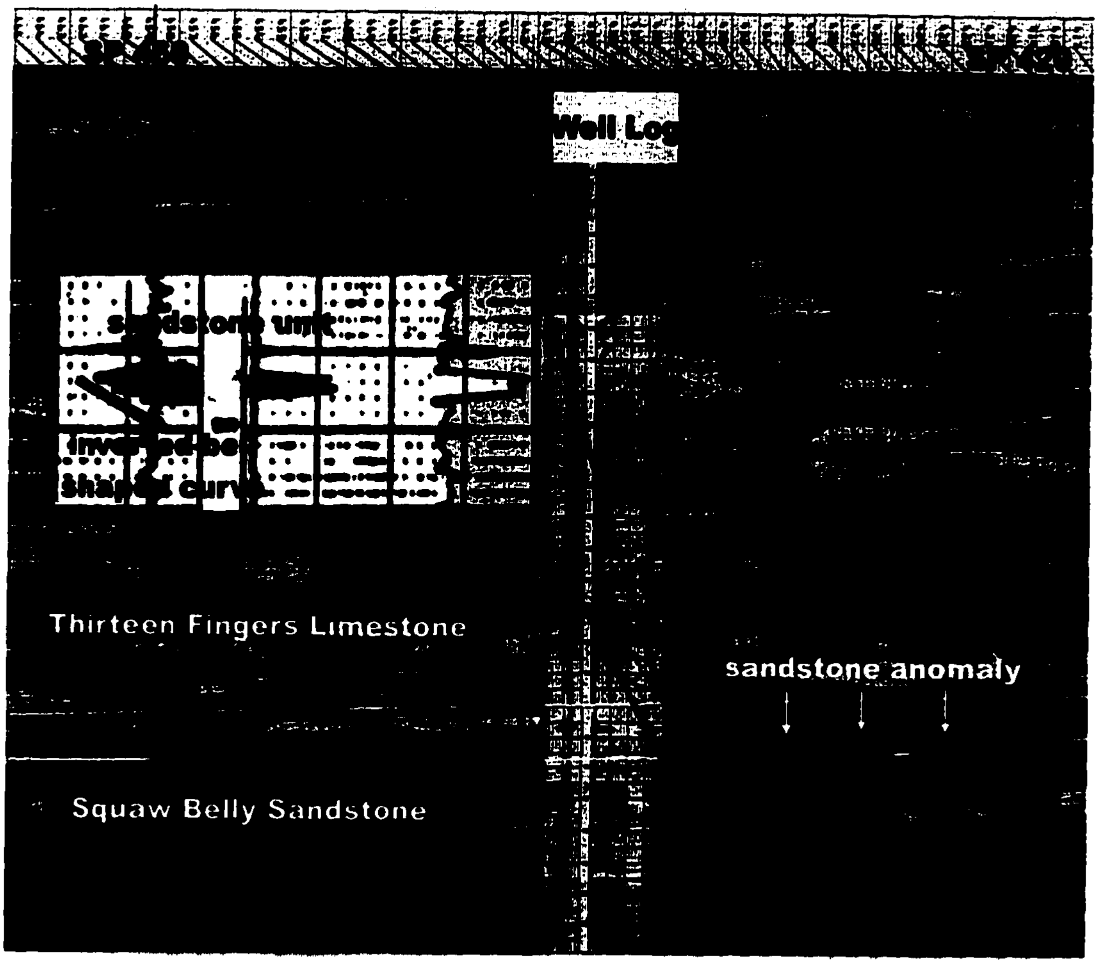

Figure 27. The inverted bell-shaped log curves characteristic of a distributary channel; a portion of Seismic Line 27 between SP 420 and 460.

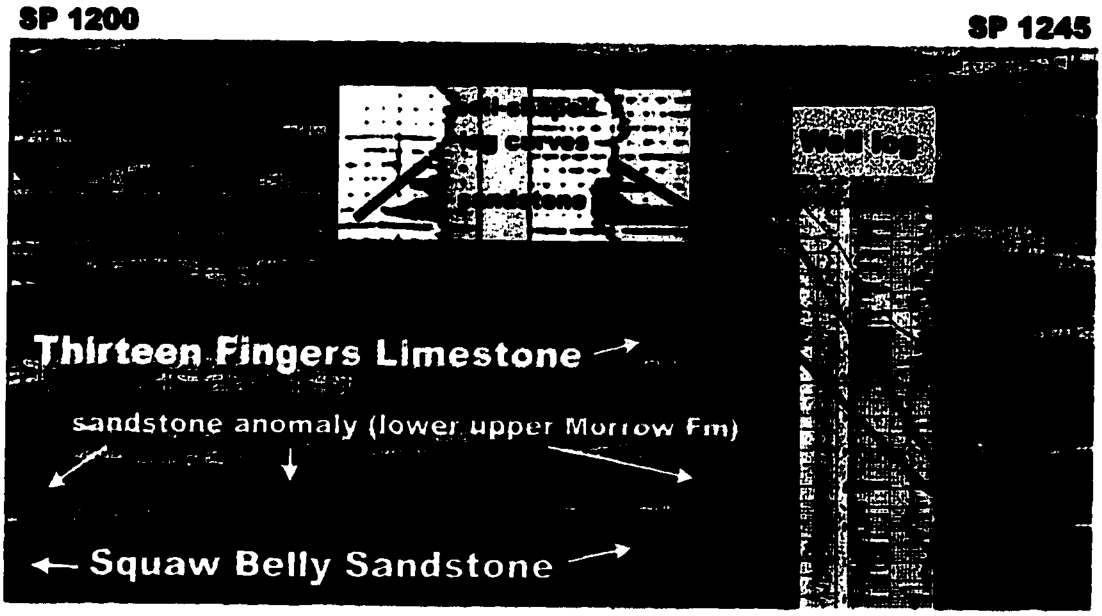

Figure 28. The bell-shaped log curves characteristic of a point bar sequence; a portion of Seismic Line 5 between SP 1200 and 1245.

The Seismic Horizon of the Middle Upper Morrow Formation

A map of the seismic horizon of the middle upper Morrow Formation is presented on Plate II, and the main trend is shown in reduced form on Figure 29. While plotting the seismic anomalies on the seismic base map prior to contouring, it became apparent that there was a sinuous pattern produced by the data seen on Seismic Lines 27, 5, 25, and 2. The contouring of the interval velocities emphasized this sinuous pattern, which is suggestive of a meandering fluvial system (Cant, 1982). The geologic model of a meandering fluvial system was then used in contouring the remainder of the anomalies seen on Seismic Lines 3, 23, and 1, where the seismic line density is less. Possible avulsion of the channel is shown at the distal, downstream end of the mapped fluvial system on Seismic Lines 23 and 1.

Well-log analysis also favors the interpretation that this seismic horizon represents a meandering fluvial system. Spontaneous potential and resistivity well logs show the bell-shaped curves that are characteristic of point bar sequences according to Swanson (1979). Anomalies of inferred clayey siltstone, laterally adjacent to interpreted sandstone anomalies, probably represent interchannel deposits temporally associated with the meandering fluvial system.

A second fluvial trend located farther northeast was also mapped (Fig. 30). Both fluvial systems trend NW-SE, parallel to the Central Lipscomb High (Fig. 31), a structural feature that was bounded on the northeast by a Mississippian reverse fault. During deposition of the upper Morrow Formation this fault was expressed as an antiform, as shown on a seismic lines studied for this project, that may have influenced the trend of the middle upper Morrow streams.

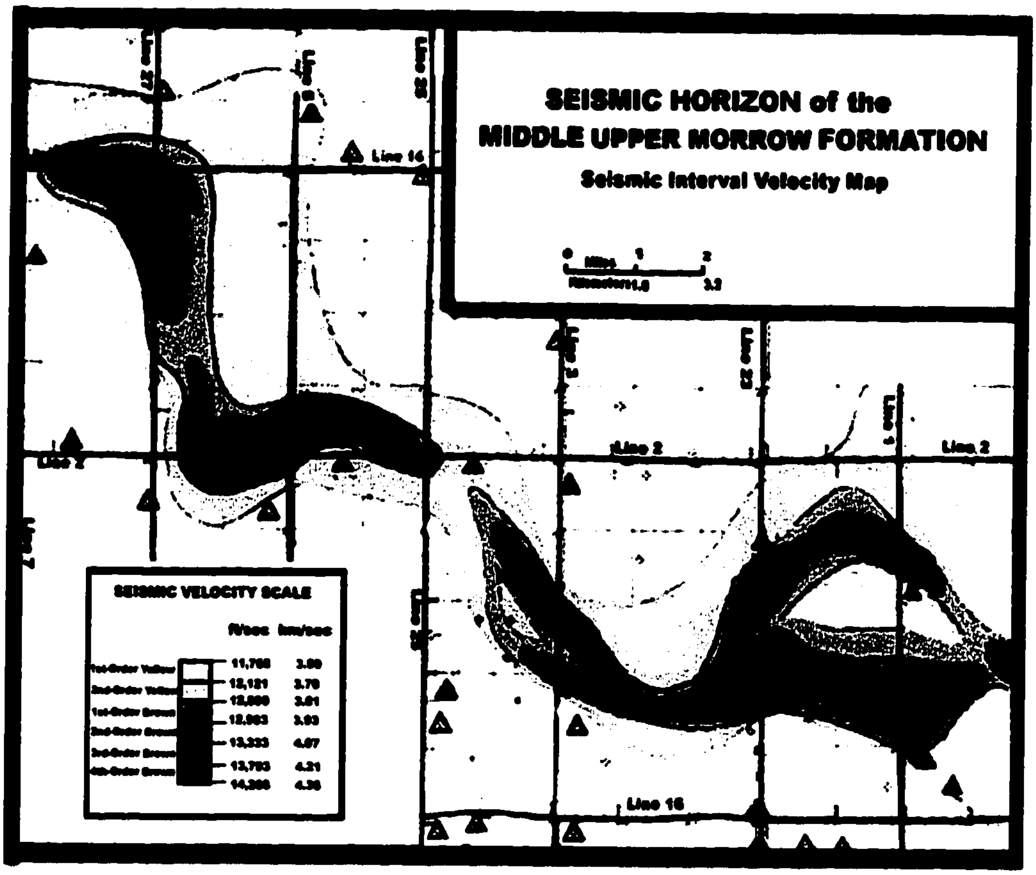

Figure 29. The mapped horizon of the southern part of the middle upper Morrow Formation. The sandstone anomalies, yellow and brown interval velocity colors, are interpreted to represent a meandering fluvial system. The cream color anomalies (1st-order yellow), laterally adjacent to the sandstone anomalies, are interpreted to represent interchannel deposits. Seismic lines are highlighted in blue; wells correlated to the seismic data are indicated by red triangles.

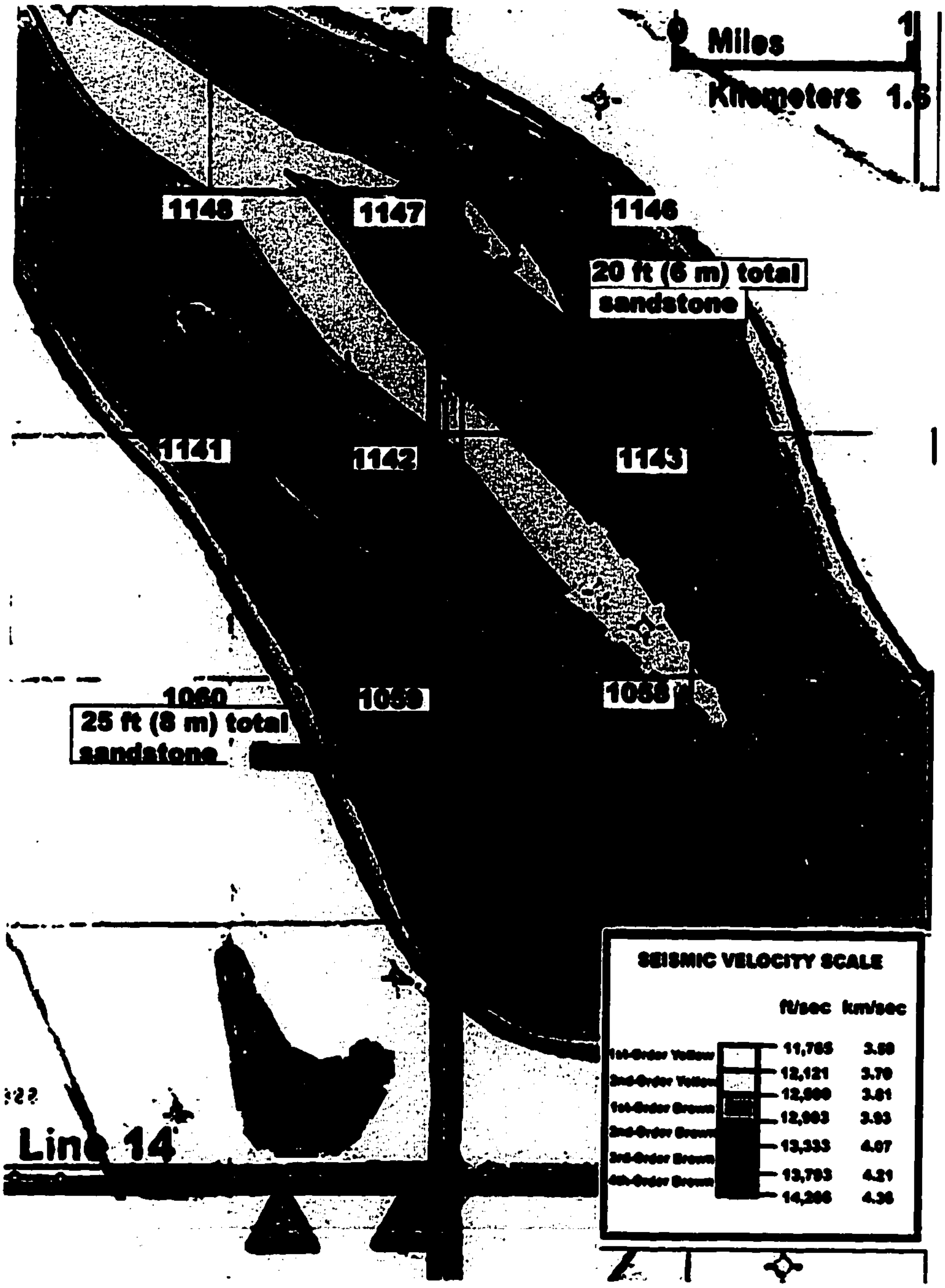

Figure 30. A map of the northern part of the seismic horizon of the middle upper Morrow Formation. Seismic lines are highlighted in blue; wells tied to the seismic data are indicated by red triangles. Blue and green spots indicate oil wells with upper Morrow production.

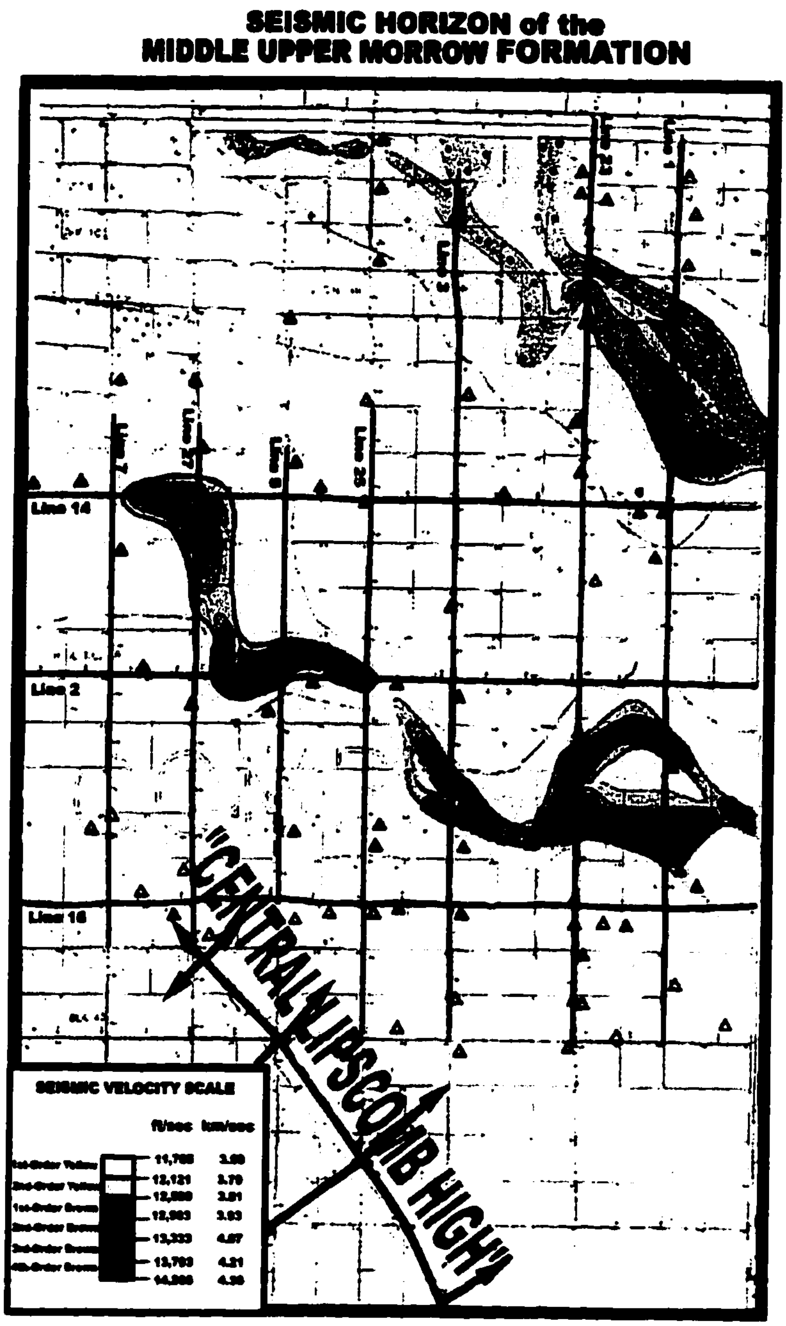

Figure 31. The Central Lipscomb High and two interpreted fluvial trends of the seismic horizon in the middle upper Morrow Formation. The northwest extension of the northern fluvial trend, highlighted in light blue, is based solely upon upper Morrow production and is speculative. Seismic lines are highlighted in blue; some of the wells tied to the seismic data are indicated by red triangles.

The Seismic Horizon of the Upper Upper Morrow Formation

A map of the seismic horizon of the upper upper Morrow Formation is shown on Figure 32. Well logs show both inverted bell-shaped curves, indicating distributary channel deposits (e.g., The Texaco, Anna Frass E-2; Sec. 72, BLK 10, H&TC Survey), and bell-shaped curves, indicating point bar sequences (e.g., The Geodyne Resources, M. P. Chew #5; Sec. 1159, BLK 10, H&TC Survey). The mapped sandstone anomalies are narrow, linear, and form two separate trends. The southern channel was mapped based upon the integration of data from Seismic Lines 7 and 27, with the published map and seismic inversion data of Darden field (Halverson, 1988).

The geomorphic expression could suggest a distributary channel that shifted position laterally during its existence, an interpretation strengthened by the inverted bell-shaped curves on well logs, the narrowness and linearity of the channels, and the relatively abrupt termination of these channels.

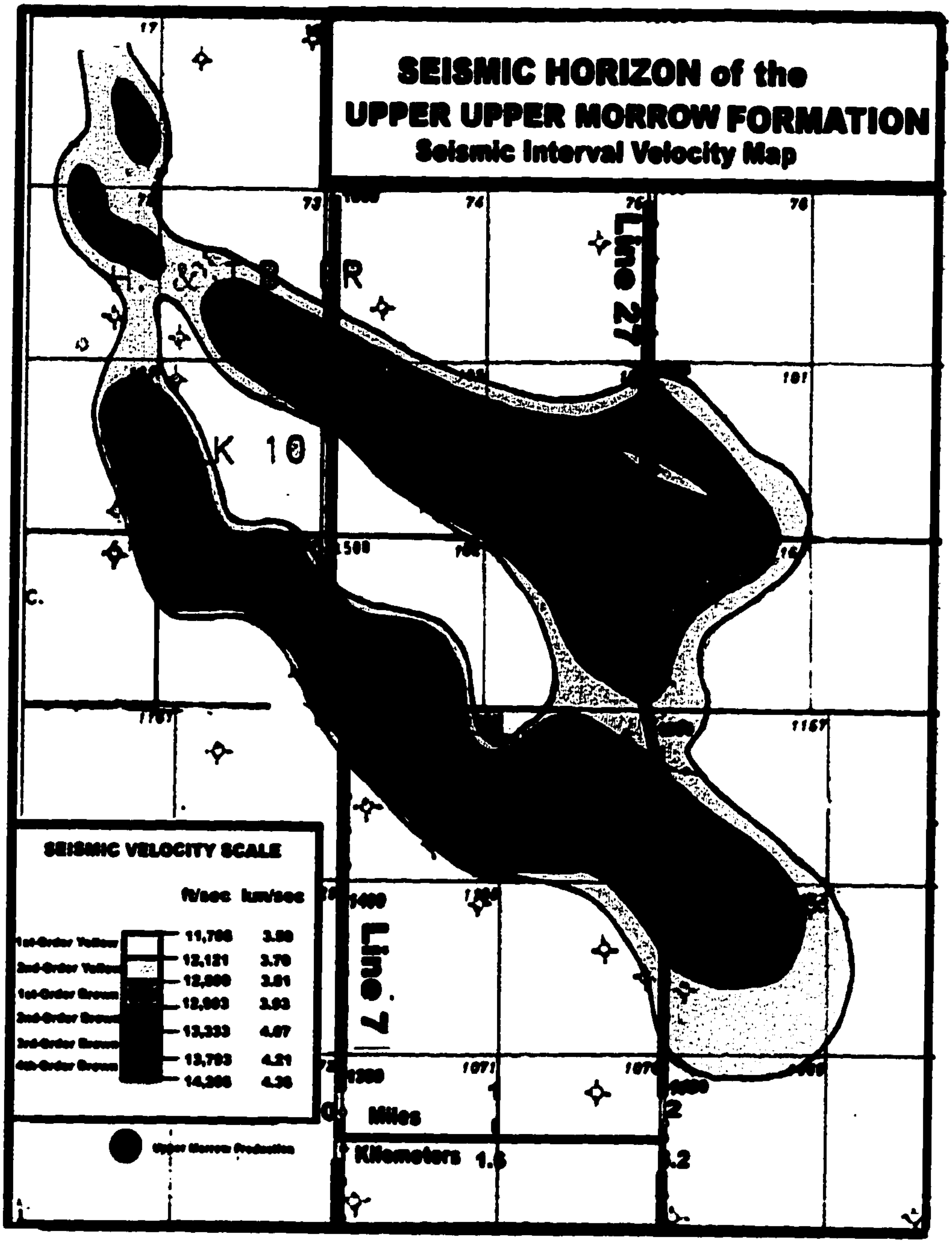

Figure 32. A map of the seismic horizon of the upper upper Morrow Formation, which is interpreted to represent a migrated distributary channel. Darden field is located within the southern channel. Seismic lines are highlighted by the blue lines and upper Morrow production is indicated by black dots within blue.

THE EVOLVING PALEOGEOGRAPHY

The general paleogeography of the Late Paleozoic in the western Anadarko Basin has been summarized by Swanson (1979). He indicated that, prior to the Morrowan, a major regression left the Upper Mississippian carbonate platform exposed and subject to erosion. This regression resulted in the development of a regional unconformity that now separates the Mississippian limestones from the overlying lower Morrow Formation.

The lower Morrow shales and sandstones, which are approximately 150 m thick within the study area, were deposited during the first, major, post-Mississippian transgression. This transgression was terminated by the seaward progradation of sediment forming the Upper Morrow Deltaic Plain. Subsequent to this progradational episode, another major transgression resulted in the deposition of the Atokan Thirteen Fingers Limestone sequence (Fig. 33).

This study demonstrates that the history of deposition of the upper Morrow Formation within the study area is somewhat more complicated than the regional interpretation indicated by Swanson (1979). The upper Morrow Formation is composed of interbedded sandstone, siltstone, and shale. The sandstone is concentrated within three zones in the upper Morrow Formation and is separated by beds composed predominantly of shale. Swanson (1979) reported fossils, including various species of foraminiferans, bryozoans, and ostracodes, that are characteristic of brackish water (C. H. Stevens, personal communication, 1997) from well cores in southwest Kansas and the Oklahoma Panhandle, a distance of 80 to 160 km northwest of the study area. One core from the well, Gulf #1 Kelly, in Texas County, Oklahoma encountered fossiliferous, shallow-marine claystone both above and below sandstones

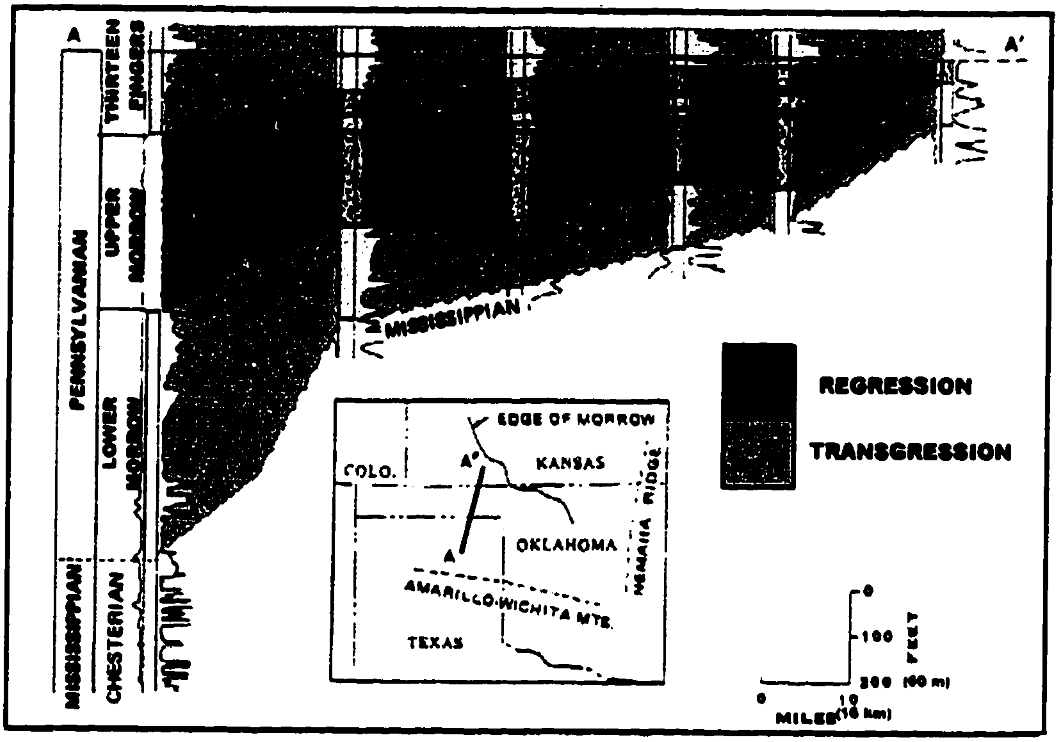

Figure 33. The gross transgressive-regressive sequence of the Morrow Formation as interpreted by Swanson (1979). The cross-section A to A' shows the major depositional events. In general terms, the upper Morrow Formation is a major progradational sequence (orange) between two major transgressions (blue).

interpreted to be deltaic deposits by Swanson (1979). Upon this basis, the similar shale units in the upper Morrow Formation in Lipscomb County, Texas are interpreted to be shallow marine in origin.

As each of the sandstone-rich seismic horizons recognized in this study is interpreted to represent a minor progradational pulse and deposition in a fluvial or deltaic environment, each major marine shale unit represents a transgression. The lowest unit of the upper Morrow Formation is a marine shale. It is overlain by the seismic horizon of the lower upper Morrow Formation, which is here interpreted to represent a prograding deltaic distributary channel system. The termination of the distributary channels seaward marks the position of the Pennsylvanian paleoshoreline at that time. The overlying marine shale indicates a minor transgression that was later terminated by progradation of sediment of the seismic horizon of the middle upper Morrow Formation, which is interpreted to represent a meandering fluvial system. During deposition of this seismic horizon, the Upper Morrow Deltaic Plain prograded farther seaward than during the deposition of the lower upper Morrow seismic horizon, and the shoreline was somewhere southeast of the study area toward the depocenter of the basin in southwestern Oklahoma. This episode was again interrupted by another marine transgression. This was followed by deposition of the seismic horizon of the upper upper Morrow Formation, which is interpreted to represent another progradation with a distributary channel that changed position laterally with time. The Paleoshoreline probably was near the termination of the distributary channel within the northwestern portion of the study area. The relative position of sea level and the evolving paleogeography as determined from this study are shown in Figure 34.

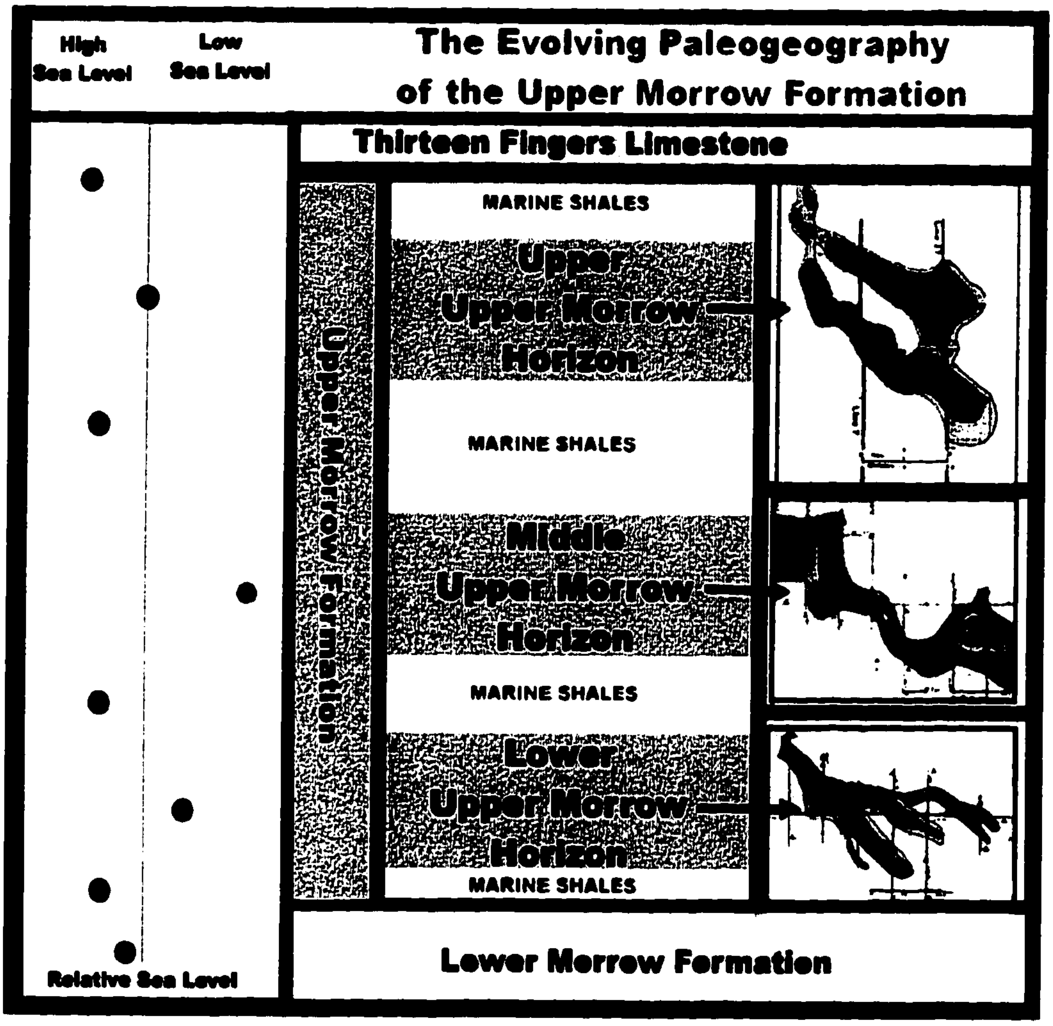

Figure 34. The changing relative sea level and the evolving paleogeography of the upper Morrow Formation. The upper Morrow Formation includes three minor progradational pulses; the paleogeography of each pulse is shown in the right column above. The relative sea level change within the study area during the deposition of the upper Morrow Formation is shown in the left column above.

More than fifty transgressive-regressive depositional sequences are represented in the Pennsylvanian and lower Permian rocks of the North American craton responding to eustatic changes of sea level of 100 to 200 m that had a recurrence interval of 1.2 to 4 Ma (Ross and Ross, 1985). The late Morrowan is represented by one global depositional sequence (Ross and Ross, 1985), the duration of which corresponds to a 3rd-order global stratigraphic cycle (Miall, 1990). The interpretations presented in this study indicate that the upper Morrow Formation is marked by three minor progradational sequences within the study area. These smaller transgressive-regressive cycles evidently were of a shorter recurrence interval than the 3rd-order cycle that contains them and was described by Ross and Ross (1985).

Two mechanisms for these changes in sea level are possible. One explanation might be that they represent Milankovitch glacioeustatic cycles, a hypothesis strengthened by the fact that the southern hemisphere was heavily glaciated at this time (Kearey and Vine, 1990). Fourth- to 5th-order glacioeustatic cycles occur every 0.01 to 0.5 Ma (Miall, 1990), an interval more or less corresponding to the frequency of the upper Morrow cycles. A second mechanism could be the episodic tectonic depression of the foreland basin as it was thrust loaded, followed by the progradation of sediment of the Upper Morrow Deltaic Plain. Overall the rate of sedimentation kept pace with subsidence so that the Upper Morrow Deltaic Plain repeatedly built seaward and deposited sandstone over the transgressive shale.

CONCLUSIONS

The geology of the upper Morrow Formation in the northeastern Texas Panhandle was studied in the subsurface using seismic reflection data that were processed into seismic inversion data, which were then integrated with well log data. This study reveals that the sandstones in the upper Morrow Formation occur at three discrete levels herein referred to as the seismic horizon of the lower upper, middle upper, and upper upper Morrow Formation.

The depositional environment of the seismic horizon of the lower upper Morrow Formation is interpreted to be a deltaic distributary channel system characterized by the presence of inverted bell-shaped well-log curves, a "bird's foot" geomorphic pattern, and an abrupt seaward termination of the channels. The paleoshoreline was within the study area near the termination of the channels.

The depositional environment of the seismic horizon of the middle upper Morrow Formation is interpreted to be a meandering fluvial system characterized by a sinuous geomorphic pattern and bell-shaped well log curves. At this time the paleoshoreline lay farther to the southeast towards the basin's depocenter in southwestern Oklahoma than it did when the lower upper Morrow seismic horizon was deposited.

The depositional environment of the seismic horizon of the upper upper Morrow Formation is interpreted to be a distributary channel based on the narrowness and linearity of the channel and well logs showing the inverted bell-shaped curves. The paleoshoreline was in the northwestern portion of the study area during this time.

Thus, the upper Morrow Formation within the study area is interpreted herein to represent three progradational pulses separated by marine transgressions. This is in contrast to the previous regional interpretation in which the upper Morrow Formation was interpreted to represent one major progradational event. The three progradational pulses recognized in this study are interpreted to represent 4^{th}- or 5^{th}-order Milankovitch glacioeustatic cycles, with tectonically generated pulses possibly superimposed.

REFERENCES CITED

Anstey, N. A., 1980, Seismic exploration for sandstone reservoirs: Boston, Massachusetts, International Human Resources Development Corporation Publishers, 136 p.

Cant, D. J., 1982, Fluvial facies models and their application, *in* Scholle, P. A. and Spearing, D., ed., Sandstone depositional environments: American Association of Petroleum Geologists Memoir 31, p. 115 - 137.

Coleman, J. M., and Prior, D. B., 1982, Deltaic environments of deposition, *in* Scholle, P. A. and Spearing, D., ed., Sandstone depositional environments: American Association of Petroleum Geologists Memoir 31, p. 139 - 178.

Halverson, J. R., 1988, The seismic expression of the upper Morrow sands, western Anadarko Basin: Geophysics, v. 53, p. 290-303.

Hilchie, D. W., 1978, Applied openhole log interpretation: Golden, Colorado, Colorado School of Mines Publishers, 311 p.

Kasino, R. E., and Davies, D. E., 1979, Environments and diagenesis, Morrow sands, Cimarron County (Oklahoma), and significance to regional exploration, production and well completion practices, *in* Hyne, N. J., ed., Pennsylvanian sandstones of the Mid-continent: Tulsa, Oklahoma, Tulsa Geological Society Special Publication 1, p. 169-193.

Kearey, P., and Vine, F. J., 1990, Global tectonics: Cambridge, Massachusetts, Blackwell Scientific Publications, Inc., 302 p.

Lindseth, R. O., 1976, Mapping stratigraphic traps with Seislog: Abstract with Programs, 46th Annual International Meeting, Houston, Texas, Society of Exploration Geophysicists.

Miall, A. D., 1990, Principles of sedimentary basin analysis, Second edition: New York, New York, Springer-Verlag, 668 p.

Miller, W. A., Brown, L. G., Hundley-Goff, E. M., and Veal, S. L., 1991, Stockholm Southwest Field [Abstract]: American Association of Petroleum Geologists Bulletin, v. 75, p. 1397.

Moore, G. E., 1979, Pennsylvanian paleogeography of the southern Mid-continent, *in* Hyne, N. J., ed., Pennsylvanian sandstones of the Mid-continent: Tulsa, Oklahoma, Tulsa Geological Society Special Publication 1, p. 2-12.

Neidell, N. S., and Poggiagliolmi, E., 1977, Stratigraphic modeling and interpretation--Geophysical principles and techniques, *in* Payton, C. E., ed., Seismic stratigraphy--Applications to hydrocarbon exploration: American Association of Petroleum Geologists Memoir 26, p. 389-416.

Patterson, E., 1985, Morrow fluvial and deltaic sandstones of Anadarko basin in southeastern and east-central Colorado [Abstract]: American Association of Petroleum Geologists, v. 69, p. 858.

Perry, W. J., Jr., 1989, Tectonic evolution of the Anadarko Basin region, Oklahoma: United States Geological Survey Professional Paper 1866, 19 p.

Ross, C. A., and Ross, J. R. P., 1985, Late Paleozoic depositional sequences are synchronous and worldwide: Geology, v. 13, p. 194-197.

Sheriff, R. E., 1984, Encyclopedic dictionary of exploration geophysics: Tulsa Oklahoma, Society of Exploration Geophysicists, 323 p.

Swanson, D. C., 1979, Deltaic deposits in the Pennsylvanian upper Morrow Formation of the Anadarko Basin, *in* Hyne, N. J., ed., Pennsylvanian sandstones of the Mid-continent: Tulsa, Oklahoma, Tulsa Geological Society Special Publication 1, p. 115-168.

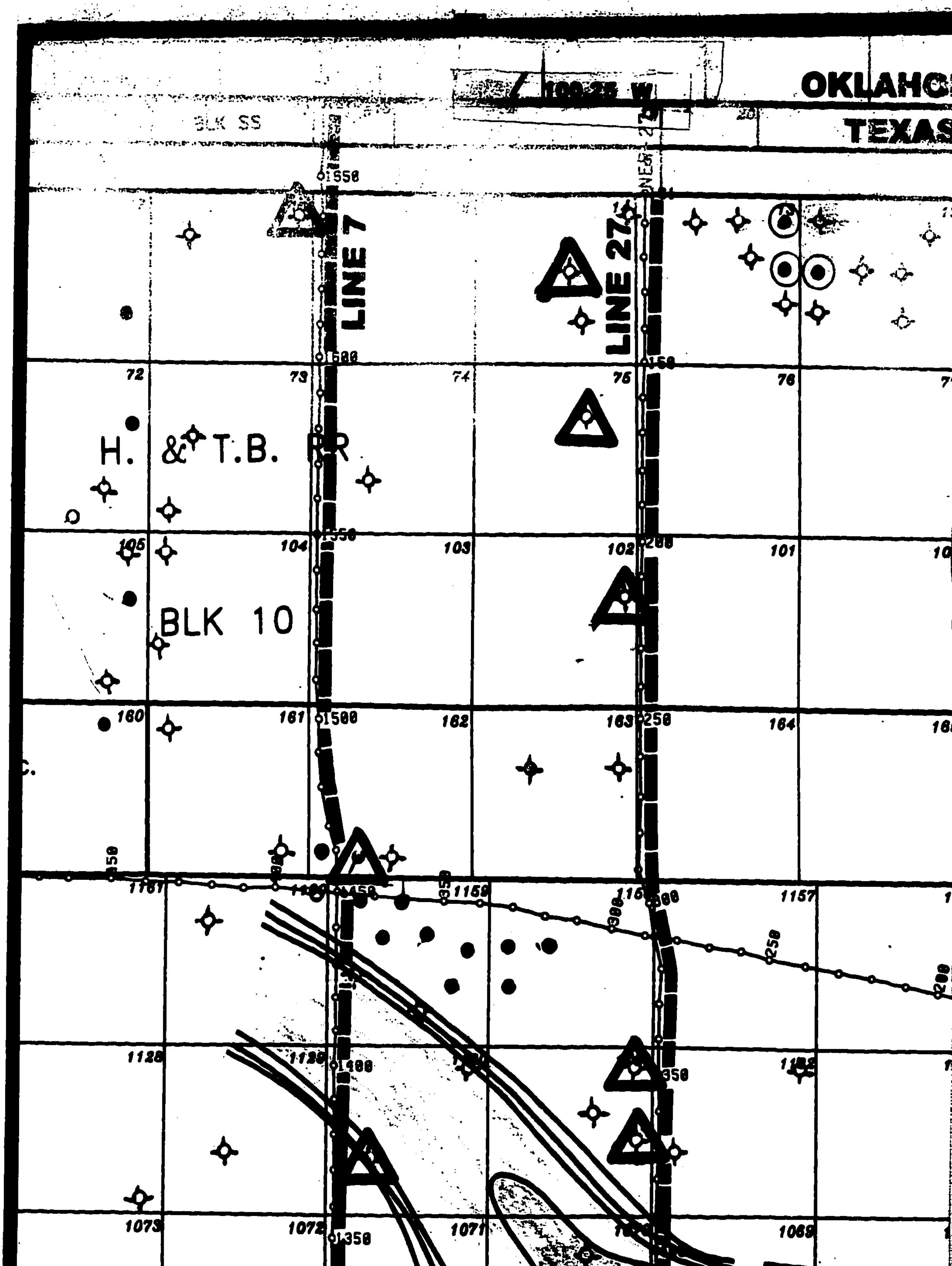

TEXAS
LINE 7
LINE 27
H. & T.B. RR
BLK 10
72
73
74
75
76
105
104
103
102
101
160
161
162
163
164
1157
1128
1073
1072
1071
1069

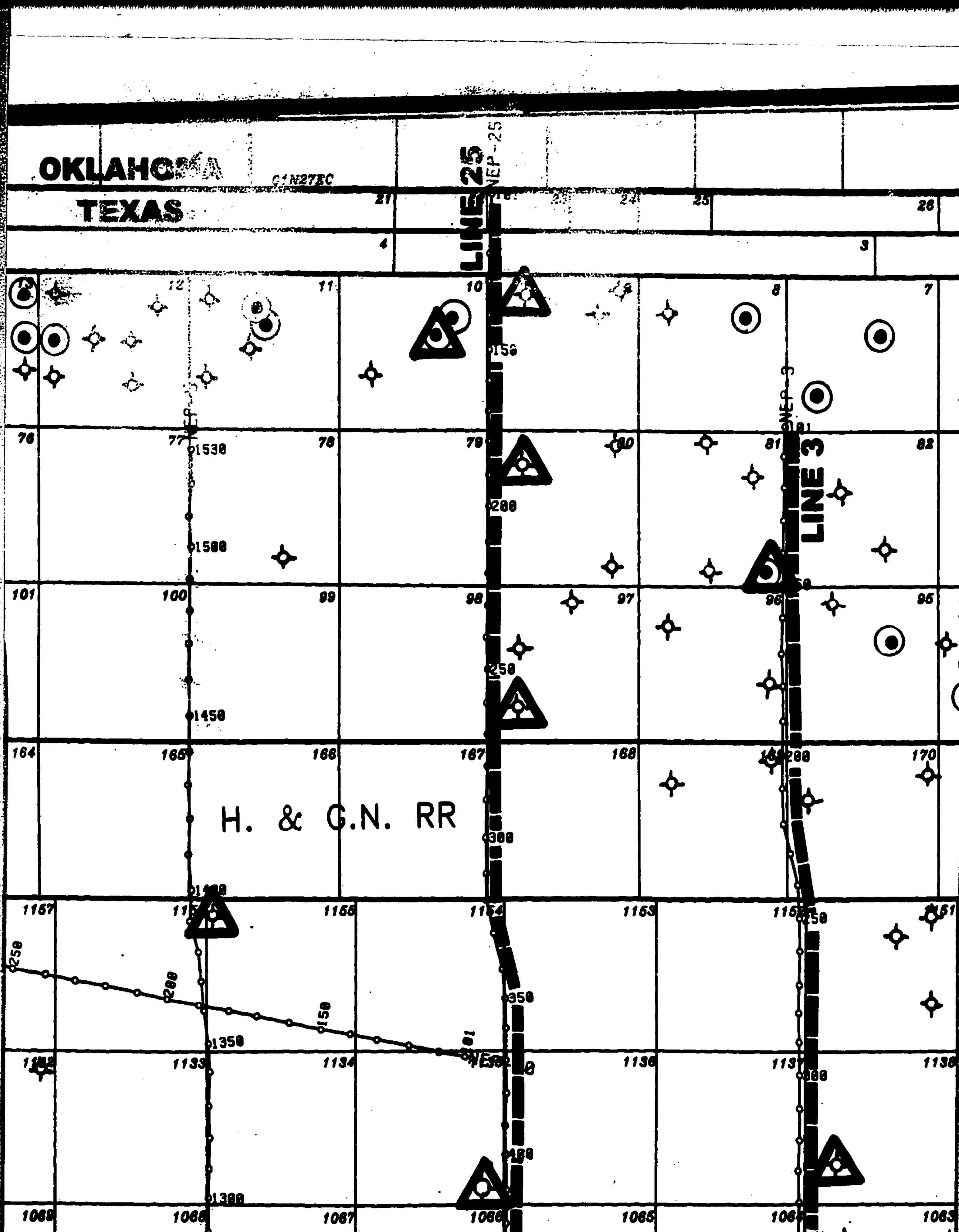

TEXAS
LINE 25
LINE 3
H. & G.N. RR
21
4
26
3
12
11
10
8
7
76
77
78
79
81
82
101
100
99
98
97
96
95
164
165
166
167
168
170
1157
1155
1153
1151
1133
1134
1136
1138
1068
1067
1065
1063
150
200
250
300
350
400
1530
1500
1450
1350
1300

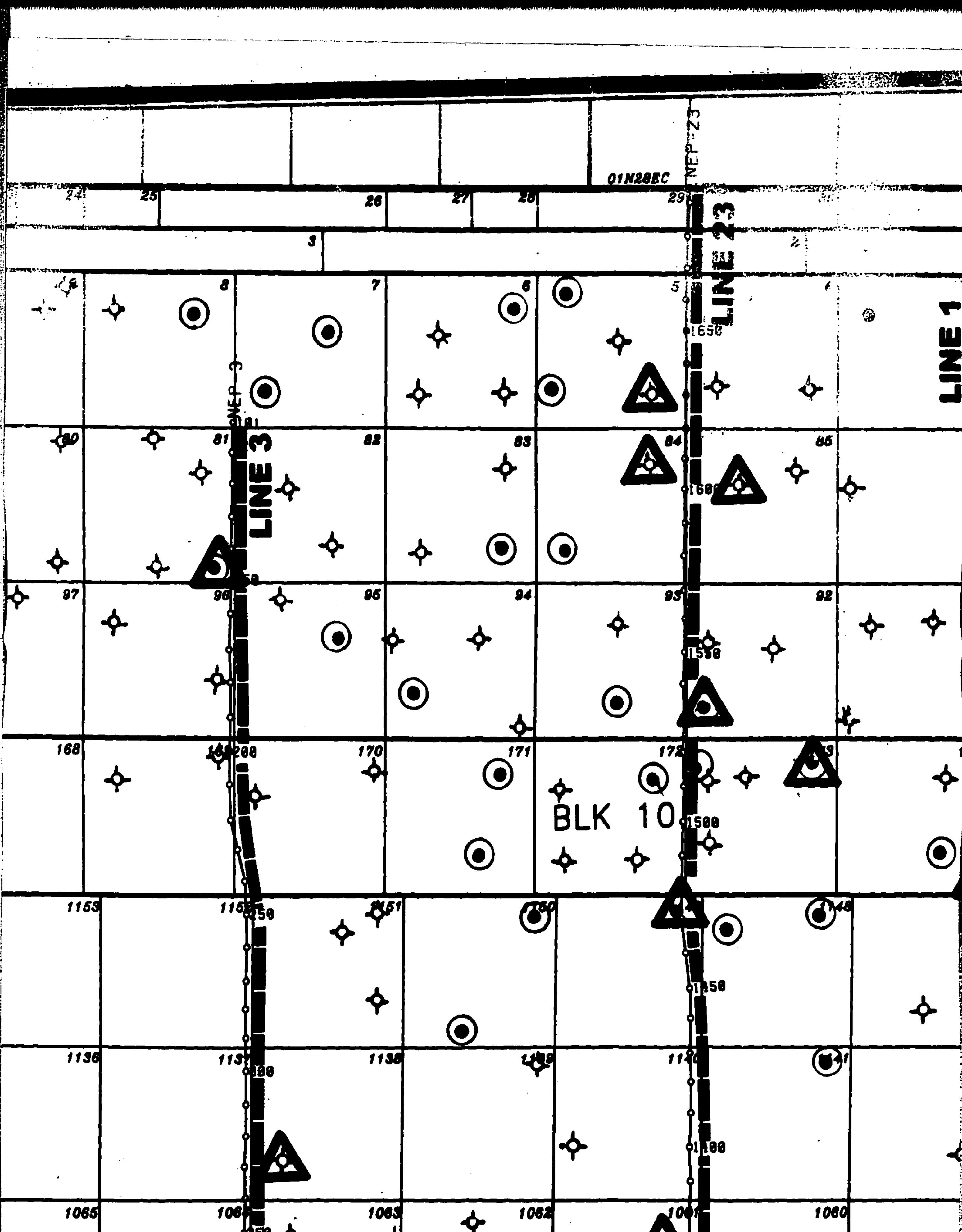

01N28EC
NEP 23
LINE 23
LINE 1
NEP 3
LINE 3
BLK 10
1650
1600
1550
1500
1450
1400
24
25
26
27
28
29
3
8
7
6
5
80
81
82
83
84
86
97
96
95
94
93
92
168
170
171
172
1153
1136
1138
1065
1063
1062
1060

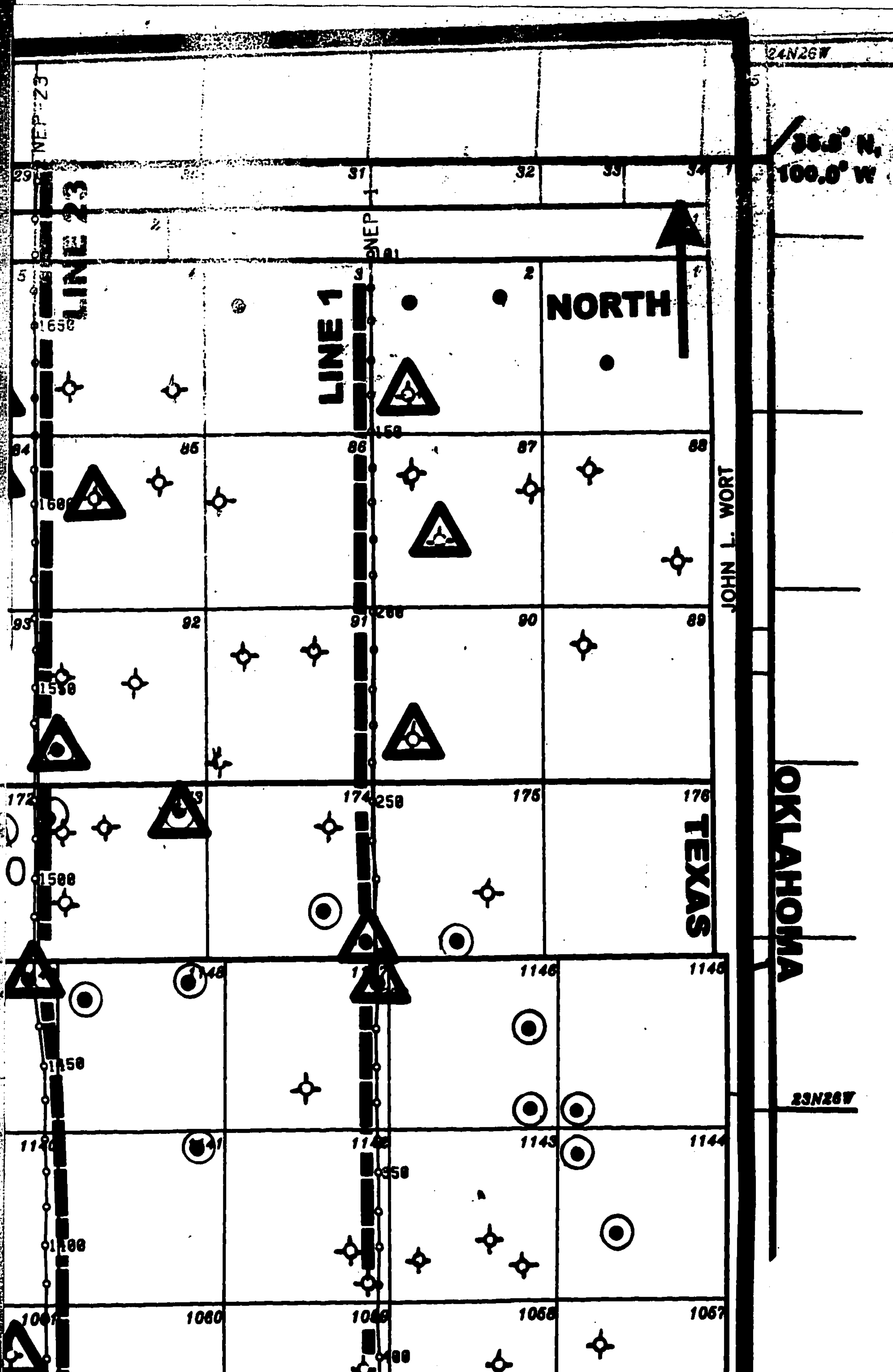
24N26W
36.5° N,
100.0° W
NEP-23
LINE 23
NEP-1
LINE 1
NORTH
JOHN L. WORT
TEXAS
OKLAHOMA
23N26W
1650
1600
1550
1500
1450
1400
150
200
250
350
400

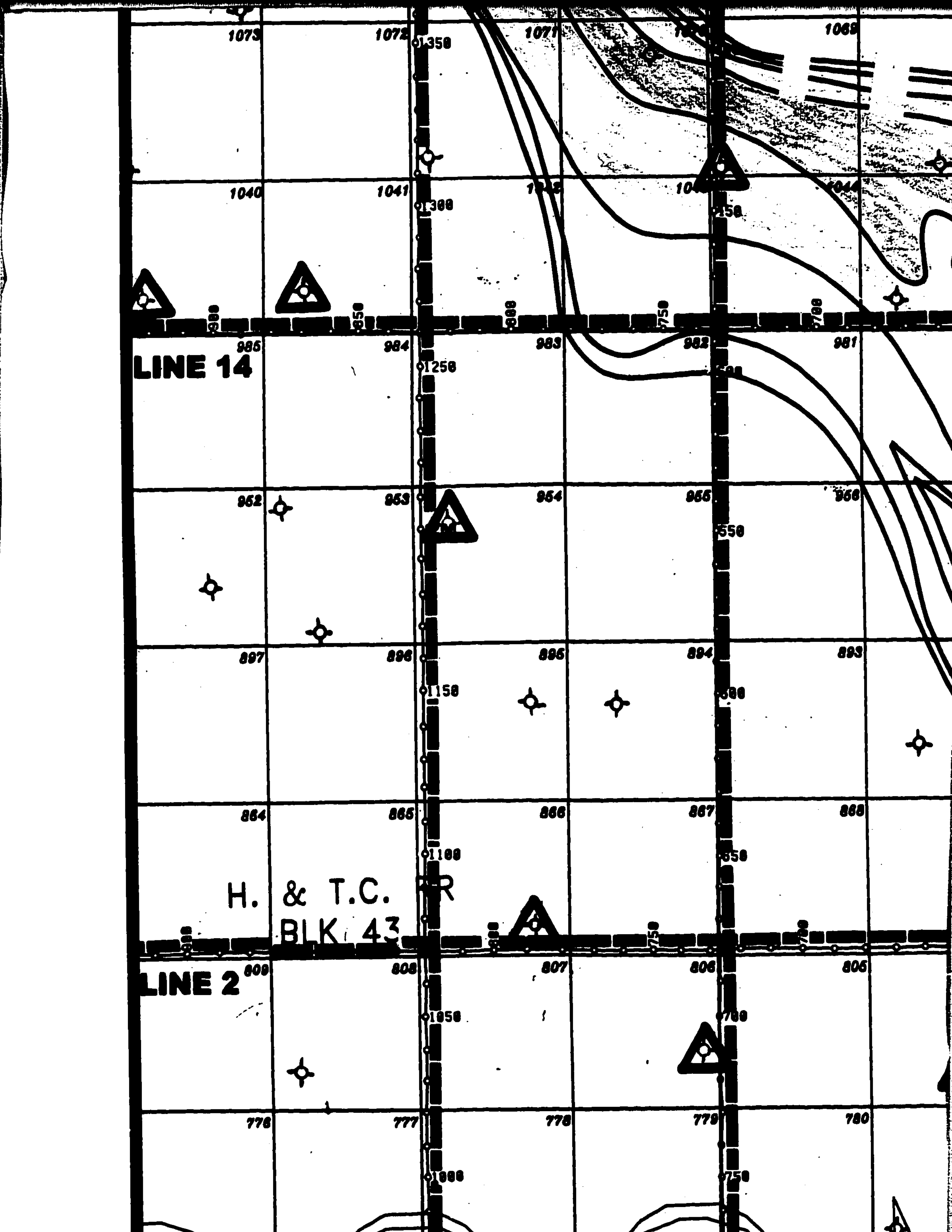

LINE 14
LINE 2
H. & T.C.
BLK 43
1073
1072
1071
1069
1040
1041
985
984
983
982
981
952
953
954
955
956
897
896
895
894
893
864
865
866
867
868
809
808
807
806
805
776
777
778
779
780

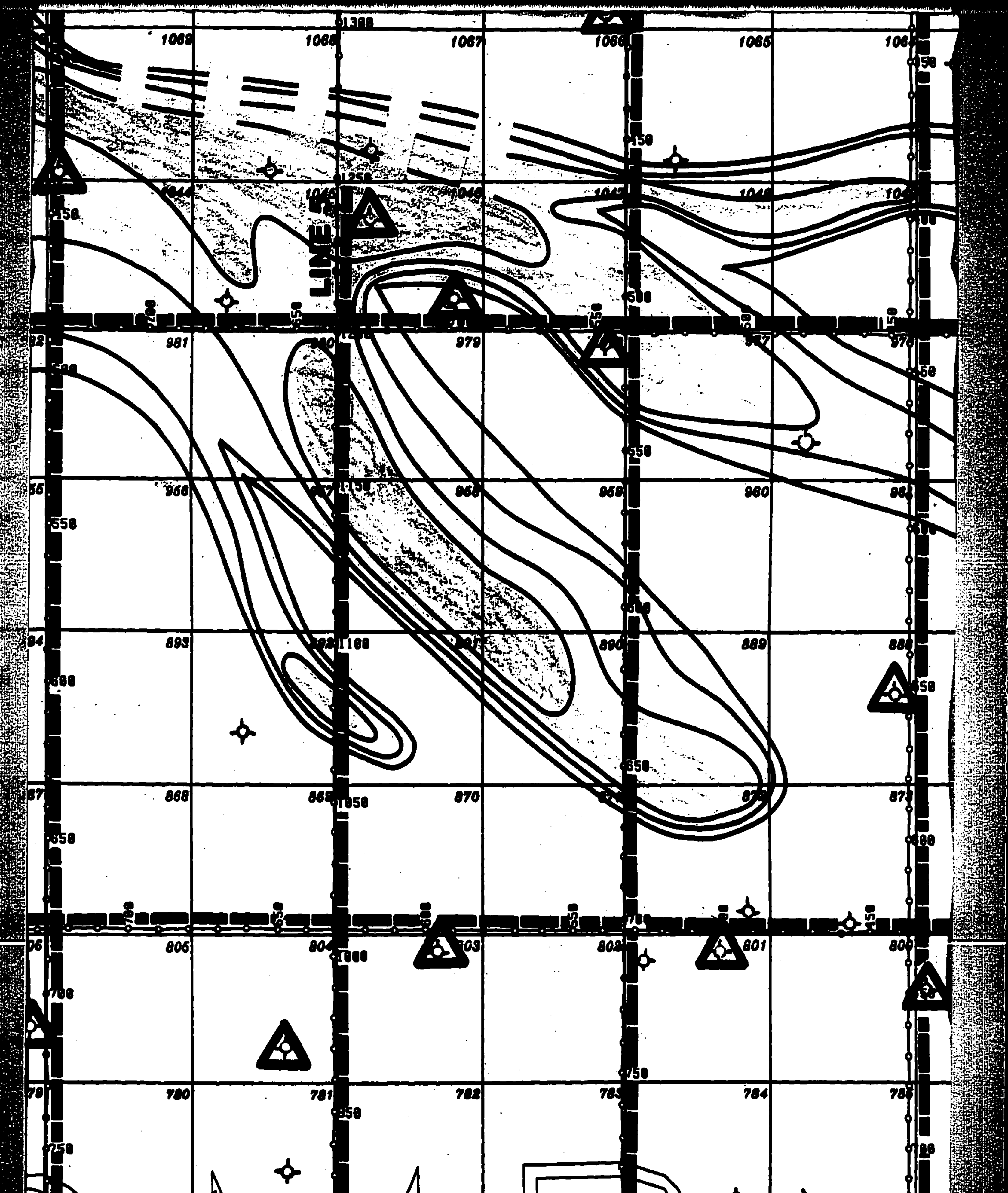

LINE
1069
1068
1067
1066
1065
981
979
958
959
960
893
889
868
870
805
801
780
782
784

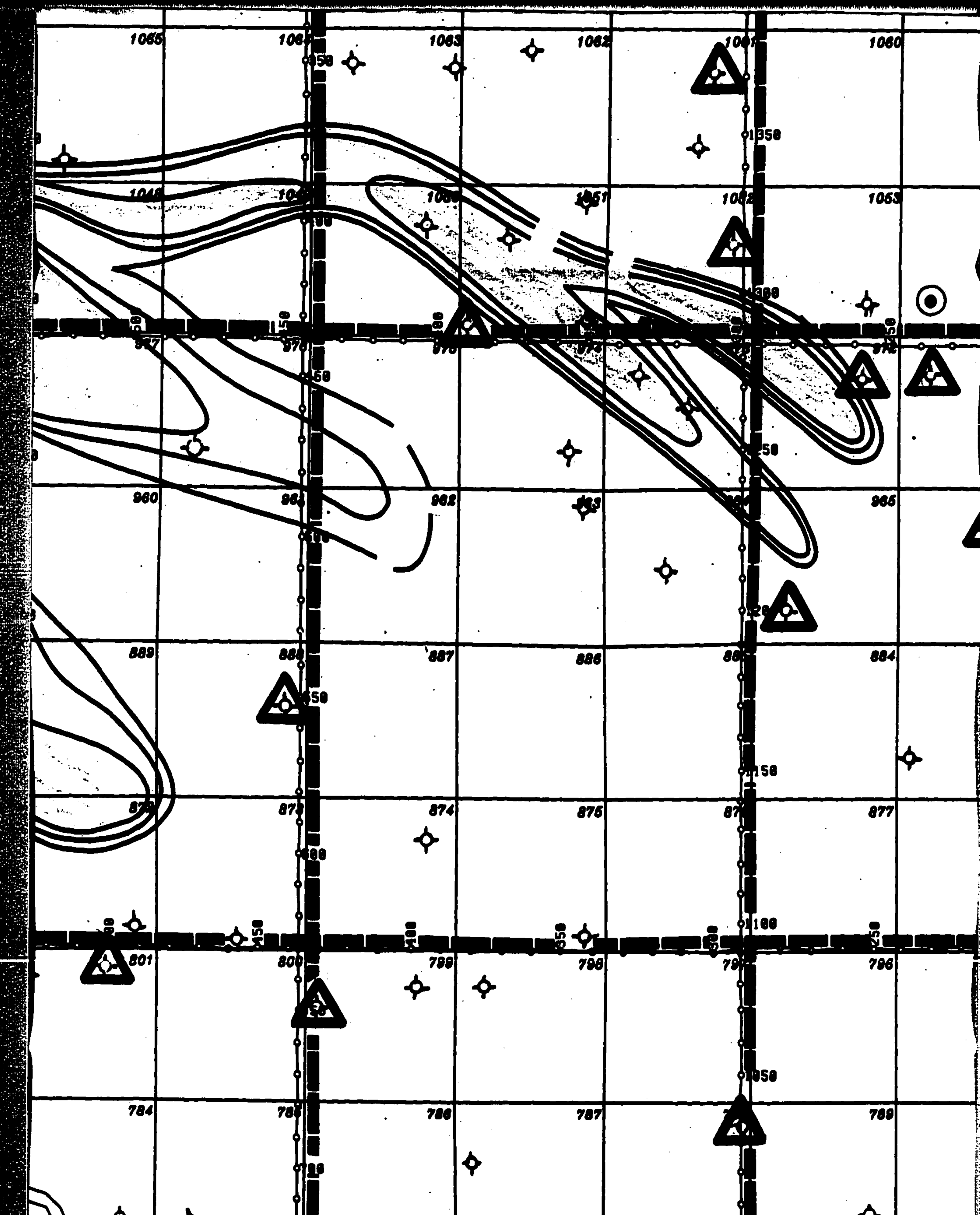

1065
1063
1062
1060
1063
960
962
965
889
887
886
884
874
875
877
801
799
798
796
784
786
787
789

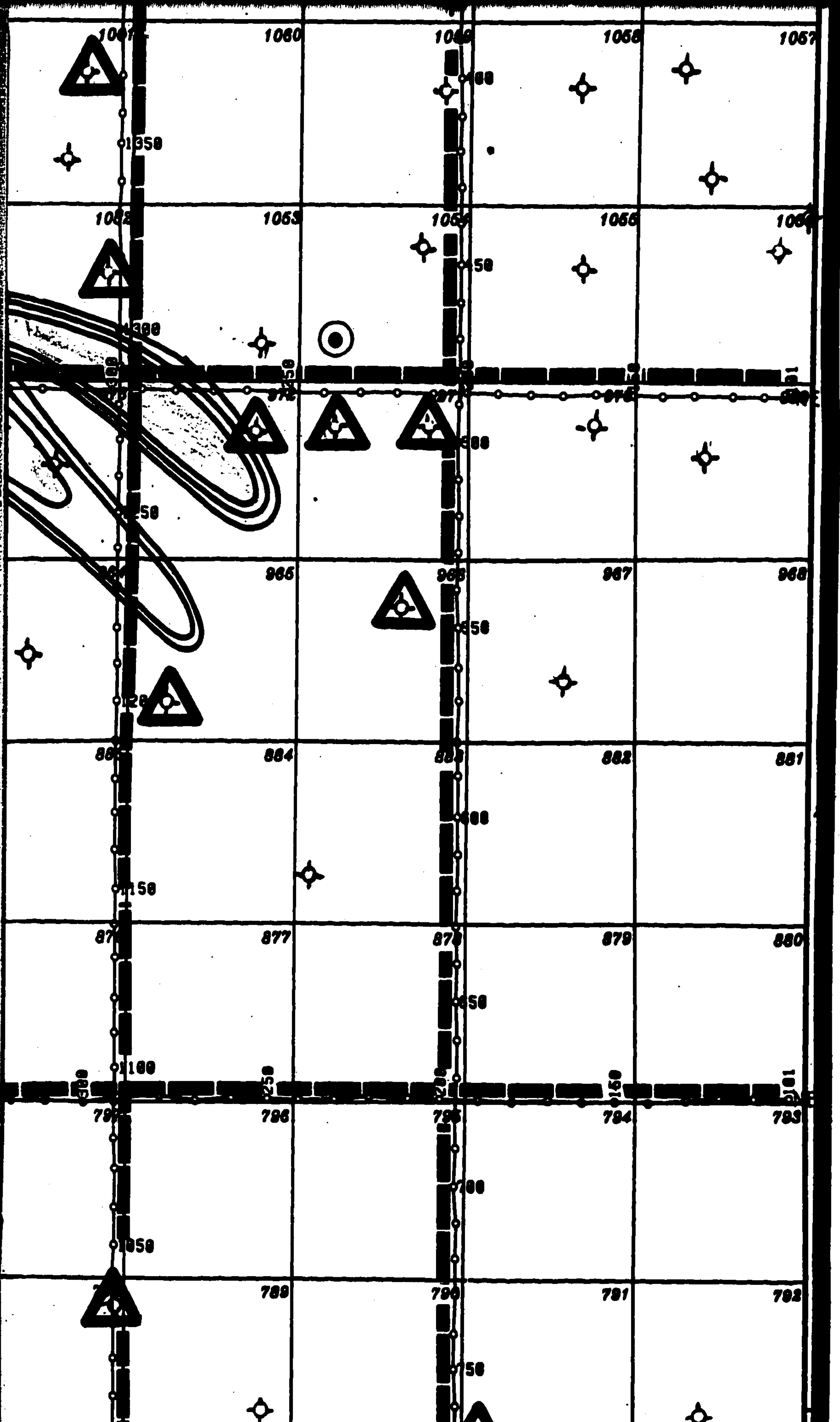

1060
1058
1057
1053
1056
965
967
968
884
882
881
877
879
880
796
794
793
789
791
792

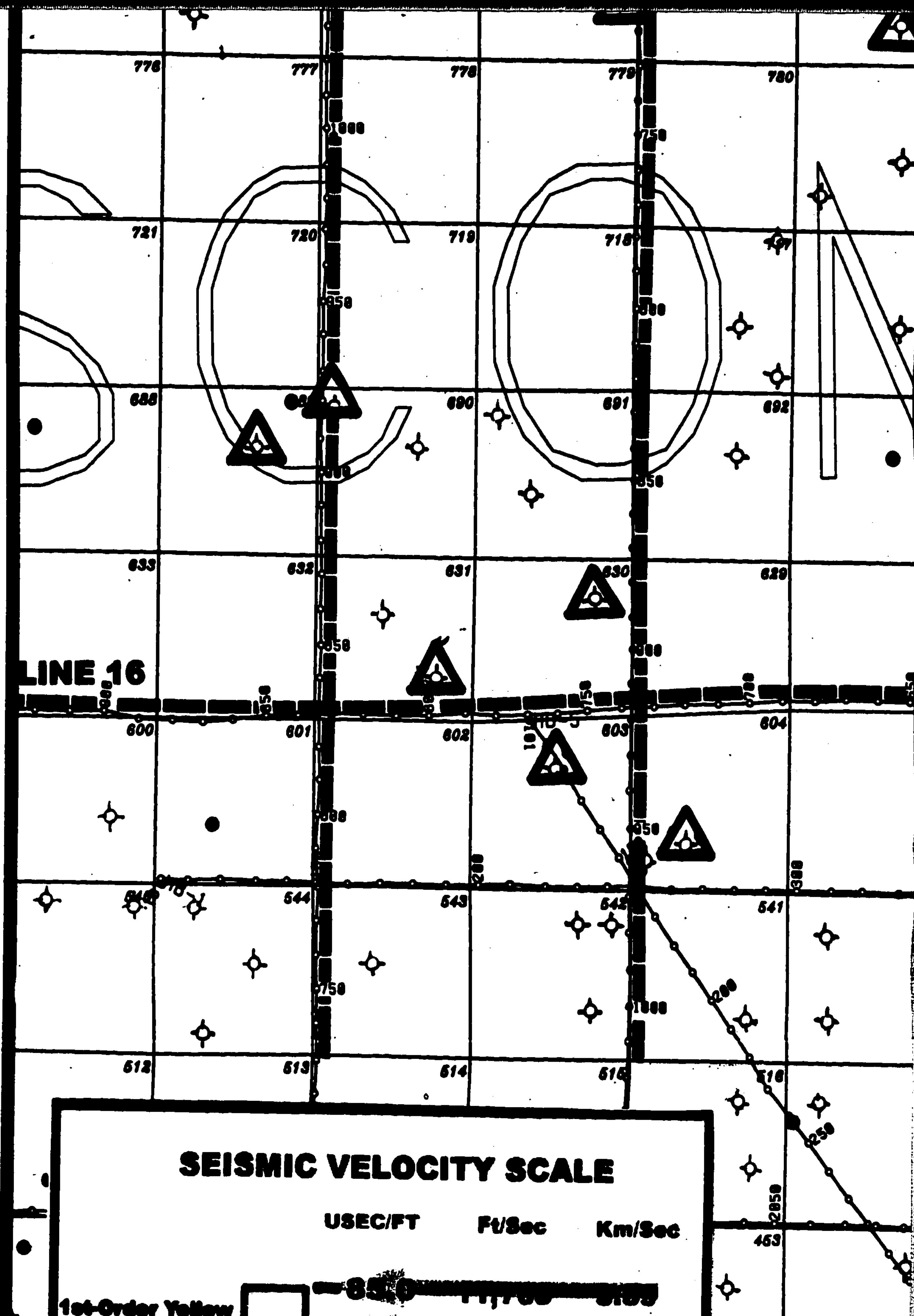

776
777
778
779
780
721
720
719
718
688
690
691
692
633
632
631
630
629
LINE 16
600
601
602
603
604
544
543
542
541
512
513
514
516
453
SEISMIC VELOCITY SCALE
USEC/FT
Ft/Sec
Km/Sec
1st-Order Yellow

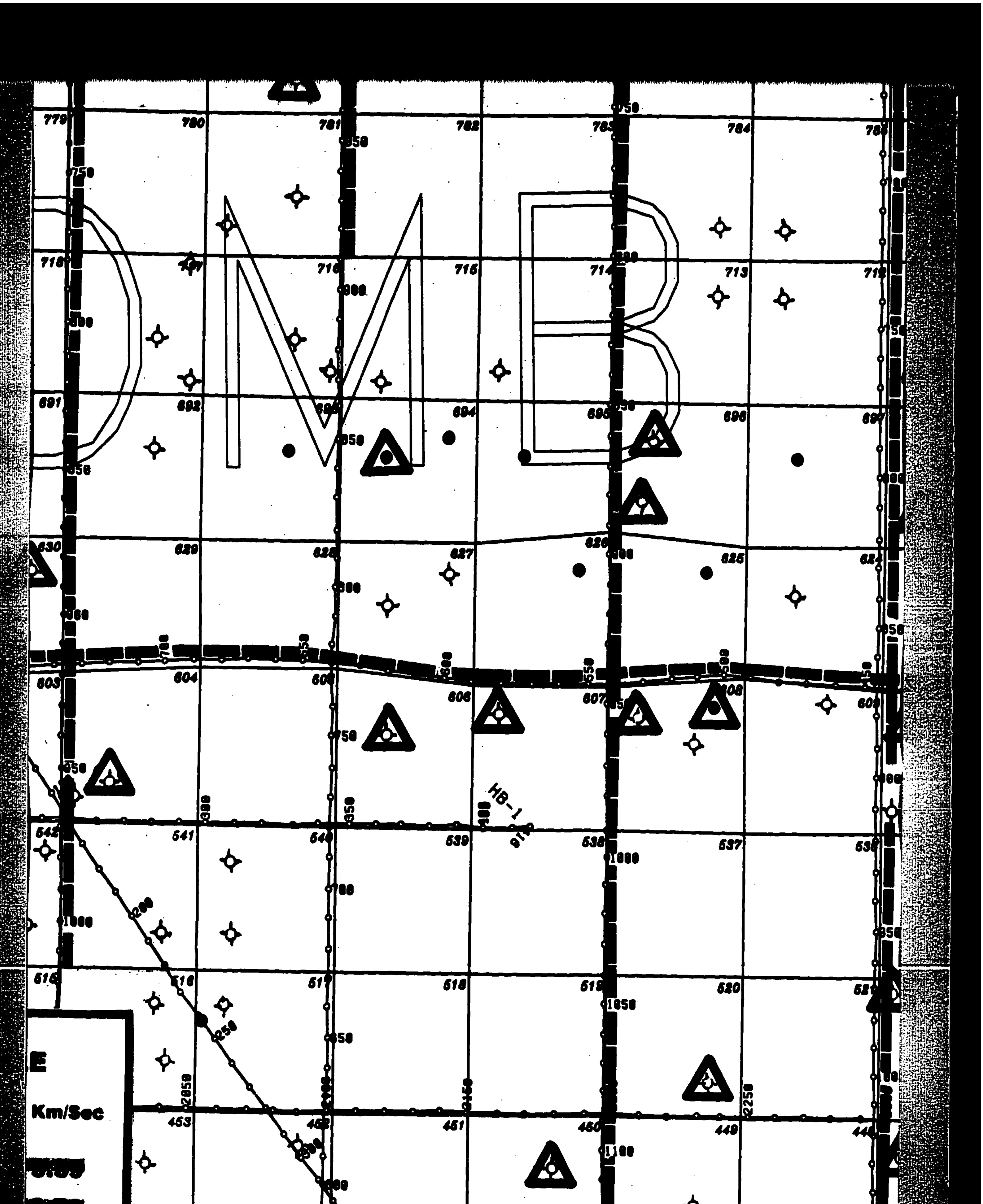

780
781
782
784
715
714
713
691
692
694
696
629
627
625
604
606
608
541
539
537
518
520
453
451
449
HB-1
Km/Sec

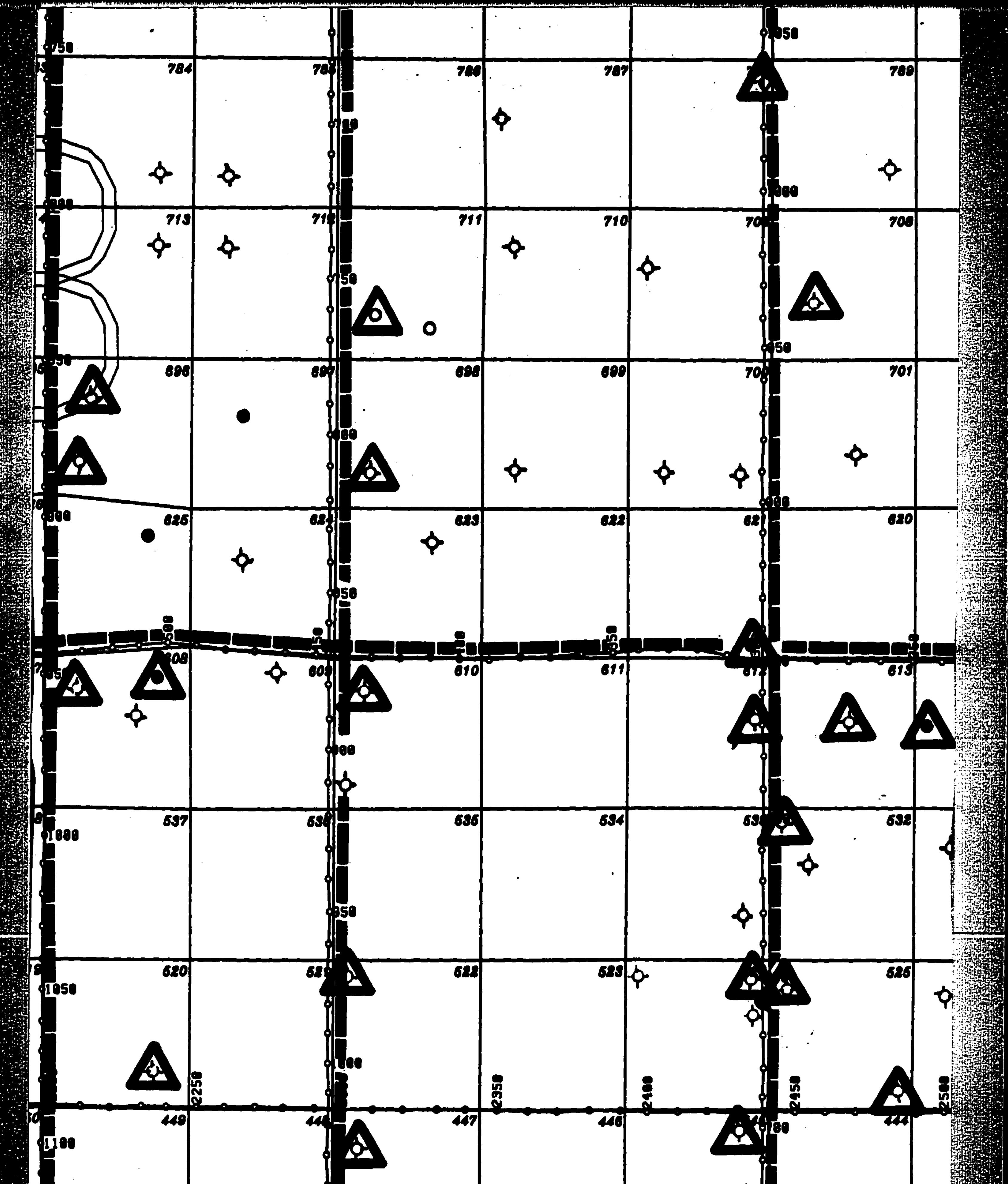

784
786
787
789
713
711
710
708
698
699
701
625
623
622
620
610
611
613
537
535
534
532
520
522
523
525
449
447
446
444
2250
2350
2400
2450
2500

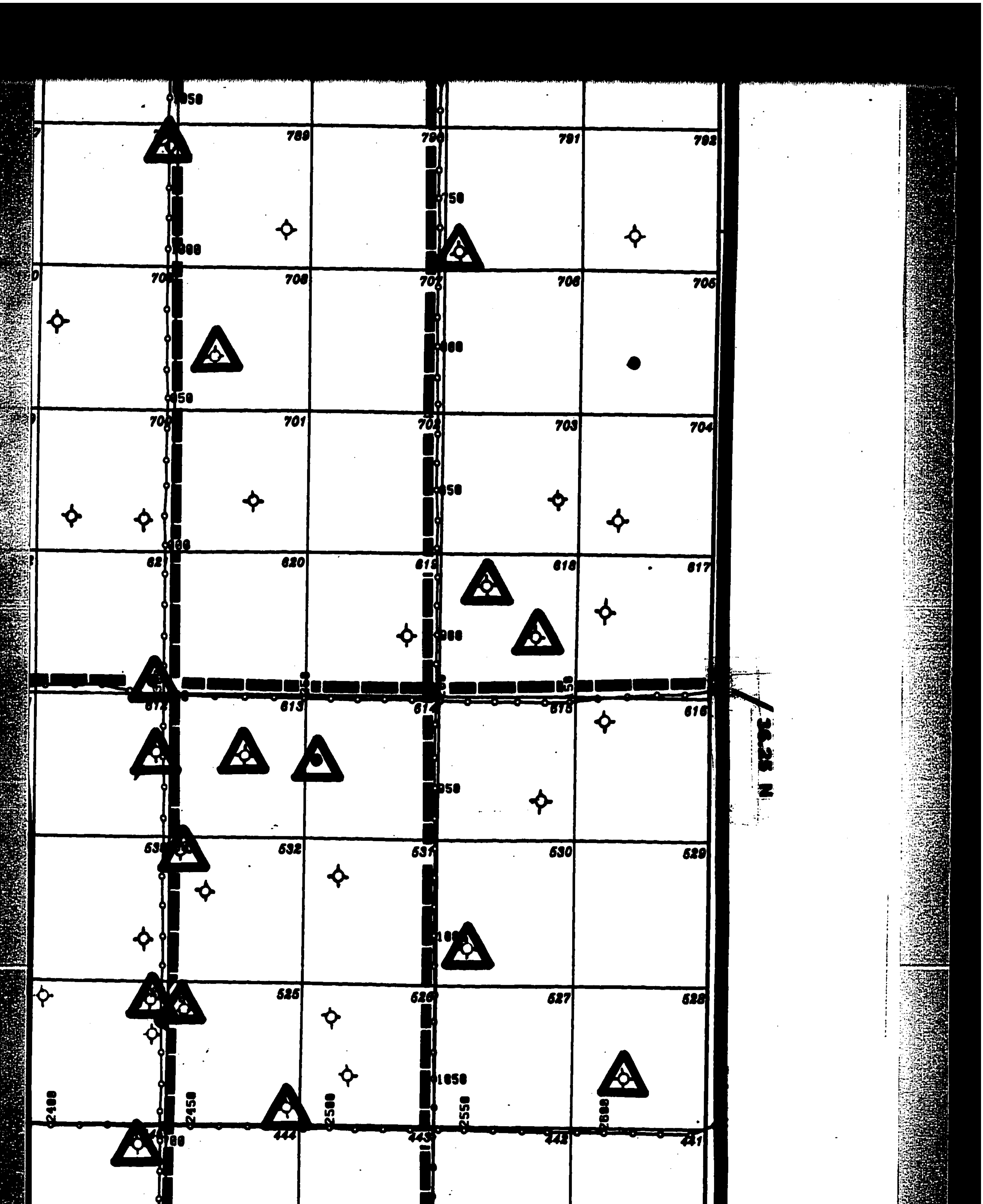
789
790
791
792
708
707
706
705
701
702
703
704
620
619
618
617
613
614
615
616
532
531
530
529
525
526
527
528
444
443
442
441
750
2400
2450
2500
2550
2600
1650

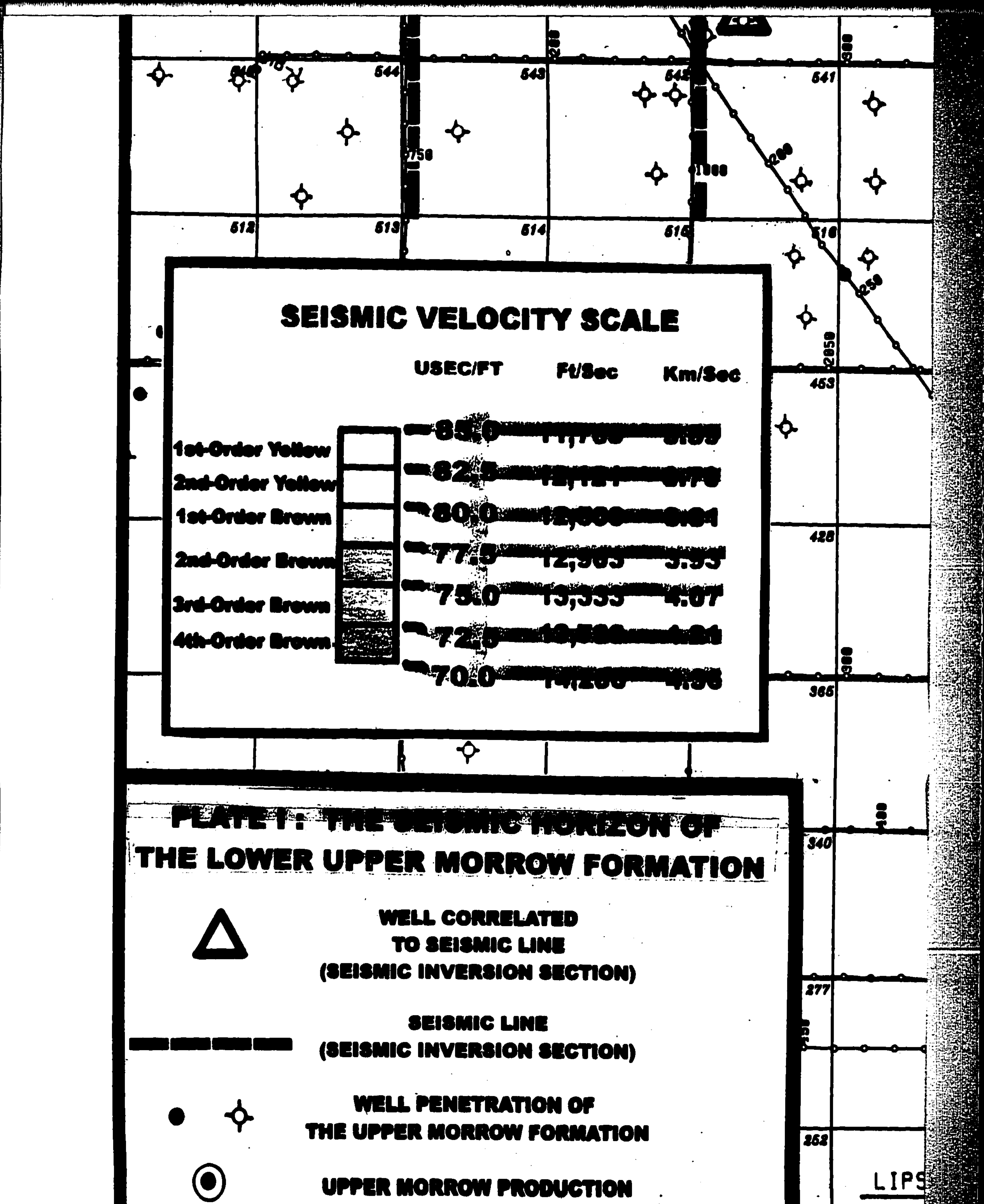

SEISMIC VELOCITY SCALE
USEC/FT
Ft/Sec
Km/Sec
1st-Order Yellow
2nd-Order Yellow
1st-Order Brown
2nd-Order Brown
3rd-Order Brown
4th-Order Brown
85.0
82.5
80.0
77.5
75.0
72.5
70.0
PLATE I : THE SEISMIC HORIZON OF
THE LOWER UPPER MORROW FORMATION
WELL CORRELATED
TO SEISMIC LINE
(SEISMIC INVERSION SECTION)
SEISMIC LINE
(SEISMIC INVERSION SECTION)
WELL PENETRATION OF
THE UPPER MORROW FORMATION
UPPER MORROW PRODUCTION
544
543
542
541
512
513
514
515
516
453
428
365
340
277
252
LIPS

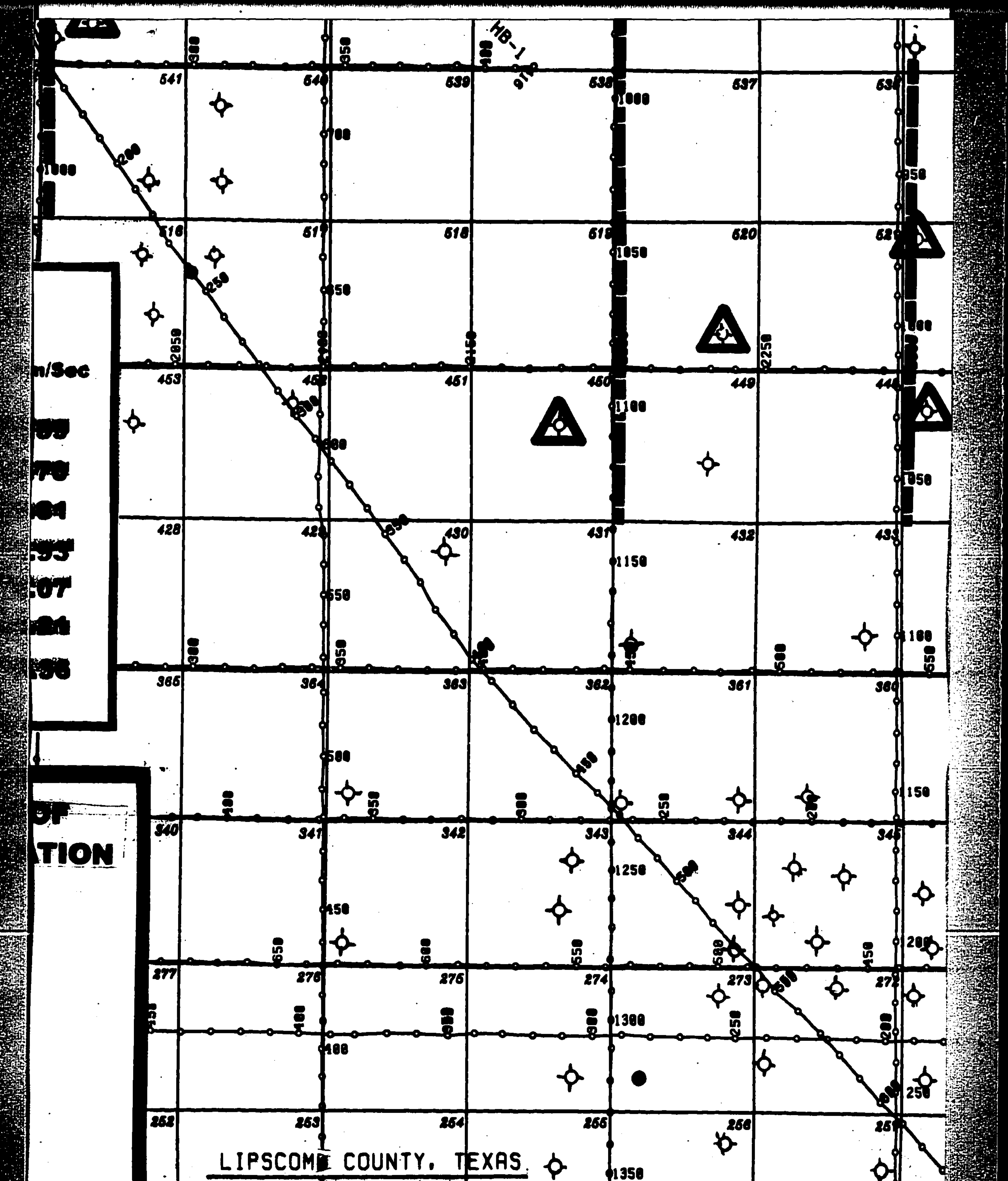

HB-1
541
540
539
538
537
536
516
517
518
519
520
521
453
452
451
450
449
448
428
429
430
431
432
433
365
364
363
362
361
360
340
341
342
343
344
345
277
278
276
274
273
272
252
253
254
255
256
257
LIPSCOMB COUNTY, TEXAS

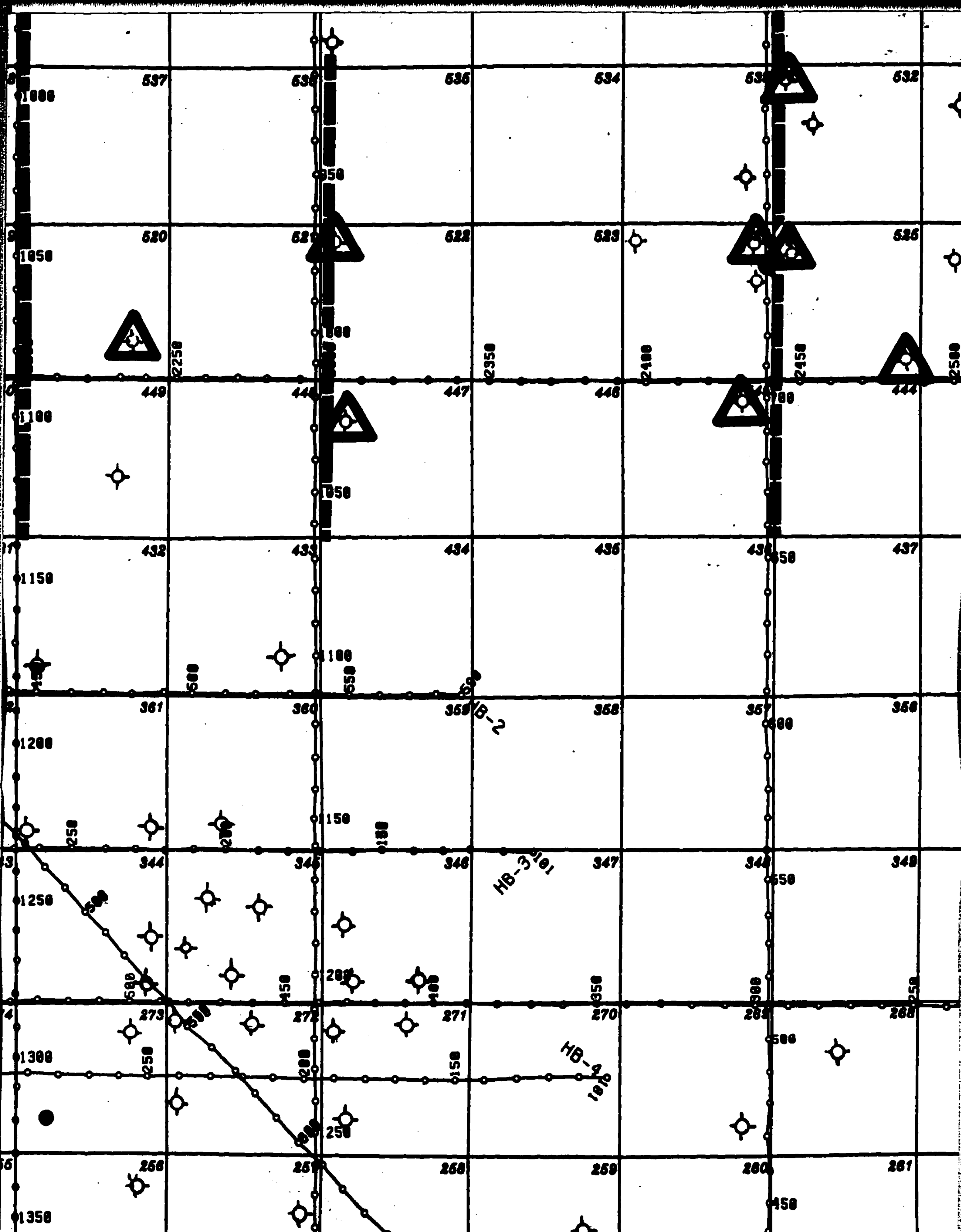

537
535
534
532
520
522
523
525
449
447
446
444
432
434
437
361
360
358
356
344
346
347
270
256
258
259
261
HB-2
HB-3
HB-4

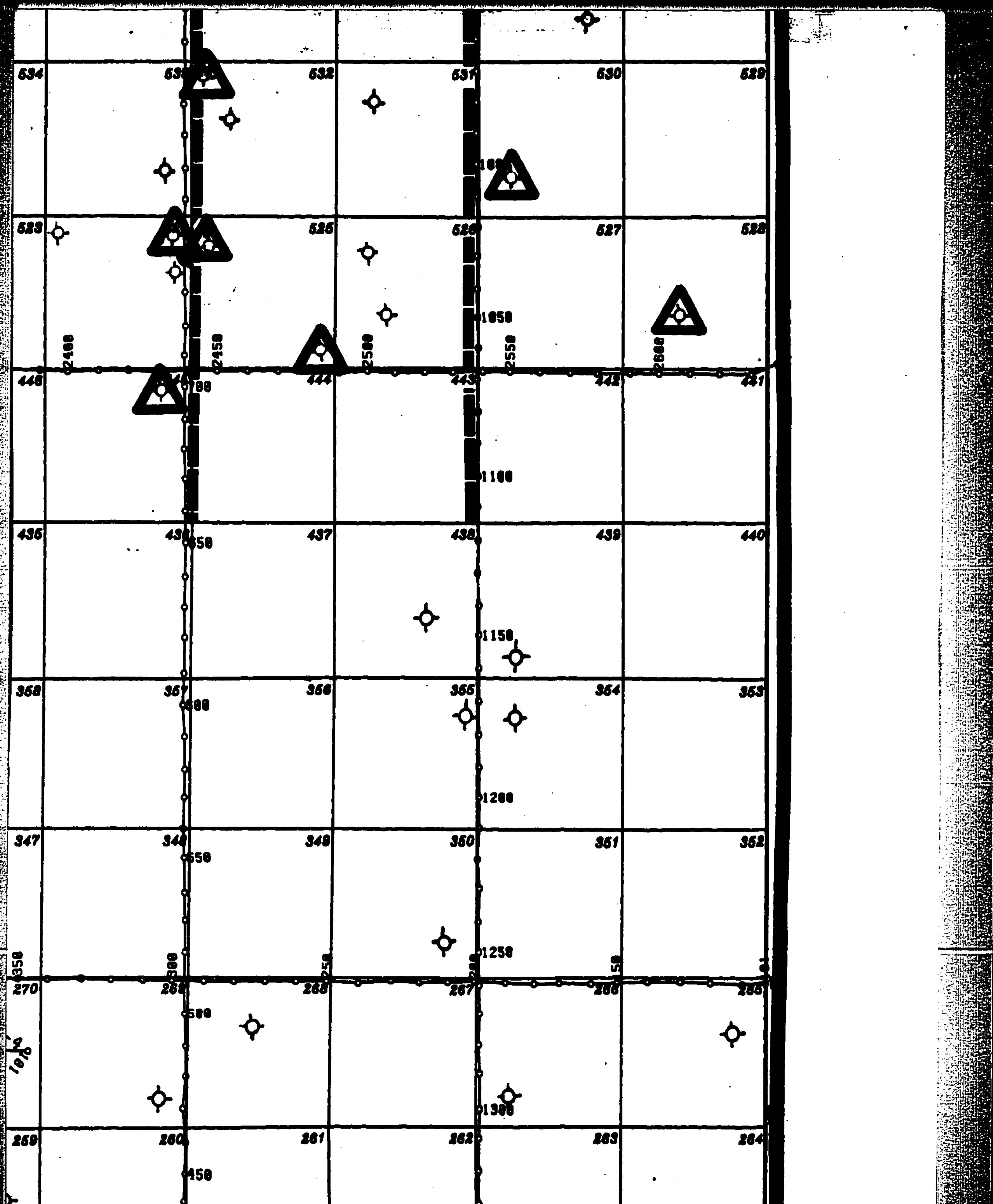
534
532
530
529
526
527
528
2400
2450
2500
2550
2600
1050
444
442
441
1100
435
437
438
439
440
1150
356
355
354
353
1200
347
349
350
351
352
1250
270
268
267
1300
259
260
261
262
263
264

PLEASE NOTE:

Oversize maps and charts are filmed in sections in the following manner:

LEFT TO RIGHT, TOP TO BOTTOM, WITH SMALL OVERLAPS

The following map or chart has been refilmed in its entirety at the end of this dissertation (not available on microfiche). A xerographic reproduction has been provided for paper copies and is inserted into the inside of the back cover.

Black and white photographic prints (17" x 23") are available for an additional charge.

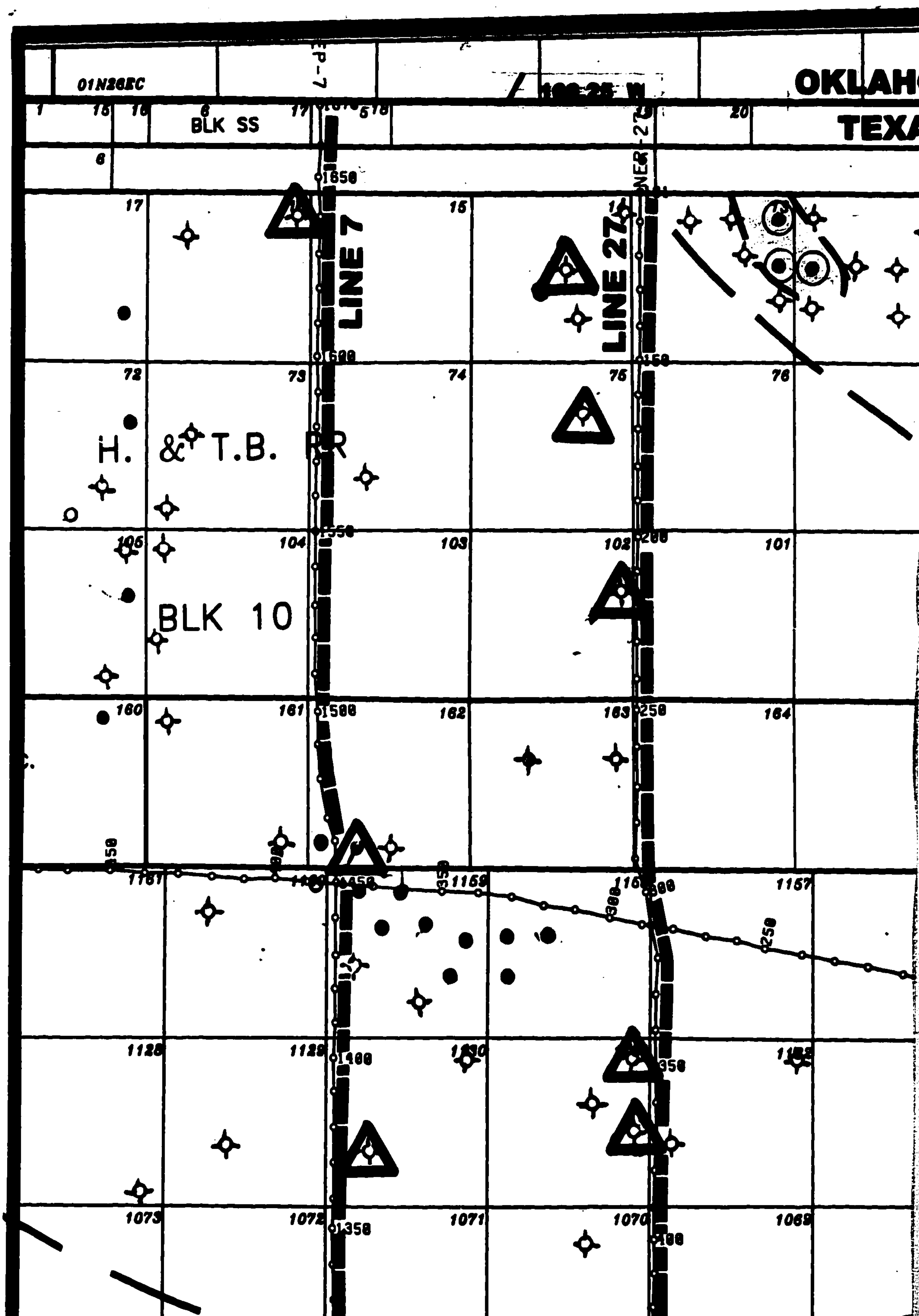
01N26EC
OKLAHO
TEXA
BLK SS
LINE 7
LINE 27
H. & T.B. RR
BLK 10
17
15
72
73
74
75
76
105
104
103
102
101
160
161
162
163
164
1161
1159
1157
1128
1129
1070
1071
1072
1073
1650
1600
1550
1500
1450
1400
1350

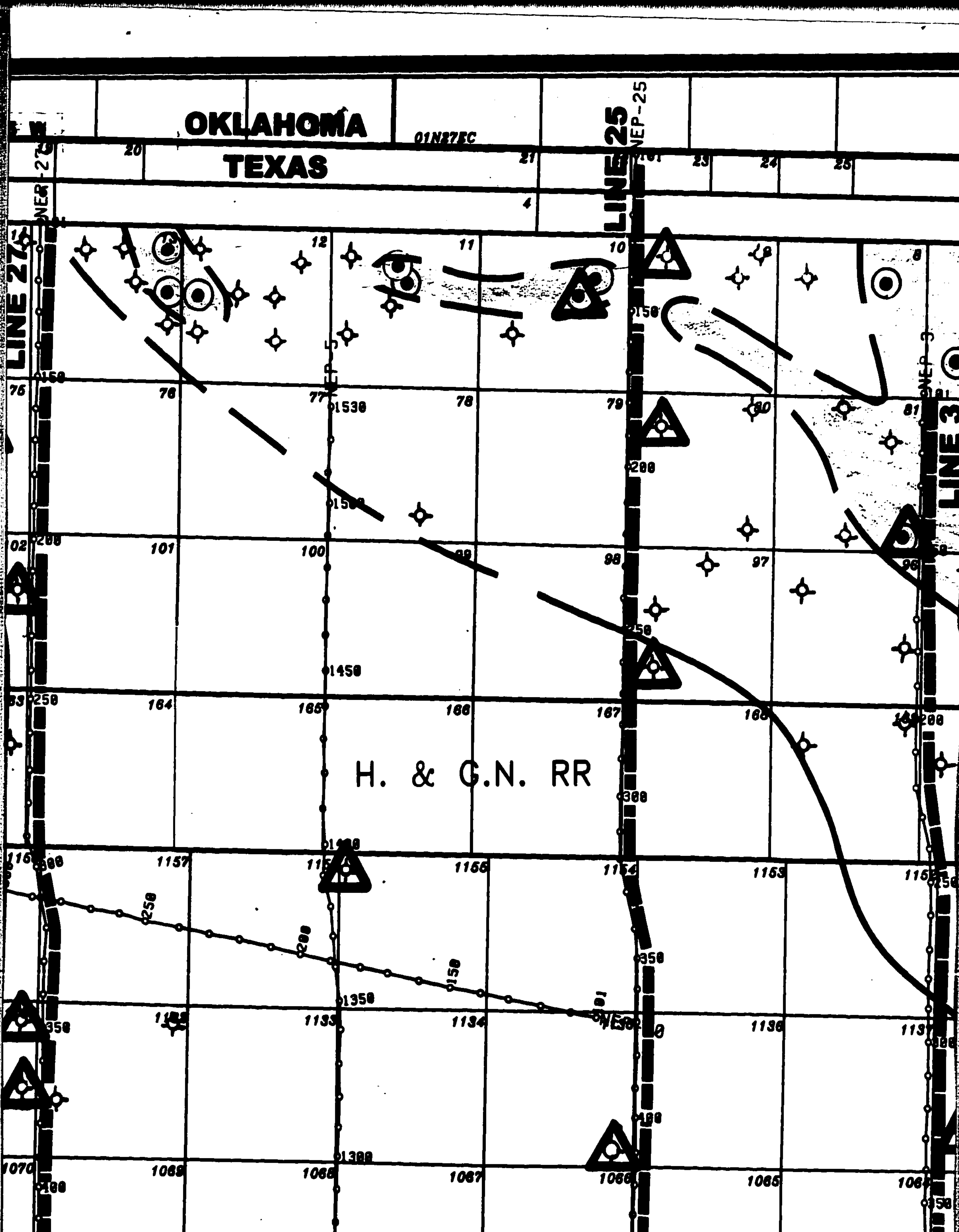
OKLAHOMA
TEXAS
01N27EC
LINE 27
LINE 25
NEP-25
NEP-5
NEP-3
LINE 3
H. & G.N. RR
20
21
23
24
25
4
12
11
10
8
75
76
77
78
79
80
81
102
101
100
98
97
96
164
165
166
167
168
1157
1155
1154
1153
1133
1134
1136
1070
1069
1068
1067
1066
1065
150
200
250
300
350
400
1530
1500
1450
1400
1350
1300

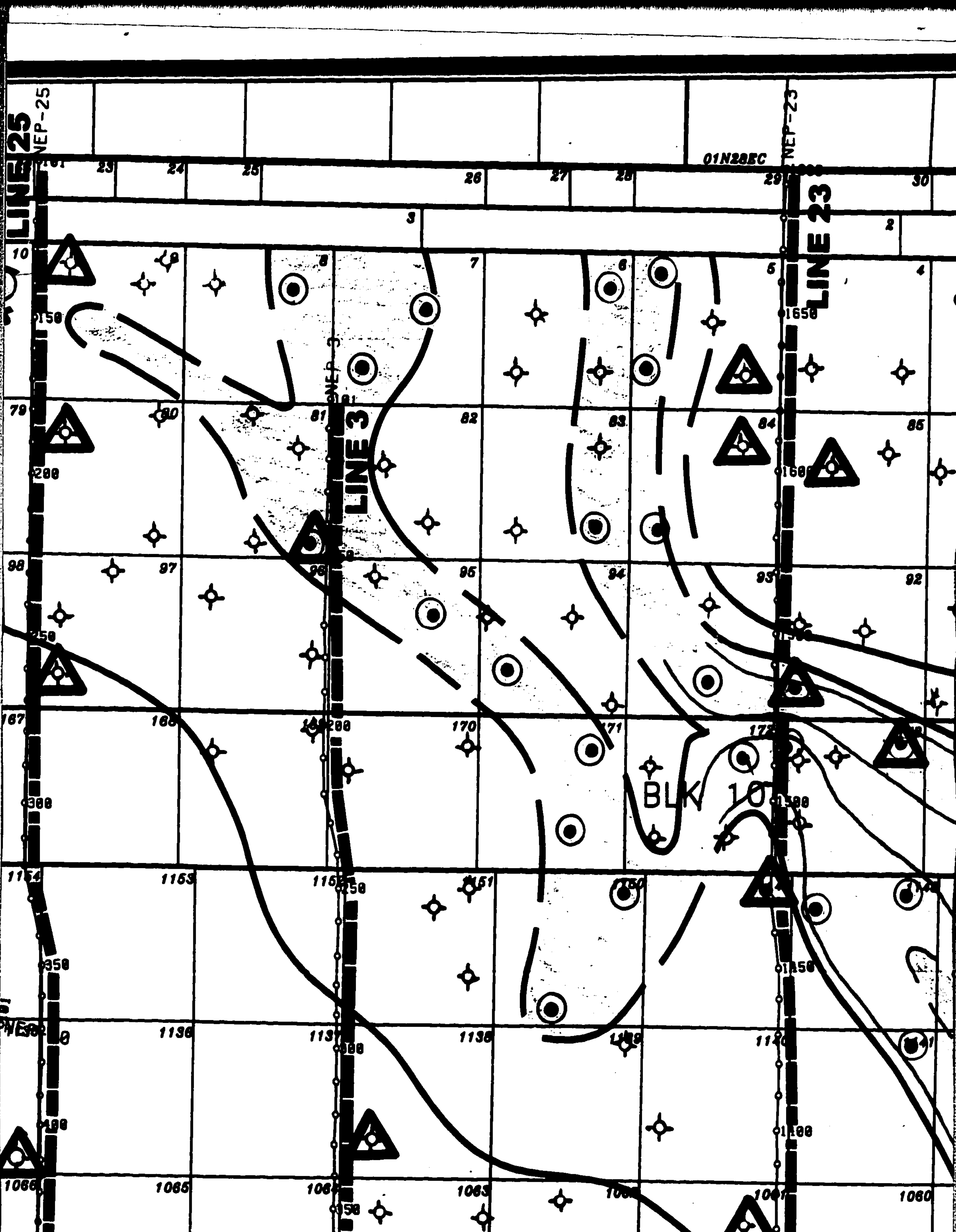

LINE 25
NEP-25
01N28EC
NEP-23
LINE 23
NEP-3
LINE 3
BLK 10
23
24
25
26
27
28
29
30
3
2
10
8
7
6
5
4
1650
79
80
81
82
83
84
85
200
1600
98
97
96
95
94
93
92
250
167
168
200
170
171
172
300
1300
1153
350
1450
1136
1138
1066
1065
1063
1060

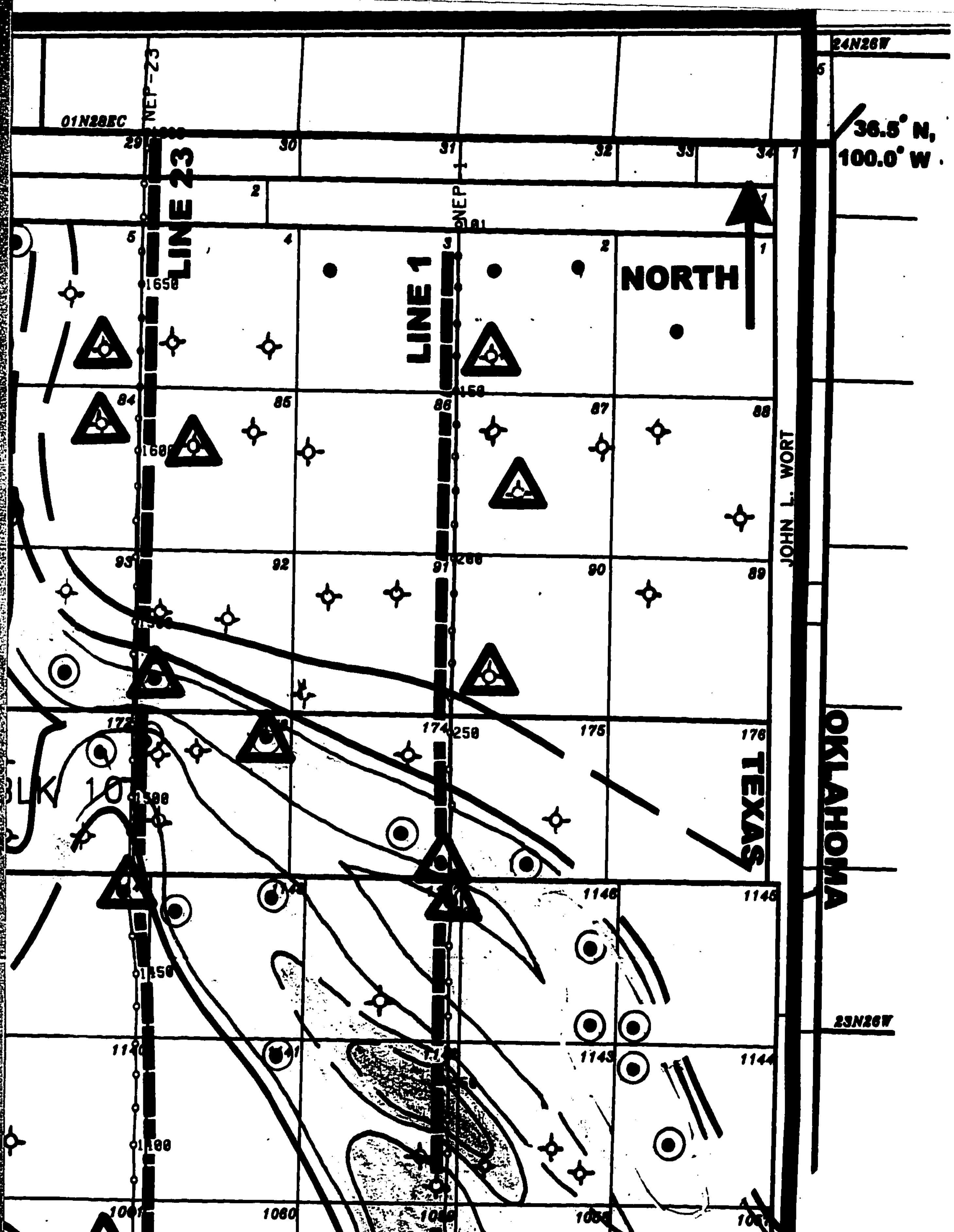

24N26W
01N28EC
NEP-23
LINE 23
NEP-1
LINE 1
36.5° N,
100.0° W
NORTH
JOHN L. WORT
TEXAS
OKLAHOMA
BLK 10
23N26W

1073
1072
1350
1071
1070
1069
1040
1041
1300
1042
1044
985
984
LINE 14
1250
981
952
953
954
956
550
897
896
895
893
1150
864
865
866
867
1100
650
H. & T.C. RR
BLK 43
LINE 2
809
808
807
806
1050
776
777
778
779
780
1000
750

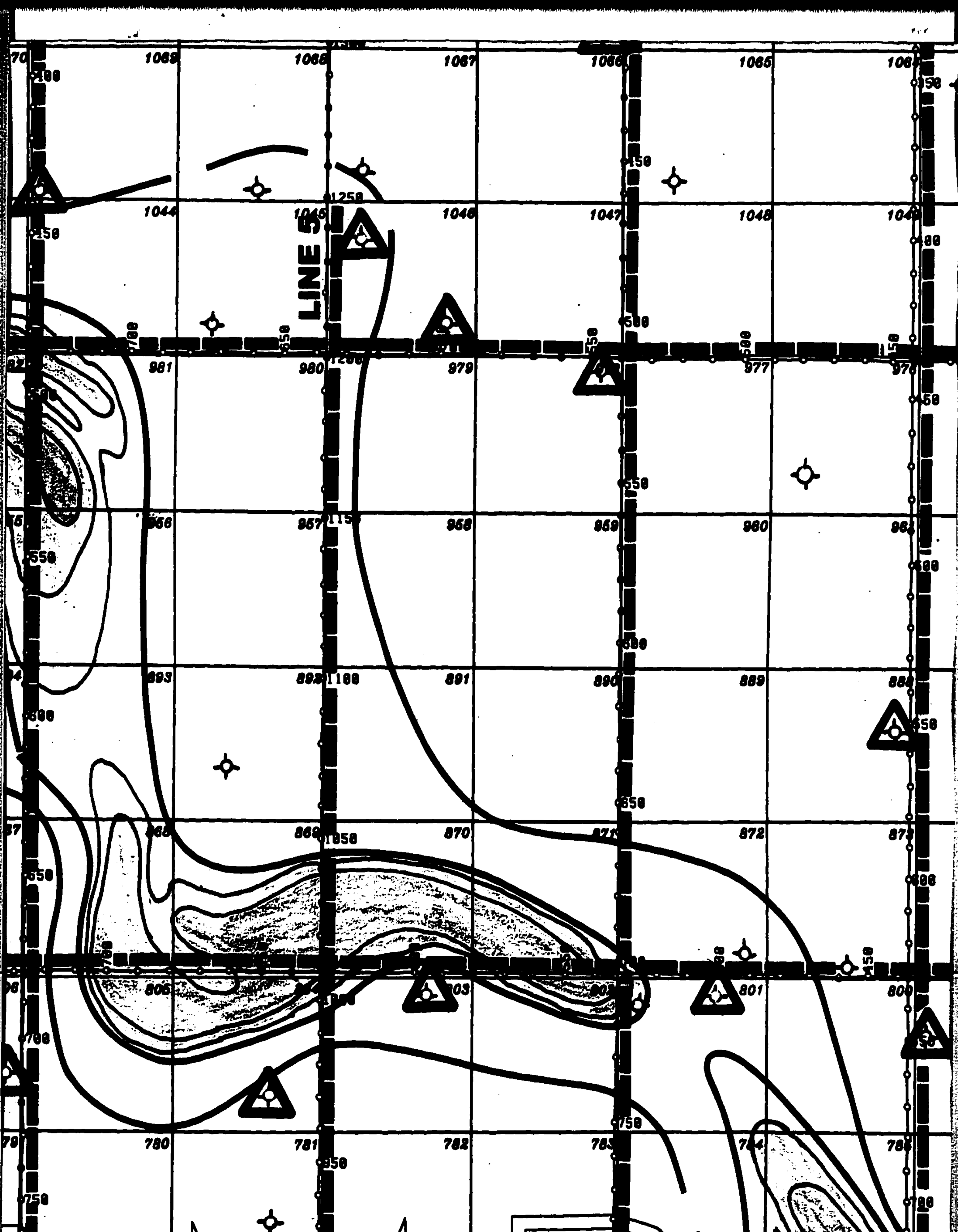

LINE 5
1069
1068
1067
1066
1065
1044
1045
1046
1047
1048
981
980
979
977
966
957
958
959
960
893
892
891
890
889
870
872
806
803
801
780
781
782
1250
1200
1150
1100
1050
950
450
500
550
600
650
700
750

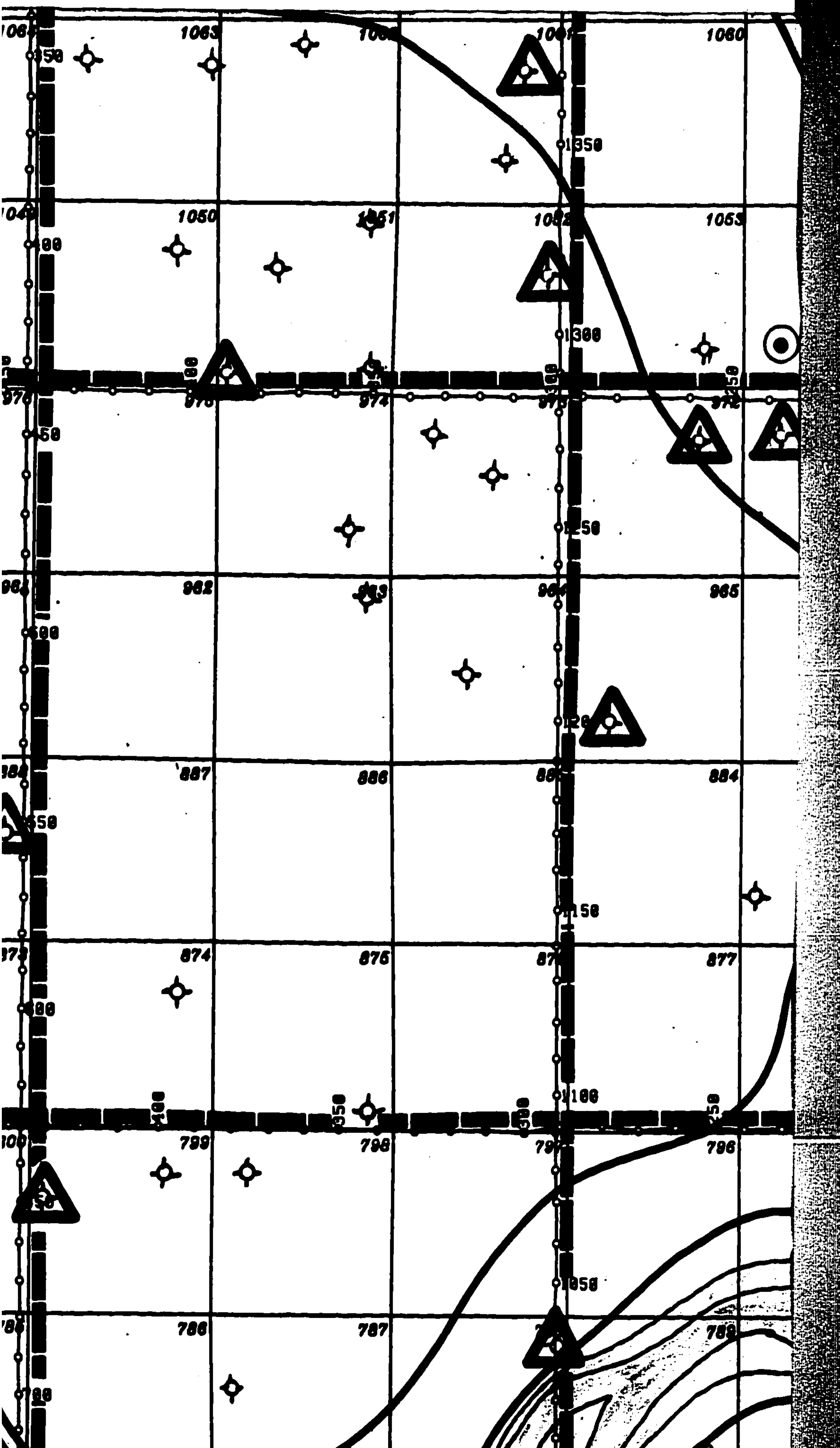

1063
1060
1350
1050
1053
1300
974
1250
962
965
887
886
884
1150
874
875
877
1100
799
798
796
1050
786
787
788

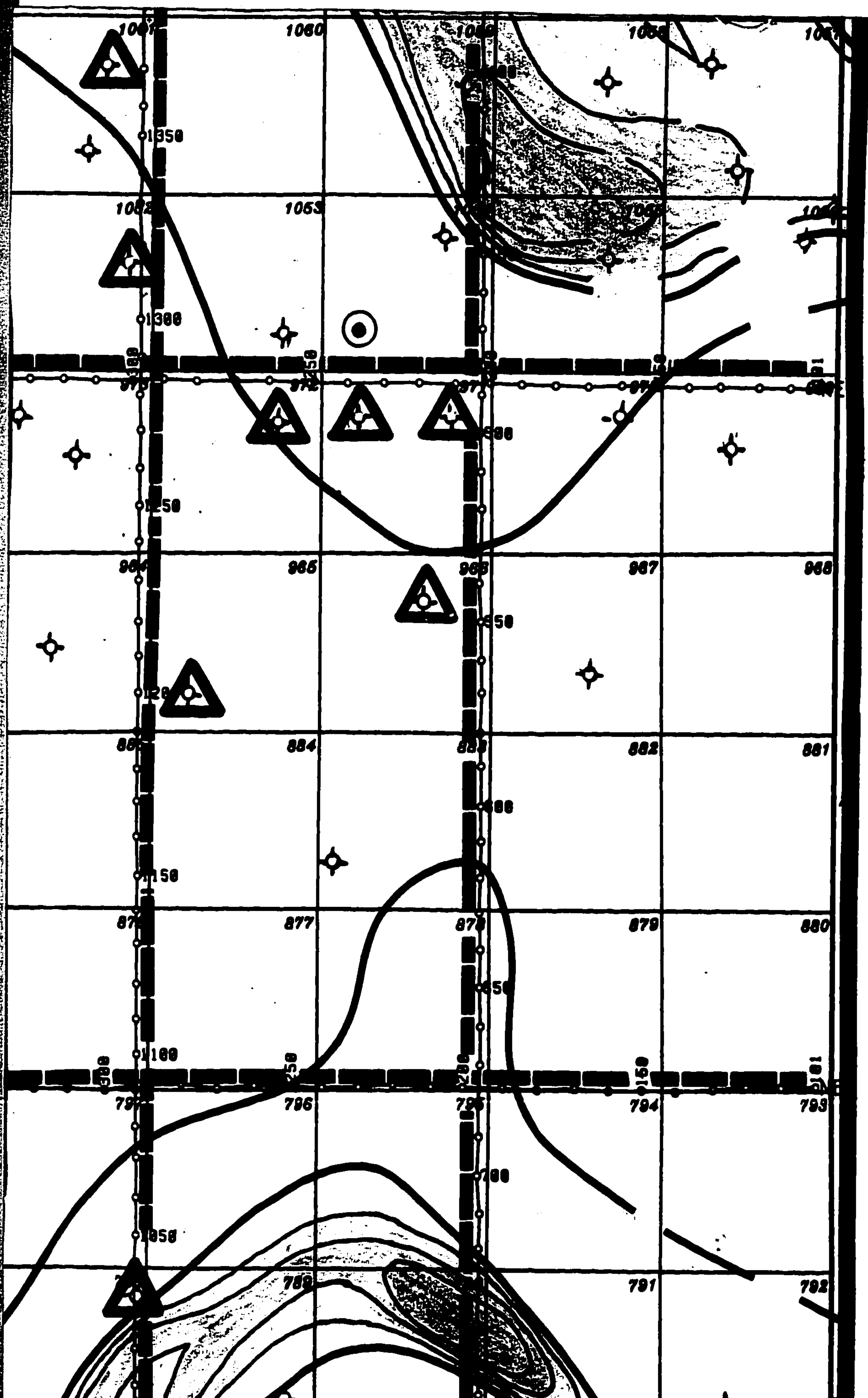

1060
1053
965
967
968
884
882
881
877
879
880
796
794
793
789
791
792
1350
1300
1250
1150
1100
1050

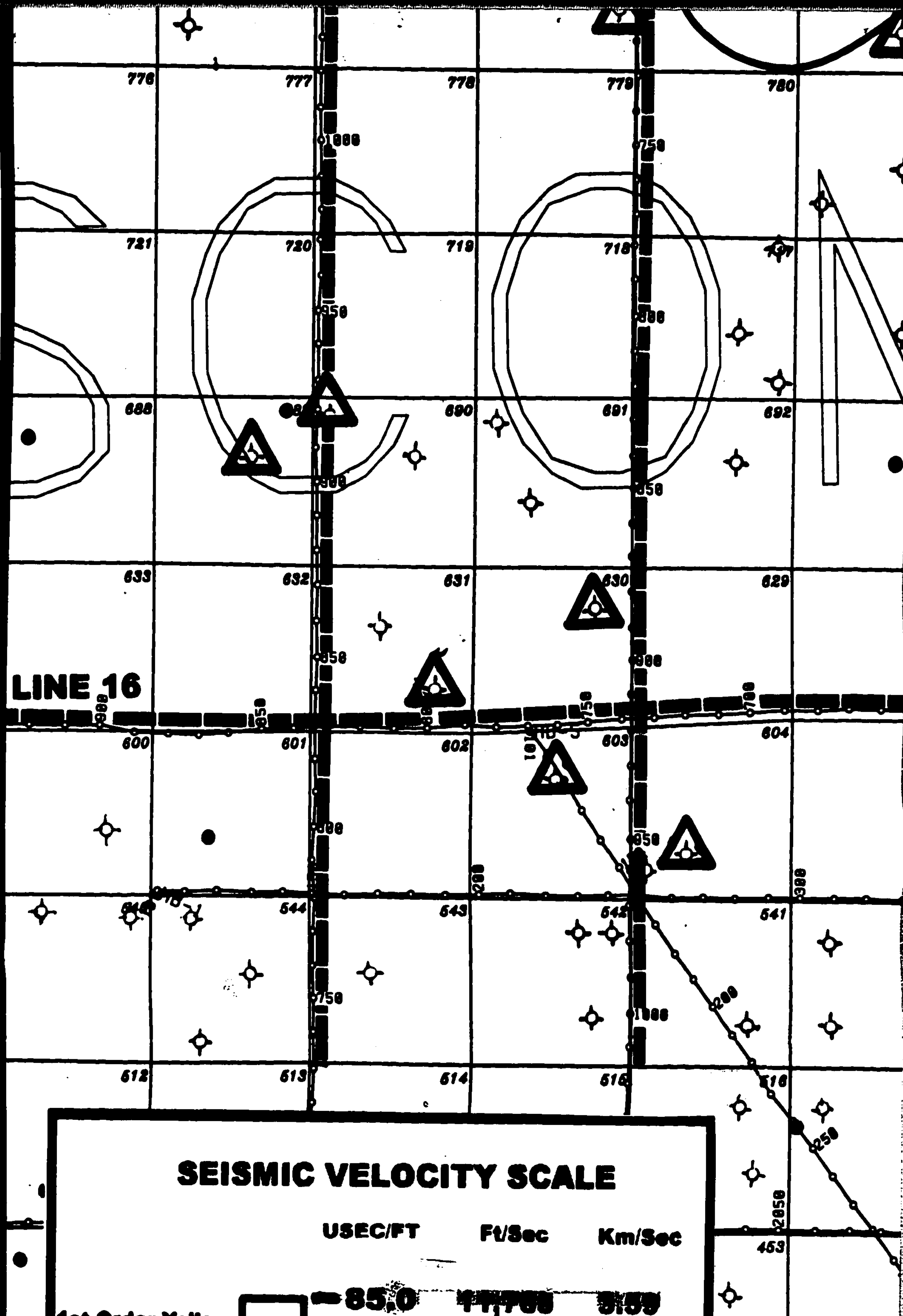

LINE 16
776
777
778
779
780
721
720
719
718
688
690
691
692
633
632
631
630
629
600
601
602
603
604
544
543
542
541
512
513
514
516
453
SEISMIC VELOCITY SCALE
USEC/FT
Ft/Sec
Km/Sec

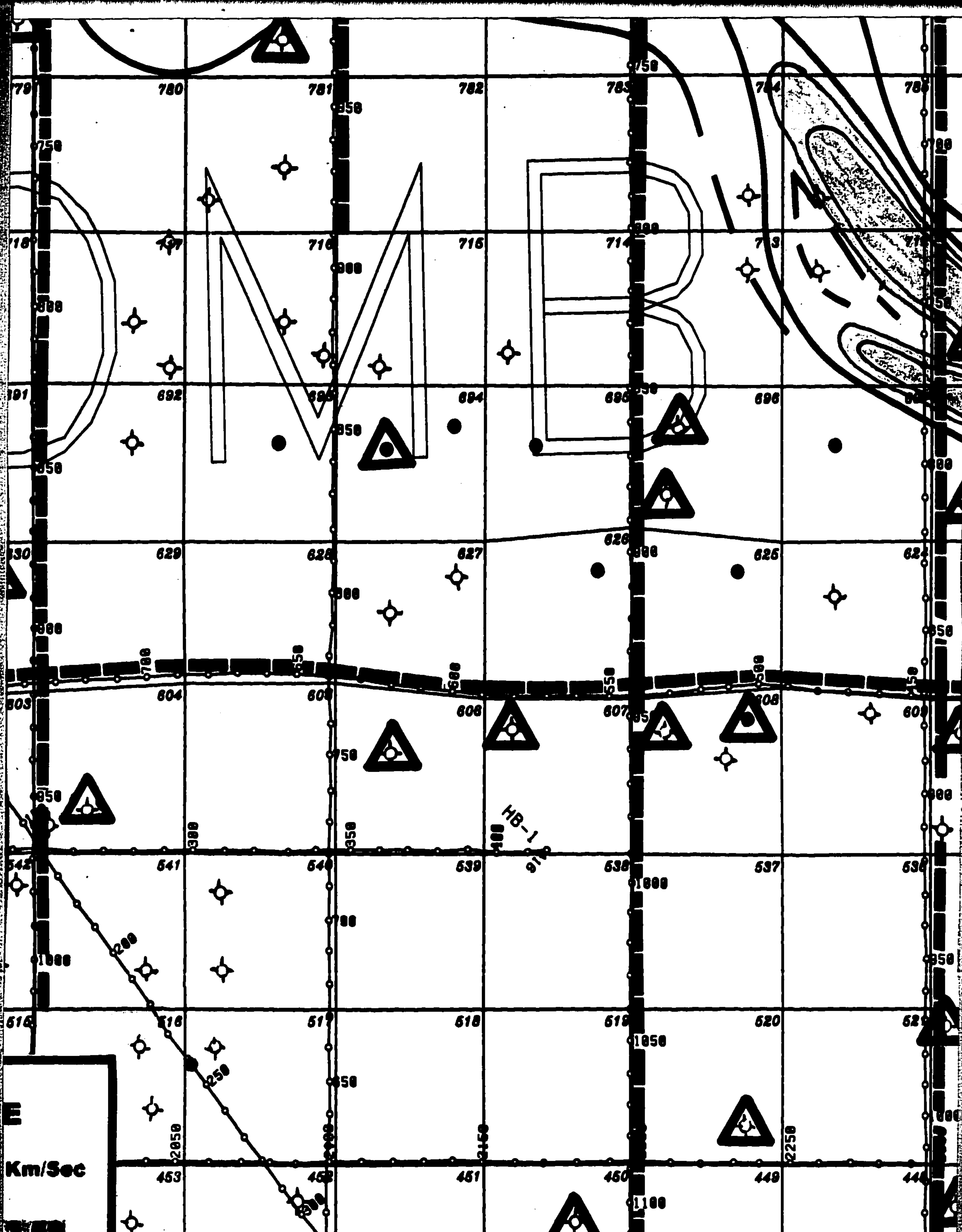

780
781
782
784
716
715
714
692
694
696
629
627
626
625
604
606
607
608
541
540
539
538
537
517
518
520
453
451
449
HB-1
1000
1050
1100
2050
2250
Km/Sec

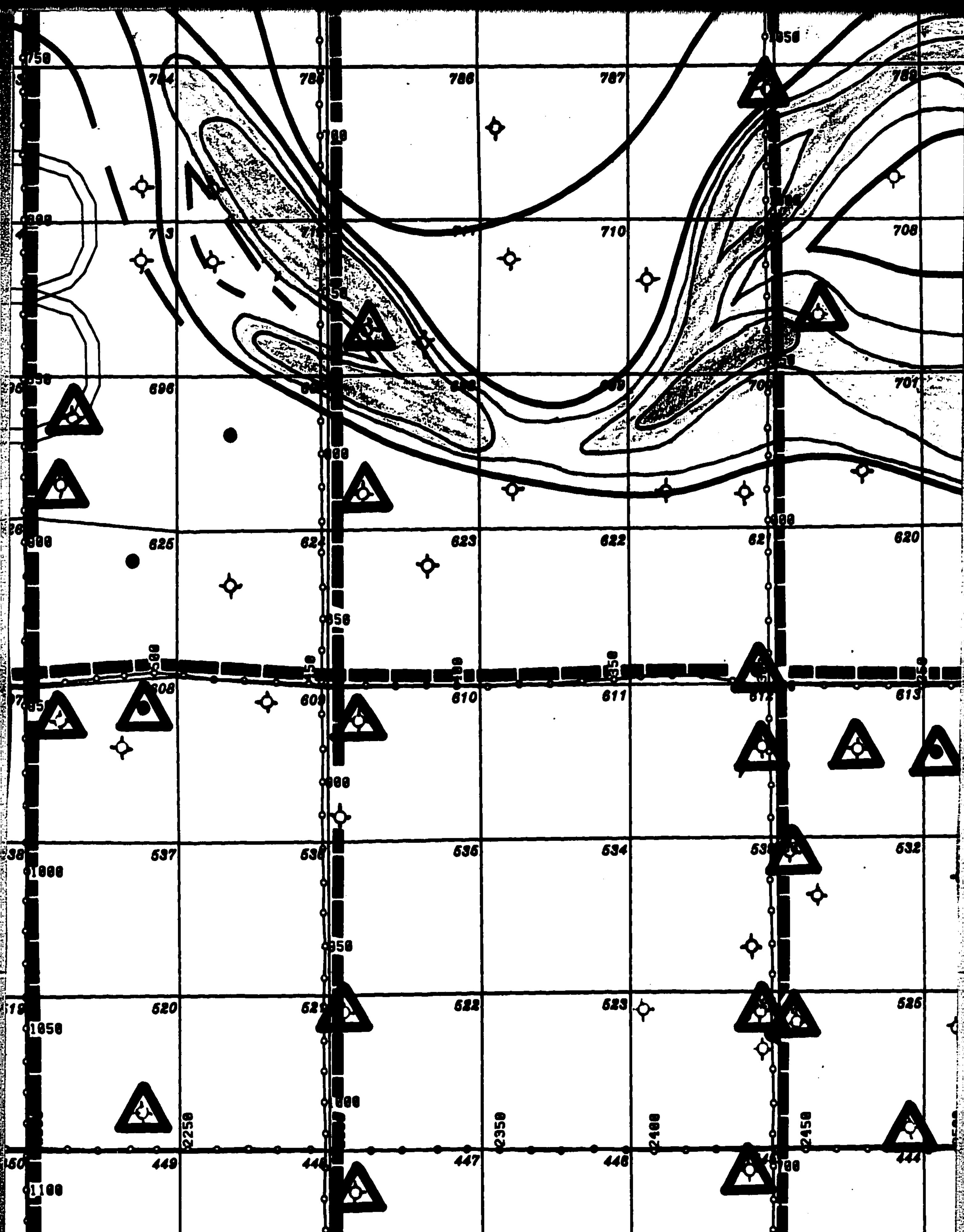

786
787
710
708
696
625
623
622
620
610
611
537
535
534
532
520
522
523
525
449
447
446
444
1000
1050
1100
2250
2350
2400
2450

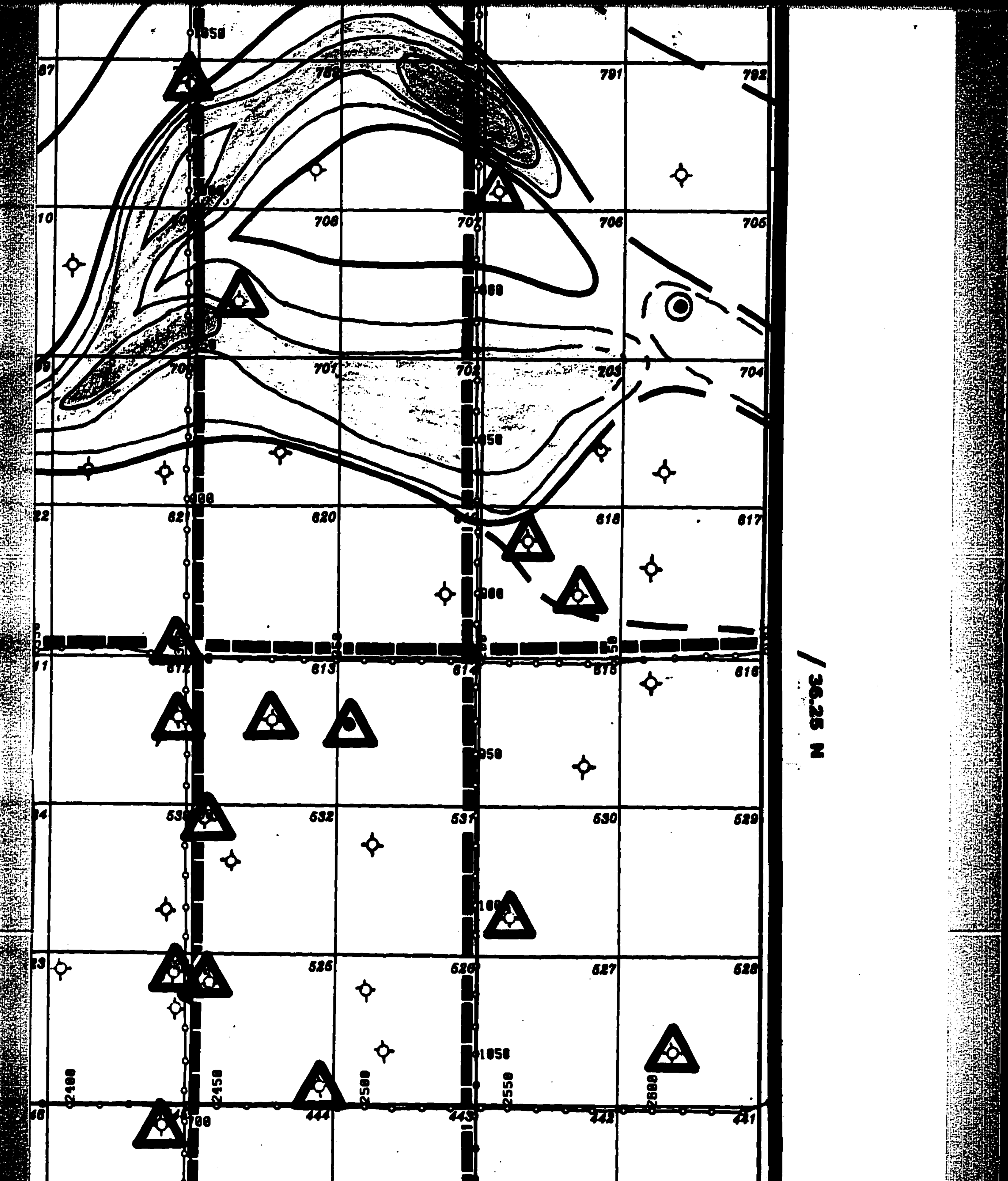

791
792
708
707
706
705
701
702
703
704
620
618
617
613
614
615
616
532
531
530
529
525
526
527
528
444
443
442
441
2400
2450
2500
2550
2600
36.25 N

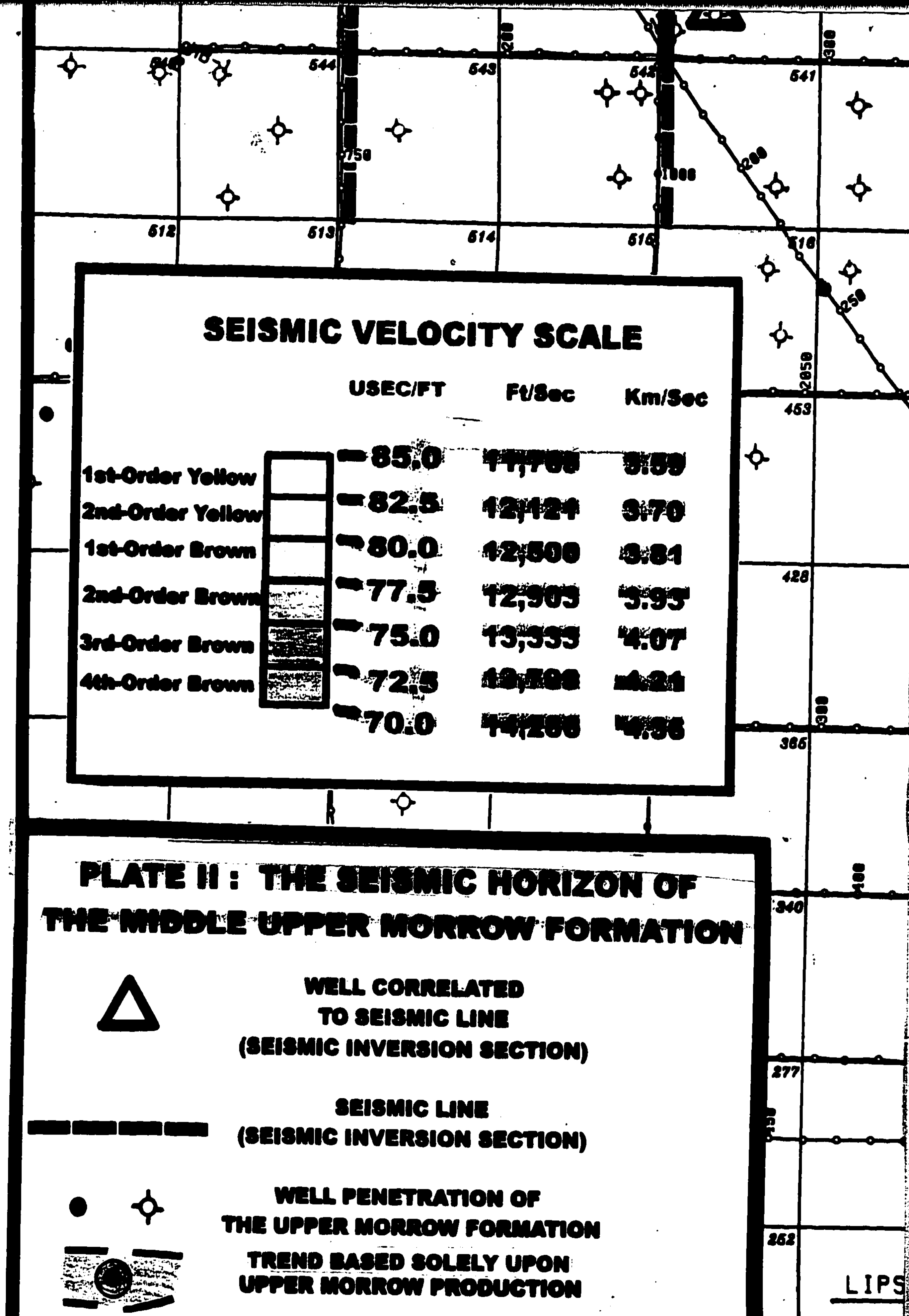

SEISMIC VELOCITY SCALE
USEC/FT
Ft/Sec
Km/Sec
1st-Order Yellow
2nd-Order Yellow
1st-Order Brown
2nd-Order Brown
3rd-Order Brown
4th-Order Brown
85.0
82.5
12,121
3.70
80.0
12,500
3.81
77.5
12,903
3.93
75.0
13,333
4.07
72.5
70.0
PLATE II : THE SEISMIC HORIZON OF
THE MIDDLE UPPER MORROW FORMATION
WELL CORRELATED
TO SEISMIC LINE
(SEISMIC INVERSION SECTION)
SEISMIC LINE
(SEISMIC INVERSION SECTION)
WELL PENETRATION OF
THE UPPER MORROW FORMATION
TREND BASED SOLELY UPON
UPPER MORROW PRODUCTION
544
543
541
512
513
514
516
453
428
365
340
277
252

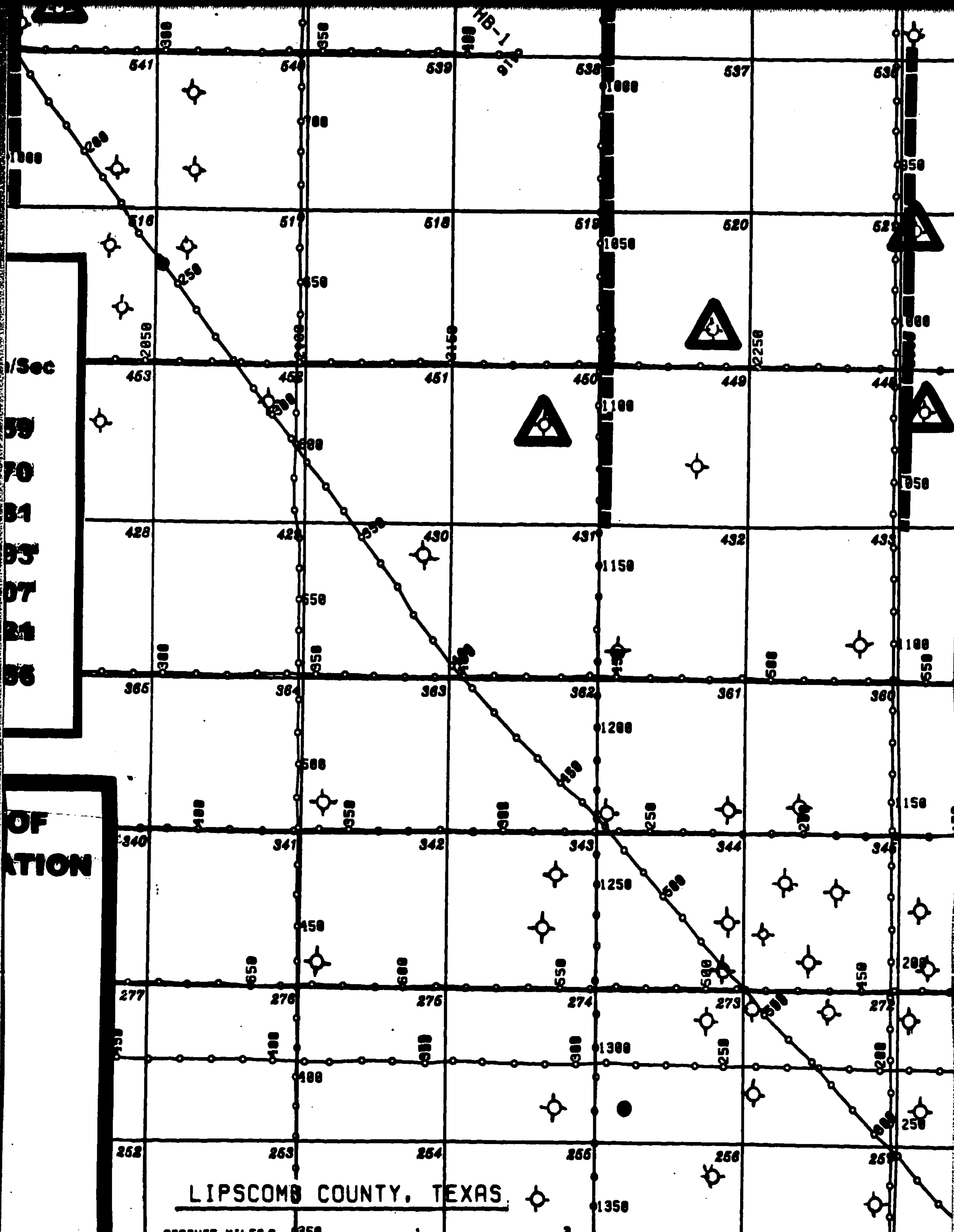

LIPSCOMB COUNTY, TEXAS
MB-1
/Sec
OF
ATION
541
540
539
538
537
536
516
517
518
519
520
521
453
452
451
450
449
448
428
429
430
431
432
433
365
364
363
362
361
360
340
341
342
343
344
345
277
276
275
274
273
272
252
253
254
255
256
257

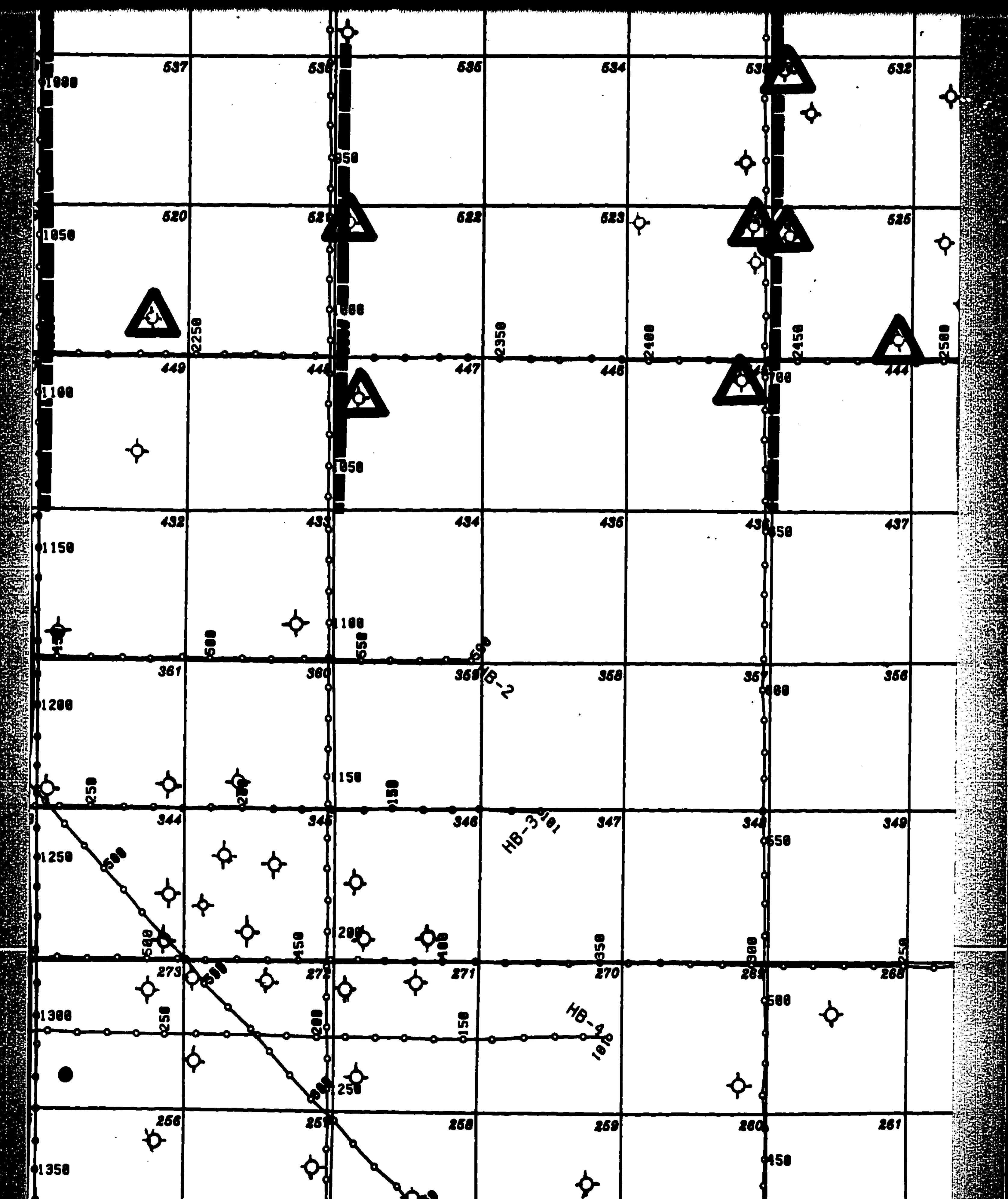
537
536
535
534
533
532
520
522
523
526
449
447
446
444
432
434
435
436
437
361
360
359
358
357
356
344
346
347
349
273
271
270
269
256
258
259
260
261
1000
1050
1100
1150
1200
1250
1300
1350
2250
2350
2400
2450
2500
HB-2
HB-3
HB-4

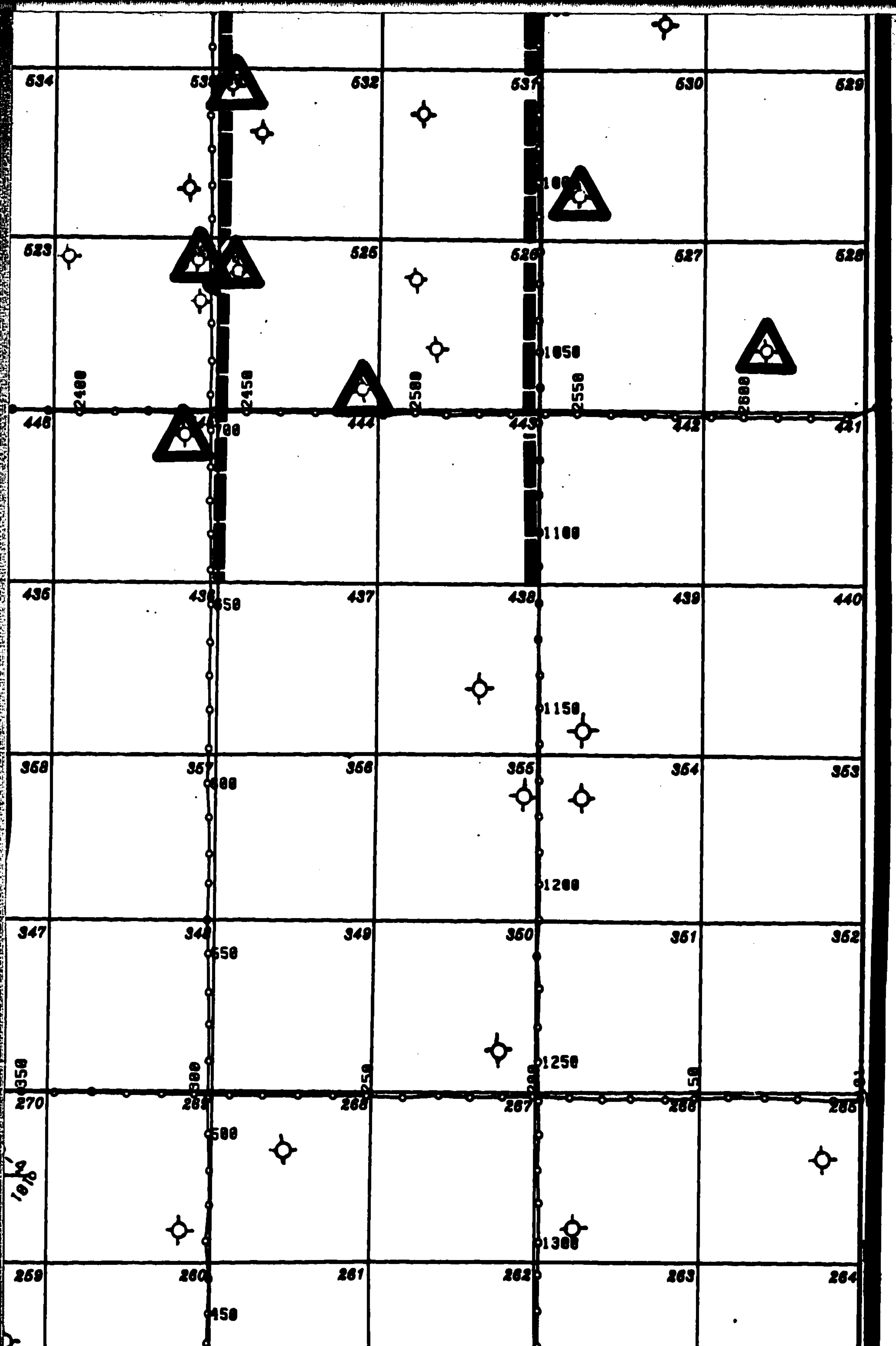
534
532
531
530
529
523
525
526
527
528
2400
2450
2500
2550
2600
1050
446
444
443
442
441
1100
436
437
438
439
440
1150
368
357
356
355
364
363
1200
347
349
350
351
352
1250
270
268
267
266
265
1300
259
260
261
262
263
264